From Department of Physiology and Pharmacology,
Karolinska Institutet, Stockholm, Sweden

BRAIN IMMUNE MECHANISMS IN SCHIZOPHRENIA – EXPERIMENTAL AND CLINICAL CHARACTERIZATION

Maximilian Tufvesson Alm

Karolinska Institutet

Stockholm 2019

Published by Karolinska Institutet.
Printed by Eprint AB 2019
Cover by Ivana Lindström

ISBN 978-91-7831-645-8

Brain immune mechanisms in schizophrenia – experimental and clinical characterization

THESIS FOR DOCTORAL DEGREE (Ph.D.)

By

Maximilian Tufvesson Alm

Principal Supervisor:
Professor Göran Engberg
Karolinska Institutet
Department of Physiology and Pharmacology

Co-supervisor(s):
Professor Sophie Erhardt
Karolinska Institutet
Department of Physiology and Pharmacology

Dr. Lilly Schwieler
Karolinska Institutet
Department of Physiology and Pharmacology

Dr. Simon Cervenka
Karolinska Institutet
Department of Clinical Neuroscience

Dr. Kristian Sandberg
Uppsala Universitet
Department of Medicinal Chemistry

Opponent:
Professor Trevor Stone
University of Oxford
The Kennedy Institute
NDORMS

Examination Board:
Professor Sven Ove Ögren
Karolinska Institutet
Department of Neuroscience

Professor Finn Bengtsson
Linköpings Universitet
Department of Medicine and Health Sciences

Dr. Karima Chergui
Karolinska Institutet
Department of Physiology and Pharmacology

Till min familj

ABSTRACT

The role of inflammation has become increasingly evident in the pathophysiology of schizophrenia and thought to one of the major causes of the symptoms. Interestingly, immune activation has been linked to the kynurenine pathway of tryptophan degradation, which produces an array of neuroactive metabolites. Most notably, the end-metabolite kynurenic acid (KYNA) has been described as an endogenous antagonist on the obligatory glycine-site of the *N*-methyl-D-aspartate (NMDA) receptor. In similarity to other NMDA receptor antagonists, KYNA has been shown to produce symptoms similar to those seen in schizophrenia. Accordingly, elevated levels of KYNA has been found in the cerebrospinal fluid (CSF) and post-mortem brains of patients with schizophrenia, along with an elevation of pro-inflammatory cytokines.

The identification of elevated brain KYNA as a potential cause for the symptoms in schizophrenia offers exciting opportunities for new treatment options for schizophrenia. In the present thesis, we show that a specific inhibitor of KAT II, the primary enzyme responsible for the production of KYNA, causes a robust decrease in ventral tegmental area dopamine cell activity, suggesting beneficial effects of the inhibitor for psychosis. However, in order to properly evaluate novel antipsychotic drugs explicitly targeting the kynurenine pathway, proper modeling has to be considered.

This thesis aimed to provide a platform where such drugs can be tested appropriately. Thus, in the present thesis, we characterize different ways of modeling elevated KYNA in rodents, anchored to clinical findings, with regards to behavioral aspects relevant to schizophrenia and dopamine activity. We highlight the importance of proper modeling in KMO K/O mice, where we saw different effects of established antipsychotics and drugs that were previously shown to lower KYNA based on endogenous KYNA levels.

Additionally, we characterize different processes involved in the pathophysiology of schizophrenia using CSF and serum of a small first-episode psychosis cohort. Our analysis provides an unbiased confirmation for the involvement of inflammation and the kynurenine pathway in schizophrenia through metabolomics.

LIST OF SCIENTIFIC PAPERS

I. Klas Linderholm*, Maximilian Tufvesson Alm*, Markus Larsson, Sara Olsson, Michel Goiny, Mihaly Hajos, Sophie Erhardt, Göran Engberg. *Inhibition of kynurenine aminotransferase II reduces activity of midbrain dopamine neurons.* Neuropharmacology, 2016. doi: 10.1016/j.neuropharm.2015.10.028

II. Maximilian Tufvesson-Alm, Lilly Schwieler, Robert Schwarcz, Michel Goiny, Sophie Erhardt, Göran Engberg. *Importance of kynurenine 3-monooxygenase for spontaneous firing and pharmacological responses of midbrain dopamine neurons: Relevance for schizophrenia.* Neuropharmacology, 2018. doi: 10.1016/j.neuropharm.2018.06.003

III. Maximilian Tufvesson-Alm, Sophie Imbeault, Xicong Liu, Lilly Schwieler, Göran Engberg, Sophie Erhardt. *Dual administration of LPS causes behavioral disturbances associated with the psychopathology of schizophrenia.* Manuscript.

IV. Carl Sellgren*, Sophie Imbeault*, Markus Larsson, Alfredo Oliveros, Ida Nilsson, Jessica Gracias, Simone Codeluppi, Maria Bhat, Maximilian Tufvesson-Alm, Funda Orhan, Magdalena Kegel, Anthi Faka, Marie Svedberg, Susan Powell, S. Caldwell, M. Kamenski, Michel Goiny, Camilla Svensson, Martin Schalling, Tomas Hökfelt, Lilly Schwieler, Simon Cervenka, Doo-Sup Choi, Mikael Landén, Göran Engberg, Sophie Erhardt. *Functional aspects of GRK3 in brain immune activation and psychosis.* Manuscript.

V. Daniel Lindberg, Maximilian Tufvesson-Alm, Funda Orhan, Surendra Dasari, Lee Peyton, Fredrik Piehl, Karolinska Schizophrenia Project (KaSP) Consortium, Simon Cervenka, Sophie Erhardt, Doo-Sup Choi. *Identification of metabolomic biomarkers associated with first-episode psychosis and antipsychotic treatment within the cerebrospinal fluid and serum.* Manuscript.

*Both authors contributed equally

CONTENTS

LIST OF ABBREVIATIONS

3-HANA	3-hydroxyanthranilic acid
3-HK	3-hydroxykynurenine
AMPA	α-amino-3-hydroxi-5-metyl-4-isoxazol-propansyra
CSF	Cerebrospinal fluid
COX	Cyclooxygenase
eQTL	Expression quantitative trait loci
EPS	Extrapyramidal symptoms
FGA	First-generation antipsychotic
GABA	Gamma-aminobutyric acid
GRK	G-protein coupled receptor kinase
IC_{50}	Half maximal inhibitory concentration
IDO	Indoleamine 2,3-dioxygenase
IFN	Interferon
IL	Interleukin
i.p.	Intraperitoneal
i.v.	Intravenous
K/O	Knock-out
PPI	Prepulse inhibition
KYNA	Kynurenic acid
KAT	Kynurenine aminotransferase
LPS	Lipopolysaccharides
K*m*	Michaelis-Menten constant
MLA	Methyllycaconitine
nACh	Nicotinic acetylcholine receptor
NAD^+	Nicotinamide adenine dinucleotide
NMDA	*N*-methyl-D-aspartate
NAc	Nucleus accumbens
PFC	Prefrontal cortex
QUIN	Quinolinic acid
SGA	Second-generation antipsychotic

SNP	Single nucleotide polymorphism
TDO	tryptophan 2,3-dioxygenase
TNF	Tumor necrosis factor
VTA	Ventral tegmental area
WT	Wild-type

1 INTRODUCTION

1.1 SCHIZOPHRENIA

Characterized by distortions of reality and altered perception of the world, schizophrenia has been a constant presence through-out human history as evidence of its occurrence dates back more than 3500 years (Burton, 2012). Schizophrenia is considered one of the most severe and detrimental psychiatric disorders and affects up to 1% of the human population world-wide (Bromet and Fennig, 1999; McGrath et al., 2008). The onset of the disorder typically occurs during adolescence or early adulthood and is in many aspects considered a chronic disorder (Carpenter and Buchanan, 1994; Kahn et al., 2015). Notably, patients suffering from schizophrenia have a reduced life expectancy of 15-20 years, mainly attributed to increased somatic health complications and suicide (Brown et al., 2000; Laursen et al., 2014; Saha et al., 2007). Beyond personal suffering, it is important to mention the massive socioeconomical costs associated with this crippling disorder, accounting for both direct and indirect cost, such as healthcare and loss of productivity (Desai et al., 2013; Ekman et al., 2013; Gustavsson et al., 2011).

1.1.1 Symptoms and clinical presentation

Although schizophrenia is mainly characterized by psychosis, it is in many aspects a heterogenous disorder and includes a broad spectrum of symptoms. Broadly, the symptoms of schizophrenia are commonly divided in three main categories (Andreasen, 1995; Andreasen and Olsen, 1982; Green et al., 2000):

- *Positive symptoms* refer to psychotic features and includes hallucinations, delusions as well as distortions of reality and perception of the world.
- *Negative symptoms* refer to a reduction, or loss, of normal functions and are often presented as anhedonia, blunted affect, apathy, avolition, alogia and social withdrawal.
- *Cognitive deficits* include impairment of memory, attention, executive function as well as lack of judgment or insight.

Generally, positive symptoms occur in episodes, while the intensity of those episodes declines over time. Conversely, the negative symptoms and cognitive deficits persist, and might worsen as the disease progresses (Andreasen, 1995; Carpenter and Buchanan, 1994).

1.1.2 Risk factors

Explaining the occurrence of schizophrenia have proved to be of no simple matter. Risk factors for developing schizophrenia include both genetic and environmental factors, most likely interacting in a sophisticated fashion (Tsuang, 2000). For the genetic influence, familial studies have provided strong evidence. However, the genetic susceptibility appears not restricted to a single or a few genes. Instead, a complex interaction between an abundance of risk genes seems more likely. Thus, genome-wide association studies (GWAS) have identified more than 100 genetic loci associated with schizophrenia, highlighting the genetic complexity involved in the disorder (Foley et al., 2017; Harrison, 2015). Nevertheless, studies using monozygotic twins indicate heritability rates as high as 80% (Cannon et al., 1998; Sullivan et al., 2003), which undeniably points to a profound genetic contribution. However, the lack of complete concordance suggests a role for environmental factors as well. Interestingly, dizygotic twins are twice as likely to be affected compared to non-twin siblings, even though they theoretically share the same number of genes (Tsuang, 2000). Thus, the prenatal environment may be of importance and factors such as prenatal infection, maternal stress and malnutrition, obstetric complications and smoking during pregnancy have all been shown to increase the risk of developing schizophrenia in the offspring (Brown & Derkits, 2010; Mortensen et al., 1999; Susser & Lin, 1992; Van Os & Selten, 1998; Yolken & Torrey, 2008). In particular, prenatal infection and the role of the immune system, both prenatally and later in life, have gained increasing attention and is supported by genetic studies where several immune-related genes have been associated with schizophrenia (Aberg et al., 2013; Müller et al., 2015; Shi et al., 2009). Beyond pure biology, a number of psychosocial risk factors have been described, such as social isolation, lower social status, migrations, urban living and drug abuse (Cantor-Graae and Selten, 2005; Di Forti et al., 2009; Kirkbride et al., 2007; Pedersen and Mortensen, 2001; Stilo and Murray, 2010; Susser and Bresnahan, 2002). However, when it comes to many of the environmental risk factors, it is important to mention that correlation does not necessarily imply causation, and the etiology behind schizophrenia remains largely unanswered. Instead, pharmacological advances have been more impactful in generating hypotheses to explain the pathophysiological mechanisms of schizophrenia.

1.1.3 Pharmacological aspects

1.1.3.1 The dopamine hypothesis and the first-generation antipsychotics

The original dopamine hypothesis postulate that the underlying mechanism giving rise to the symptoms of schizophrenia is through a hyperactive dopamine system (Carlsson and Lindqvist, 1963). The hypothesis was originally based on the actions of the first antipsychotic drugs, commonly termed typical or first-generation antipsychotics (FGA), such as chlorpromazine and haloperidol, which successfully ameliorated the psychotic symptoms in patients suffering from schizophrenia. Subsequently, it was discovered that the FGAs owed their efficacy to their ability to bind and inhibit dopamine receptors, in particular the D_2-receptor (Carlsson and Lindqvist, 1963; Creese et al., 1996; Seeman and Lee, 1975). The hypothesis was strengthened by the findings that amphetamine, known to cause excessive dopamine release, could produce psychotic features in healthy volunteers and intensify symptoms in patients (Angrist et al., 1974; Laruelle et al., 1996; Snyder, 1973). This led to the belief that hyperactive dopaminergic signaling was the underlying cause of schizophrenia. However, the hypothesis falls short in explaining the negative and cognitive symptoms. The FGAs were unsuccessful in treating these symptom domains, and amphetamine appeared to produce mainly psychotic symptoms. Consequently, the dopamine hypothesis was revised to propose a dysregulation of dopamine signaling, rather than an overall hyperactivation (Abi-Dargham and Laruelle, 2005; Breier, 1999; Davis et al., 1991; King, 1998). Thus, the positive symptoms are believed to arise from increased dopaminergic signaling along the mesolimbic pathway, from the ventral tegmental area (VTA) to subcortical limbic structures, e.g., nucleus accumbens (NAc; Carlsson et al., 2001). In contrast, the negative and cognitive symptoms are believed to arise from decreased dopaminergic signaling along the mesocortical pathway, from the VTA to cortical areas, and in particular, the prefrontal cortex (PFC; Slifstein et al., 2015). Sadly, due to excessive dopamine receptor blockade, the FGAs are associated with extrapyramidal symptoms (EPS), arising from blockade of nigrostriatal D_2-receptors (Marsden and Jenner, 1980).

1.1.3.2 Clozapine, the first second-generation antipsychotic

The dopamine hypothesis was further questioned when the first atypical, or second-generation antipsychotic (SGA) clozapine was introduced in 1972. Clozapine appeared superior to FGAs as it was successful in treating not only the positive symptoms but the other symptoms as well, while producing essentially no EPS (Breier et al., 1994; Claghorn et al., 1987; Hagger et al., 1993). While the FGAs display a D_2-receptor occupancy above 70% at

therapeutic doses, clozapine has a much lower affinity for the D_2-receptor (~40% at therapeutic doses) and as such, D_2-receptor occupancy cannot fully account for clozapine's efficacy (Farde et al., 1992; Kapur and Seeman, 2001). Clozapine has a very broad binding profile and binds to several different receptors, including various dopamine, serotonin, noradrenaline, acetylcholine and histamine receptors (Brunello et al., 1995; Bymaster et al., 2003; Coward, 1992; Meltzer and Huang, 2008; Snyder et al., 1974). In addition, clozapine has been shown to interact with the γ-aminobutyric acid (GABA) receptor and the ionotropic glutamatergic *N*-methyl-D-aspartate (NMDA) receptor (Arvanov et al., 1997; Arvanov and Wang, 1999; Jardemark et al., 2003; Millan, 2005; Ninan et al., 2003; Squires and Saederup, 1997). Despite, or perhaps rather because of, its complex pharmacological profile, clozapine is still considered the most effective treatment for schizophrenia available (Nucifora et al., 2017). In particular, clozapine has proven effective for treatment-resistant schizophrenia and is the only antipsychotic drug with a documented effect on suicide prevention in schizophrenia (Griffiths et al., 2014; Kane et al., 1988). Despite its superior efficacy, clozapine is underutilized as a number of severe adverse effects limit its use, including sedation, metabolic syndrome and increased risk of cardiovascular complications (Gardner et al., 2005). Furthermore, clozapine is associated with life-threatening agranulocytosis, and patients require careful and regular monitoring of white blood cell counts for the duration of the treatment (Idänpään-Heikkilä et al., 1977; Krupp and Barnes, 1992).

Many efforts have been made in dissecting the mechanisms of clozapine and replicating its treatment efficacy while limiting the side-effects. Many SGAs have since been developed with varying degrees of efficacy and side-effects. However, clozapine still stands superior.

1.1.3.3 The glutamate hypothesis and the NMDA receptor

Although the role of dopamine should not be disregarded and remains one of the main hallmarks for schizophrenia, the success of clozapine implicates that dopamine dysregulation could not solely explain the underlying causes of schizophrenia. Consequently, it was later demonstrated that NMDA receptor antagonists, such as ketamine and phencyclidine were able to closely mimic the symptoms of schizophrenia in healthy individuals (Krystal et al., 1994) and augment symptoms in patients suffering from schizophrenia (Lahti et al., 1995), similar to that of amphetamine. But in contrast to the amphetamine-induced psychosis, NMDA receptor antagonists can produce the full spectrum of schizophrenia symptoms (Krystal et al., 2005; Lahti et al., 2001). Consequently, these discoveries formed the basis of the glutamate deficiency hypothesis of schizophrenia, stating that disruptions in glutamatergic

signaling, in particular through the NMDA receptor, could account for the symptoms of schizophrenia (Krystal et al., 2005). The hypothesis has since been strengthened further by genetic studies, implicating both genes encoding for NMDA receptor proteins and proteins necessary for its downstream signaling (Harrison, 2015). In addition, post-mortem studies have found reduced expression and protein levels of NMDA receptor subunits in the brain of patients with schizophrenia (Catts et al., 2016; Weickert et al., 2013). Taken together, there is strong evidence for a glutamatergic deficiency in schizophrenia, and in particular with regard to NMDA receptor dysfunction.

Accordingly, glutamatergic deficiency may directly account for the negative and cognitive symptoms through cortical dysconnectivity, and a disrupted glutamate signaling may indirectly cause a downstream dysregulation of dopamine signaling (Carlsson et al., 2001; Javitt, 2007; Jentsch and Roth, 1999). Thus, the dopamine and glutamate hypotheses are not necessarily mutually exclusive as VTA dopamine neurons appear tightly regulated by glutamatergic afferents through the NMDA receptor, either directly or, more likely, indirectly through GABAergic interneurons (Erhardt et al., 2002; Linderholm et al., 2016; Schwieler et al., 2008). For instance, cortical pyramidal cells have been suggested to innervate the VTA both directly, and indirectly through inhibitory GABAergic interneurons, to regulate firing of VTA dopamine neurons via the NMDA receptor (Carr and Sesack, 2000; Erhardt and Engberg, 2002; Kalivas et al., 1993; Patton et al., 2013; Phillipson, 1979; Sesack et al., 1989; Tan et al., 2012; Van Zessen et al., 2012). In this case, NMDA receptor hypofunction would cause a reduced GABAergic influence on dopaminergic cells, consequently leading to a disinhibition of dopamine. Accordingly, clinical studies have found reduced levels of GABA in cerebrospinal fluid (CSF) of patients suffering from schizophrenia, which correlates to symptom severity (Orhan et al., 2018). Notably, glutamatergic signaling appears to regulate the mesolimbic and mesocortical dopamine circuits differently. Thus, NMDA receptor blockade causes a disinhibition of mesolimbic dopamine cells, through inhibition of GABAergic interneurons, and a subsequent increase in dopamine release in limbic areas, such as NAc (Jentsch et al., 1998b; Jentsch and Roth, 1999). In contrast, NMDA receptor inhibition reduces the activity of mesocortical dopamine signaling, causing a decrease of dopamine release in cortical areas such as the PFC (Jentsch et al., 1998a, 1997b, 1997a; Jentsch and Roth, 1999).

Interestingly, clozapine has been shown to interact with the NMDA receptor (section 1.1.3.2), an action that could contribute to its superior efficacy. Thus, electrophysiological studies point to an interaction with the obligatory glycine site of the NMDA receptor (Millan, 2005),

where clozapine appears to have a partial agonistic effect (Schwieler et al., 2008, 2004). Although the exact mechanism is subject to further investigation, clozapine has been suggested to inhibit sodium-coupled neutral amino acid transporter 2, responsible for transporting glycine from the synaptic site, causing an increase in extracellular glycine levels (Javitt et al., 2005). Accordingly, different strategies for enhancing NMDA receptor signaling have been proposed and tested as treatment options for schizophrenia (Balu, 2016; Balu and Coyle, 2015). However, robust evidence for their clinical efficacy is lacking.

1.2 THE KYNURENINE PATHWAY

With regards to glutamatergic signaling and schizophrenia, one of the most exciting finding in recent years is the impact of the kynurenine pathway (Erhardt et al., 2017b). Interestingly, in this pathway several neuroactive substances are produced which have been demonstrated to interact and influence glutamatergic signaling (Schwarcz, 2016).

The kynurenine pathway (Figure 1) is the primary route of tryptophan degradation throughout the body, including the brain (Guidetti et al., 1995; Schwarcz and Stone, 2017). Although tryptophan degradation is essential for producing serotonin, only a minor fraction of tryptophan is metabolized this way (Gál and Sherman, 1980). Indeed, the kynurenine pathway accounts for as much as 90-95% of all tryptophan metabolism (Gál and Sherman, 1980; Leklem, 1971). The initial and rate-limiting step of the kynurenine pathway is the oxidation of tryptophan into *N*-formylkynurenine by indoleamine 2,3-dioxygenase (IDO) or tryptophan 2,3-dioxygenase (TDO). *N*-formylkynurenine is then converted by formamidase into the central component of the pathway, kynurenine. From here, the pathway is commonly divided into two main branches: the kynurenic acid (KYNA) producing branch and the quinolinic acid (QUIN) producing branch (Schwarcz et al., 2012). For the first branch, kynurenine is transformed into KYNA, which is not further metabolized, by one of the kynurenine aminotransferase (KAT) I-IV enzymes (Han et al., 2010). Of note, KAT II appears to be the main responsible enzyme, accounting for about 75% of KYNA production under normal physiological conditions (Guidetti et al., 1997; Schmidt et al., 1993). As such, specific inhibition of KAT II reliably and robustly lowers the levels of KYNA (Kozak et al., 2014; Linderholm et al., 2016; Rossi et al., 2008). For the latter branch, kynurenine is metabolized into 3-hydroxykynurenine (3-HK) by kynurenine 3-monooxygenase (KMO; Chiarugi et al., 1995) and subsequently into 3-hydroxyanthranilic acid (3-HANA) by kynureninase. Alternatively, kynurenine can be metabolized by kynureninase into anthranilic acid, which, in turn, is rapidly transformed into 3-HANA by non-enzymatic oxidation (Baran

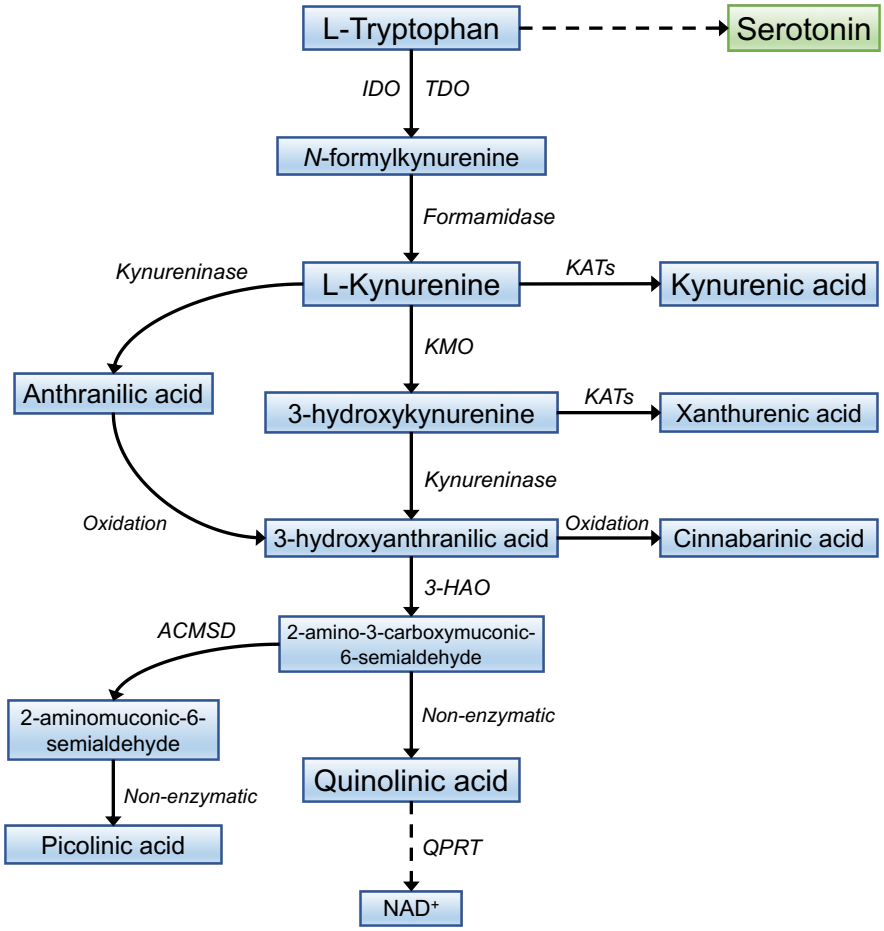

Figure 1. The kynurenine pathway of tryptophan degradation

and Schwarcz, 1990). In addition, 3-HK and 3-HANA can be converted into xanthurenic acid by the KATs or cinnabarinic acid by non-enzymatic oxidation, respectively (Fazio et al., 2017). Subsequently, 3-HANA is metabolized into QUIN, via 2-amino-3-carboxymuconic-6-semialdehyde by 3-hydroxyanthranilate oxygenase and non-enzymatic reactions (Foster et al., 1986). Alternatively, the intermediate can form picolinic acid through 2-amino-3-carboxymuconic-6-semialdehyde decarboxylase (Pucci et al., 2007). Although QUIN is sometimes considered an end-metabolite, it can be further degraded into NAD^+.

Under normal physiological conditions, the main portion of kynurenine is metabolized via the KMO enzyme into QUIN and further degraded into NAD^+. However, the KMO enzyme has a Michaelis-Menten constant (Km) in the micromolar range ($Km \approx 20$ μM) and becomes quickly saturated (Bender and McCreanor, 1985). In contrast, the KAT enzymes have a Km in the millimolar range and can rapidly turn kynurenine into KYNA (Okuno et al., 1991). As a consequence, increased activation of the kynurenine pathway leads to more kynurenine available for the KAT enzymes, which are substrate-dependent and shunts the pathway into the KYNA producing branch (Giorgini et al., 2013; Schwarcz and Pellicciari, 2002). In

addition, KYNA does not pass the blood-brain barrier, and do not, in contrast to QUIN, seem to undergo any further degradation (Schwarcz et al., 2012). Instead, clearance of KYNA is dependent on slow organic anion transporters (Fukui et al., 1991; Uwai et al., 2012) and easily accumulates in the brain as a result of activation of the kynurenine pathway (Schwarcz et al., 2012; Stone et al., 2012).

1.2.1 Kynurenine pathway in the brain

Within the brain, the two main branches of the kynurenine pathway are spatially separated as microglia express the KMO enzyme and produce QUIN, while astrocytes express the KAT enzymes and are the main producers KYNA (Guillemin et al., 2001; Schwarcz et al., 2012). Although recently, this two-compartment concept has been challenged as evidence has emerged that certain neurons, such as GABAergic interneurons, express KAT enzymes and could produce KYNA by themselves (Herédi et al., 2017). However, the significance of KYNA produced by these neurons are subject to further investigations.

As previously mentioned, several metabolites produced by the kynurenine pathway has been found to be neuroactive. Best described thus far, is the action of the two end-metabolites of the two main branches, KYNA and QUIN. In this regard, KYNA acts as an antagonist at the obligatory glycine-site of the NMDA receptor ($IC_{50} \approx$ 8-15 μM) and the α7-nicotinic acetylcholine (α7nACh) receptor ($IC_{50} \approx 7$ μM; Birch et al., 1988; Hilmas et al., 2001; Kessler et al., 1989; Parsons et al., 1997). At higher concentrations, KYNA is also able to block the glutamate recognition site of the NMDA receptor ($IC_{50} \approx$ 200-500 μM) as well as AMPA and kainite receptors at millimolar concentrations (Kessler et al., 1989; Perkins and Stone, 1982). In contrast, QUIN has an agonistic action at the NMDA receptor and promotes release and inhibits re-uptake of glutamate (Stone, 1993; Stone and Perkins, 1981; Tavares et al., 2002). Due to this action, QUIN is broadly considered as a neurotoxin and possess potent excitotoxic properties (Guillemin, 2012). Contrarily, KYNA, through its antagonistic effect on the NMDA receptor, is considered neuroprotective, and has been suggested to play an essential role in limiting excitotoxic damage, for example during a stroke event (Foster et al., 1984; Mangas et al., 2017).

Furthermore, the lesser studied xanthurenic acid and cinnabarinic acid appear to have an agonistic effect on the metabotropic glutamate (mGlu) 2/ 3 receptor and mGlu4 receptor, respectively (Fazio et al., 2017). In addition, picolinic acid has been suggested to modulate glutamate release and counteract the neurotoxic effects of QUIN (Beninger et al., 1994; Tonohiro et al., 1990; Vrooman et al., 1993).

1.2.2 Regulation of the kynurenine pathway

The initial enzymes, IDO and TDO, are the rate-limiting enzymes and their expression and activity are crucial in regulating the overall activity of the kynurenine pathway (Badawy, 2017). These enzymes are known to be influenced by the immune system where pro-inflammatory cytokines induce their expression (Campbell et al., 2014). For example, interferon (IFN)-γ has been shown to induce expression of IDO (Alberati-Giani et al., 1996; Munn and Mellor, 2016) while interleukin (IL)-1β induces TDO expression (Sellgren et al., 2016), leading to a subsequent increase in kynurenine production. Conversely, anti-inflammatory cytokines, such as IL-4, negatively affect the expression of IDO (Musso et al., 1994). Treatment with the endotoxin lipopolysaccharide (LPS) is known to induce expression of IDO through the induction of pro-inflammatory cytokines, and cause an elevation in kynurenine production (Dostal et al., 2018; O'Connor et al., 2009). Furthermore, TDO expression appears sensitive to hormonal influence, and transcription can be induced by glucocorticoids as the *TDO* gene contains glucocorticoid-responsive elements (Danesch et al., 1983). Moreover, TDO expression appears positively regulated by glucagon, but negatively regulated by insulin and adrenaline (Badawy, 2017; Nakamura et al., 1987). In addition, TDO responds to substrate availability as its expression is positively regulated by tryptophan (Badawy, 2017).

Similar to the initial enzymes, KMO appears influenced by the immune system where IL-1β and IFN-γ has been shown to induce transcription (Alberati-Giani et al., 1996; Zunszain et al., 2012). Additionally, expression of KMO increases following treatment with LPS together with an elevation of brain IL-6 (Connor et al., 2008; Molteni et al., 2013).

With regards to the production of KYNA, the most salient rate-limiting factor is the availability of kynurenine, which is dependent on the activity of the kynurenine pathway, including KMO activity (Erhardt et al., 2017b; Giorgini et al., 2013). However, there is evidence of KAT expression being sensitive to immune stimulation, and KAT enzymes in astrocytes appears more sensitive in this regard (Alberati-Giani et al., 1996; Guillemin et al., 2001; Song et al., 2018). However, further studies are needed to unravel the link between the KAT enzymes and immune system and determine its functional significance.

Intriguingly, extracellular KYNA levels also appear sensitive to neuronal input (Gramsbergen et al., 2002). In particular, dopamine appears to have a regulatory role on extracellular KYNA levels as microdialysis studies reveal that D-amphetamine cause a reduction in brain KYNA (Rassoulpour et al., 1998). The exact mode by which KYNA is released into the extracellular

space is still unknown. However, the location of KYNA in astrocytes, tightly connected to neuronal synapses, may suggest that KYNA could be an essential endogenous regulatory player in neuronal transmission.

The kynurenine pathway and production of QUIN and KYNA in the brain is highly influenced by peripheral kynurenine metabolism (Schwarcz et al., 2012). Although most of the neuroactive metabolites, such as QUIN and KYNA, are polar and do not readily pass the blood-brain barrier, the availability of those that can, e.g. tryptophan, kynurenine and 3-HK, are vital for central kynurenine metabolism (Fukui et al., 1991). Indeed, around 60% of all kynurenine metabolized in the brain originates from the periphery (Gál and Sherman, 1980). Consequently, peripheral metabolism of tryptophan and kynurenine can facilitate the activity of the kynurenine pathway in the brain by increasing available substrates essential for production of KYNA and QUIN (Agudelo et al., 2014).

Although the regulation of the kynurenine pathway is a complicated matter, and many stones are left unturned, one of the strongest influences appear to be that of the immune system. The interaction between the kynurenine pathway and the immune system is in line with findings suggesting that inflammation might be one of the responsible factors for schizophrenia (Müller, 2018; Söderlund et al., 2009). Here, the kynurenine pathway offers a bridge between immune activation and neuronal transmission through the endogenous NMDA receptor antagonist KYNA (Erhardt et al., 2017b).

1.2.3 The kynurenine pathway in schizophrenia

Due to its inhibitory action on the NMDA receptor, KYNA is of particular interest to schizophrenia. In this regard, an activated or dysregulated kynurenine pathway, leading to an increase in brain KYNA levels, could give rise to the symptoms of schizophrenia (Erhardt et al., 2017b). Accordingly, elevated levels of KYNA has repeatedly been shown in CSF ((Erhardt et al., 2001a; Linderholm et al., 2012; Nilsson et al., 2005; Plitman et al., 2017) and post-mortem tissue (Sathyasaikumar et al., 2011; Schwarcz et al., 2001) in patients with schizophrenia. These findings have, however, been hard to replicate in peripheral tissue (Plitman et al., 2017), although this discrepancy can be explained by KYNAs inability to cross the blood-brain barrier.

As an endogenous NMDA receptor antagonist, KYNA has a profound impact on neuronal signaling in the brain. Given the prominent role of dopamine in schizophrenia pathophysiology, it is noteworthy that there is a positive correlation between KYNA levels and the dopamine metabolite homovanillic acid (Nilsson et al., 2007; Sellgren et al., 2016).

Further, electrophysiological studies have repeatedly shown that KYNA potently regulates dopamine cell activity *in vivo* through its inhibitory action on the NMDA receptor. Thus, increased endogenous brain KYNA is associated with elevated spontaneous firing and activity of dopamine cells, and importantly, decreased endogenous levels slow down the firing and decrease the activity of dopamine cells (Erhardt et al., 2001b, 2003; Erhardt and Engberg, 2002; Linderholm et al., 2007, 2016; Nilsson et al., 2006; Schwieler et al., 2006; Schwieler and Erhardt, 2003; Tufvesson-Alm et al., 2018). In addition, KYNA appears to directly regulate striatal dopamine release through terminal α7nACh receptors. Notably, acute elevation of KYNA seemingly reduces dopamine release in the striatum, possibly through blockade of terminal α7nACh receptors (Giménez-Gómez et al., 2018; Rassoulpour et al., 2005). However, lasting elevation of brain KYNA levels increases striatal dopamine and dopamine responsivity to amphetamine (Olsson et al., 2009, 2012a).

Evidence supporting the role of KYNA in schizophrenia has also been found at a genetic level. For instance, genetic variations and reduced expression and activity of KMO has been linked to increased CSF levels of KYNA, and associated to schizophrenia and psychotic features in bipolar disorder (Aoyama et al., 2006; Ekelund et al., 2004; Holtze et al., 2012, 2011; Lavebratt et al., 2014; Sathyasaikumar et al., 2011; Wonodi et al., 2011). In addition, increased expression of brain TDO has been shown post-mortem in patients with schizophrenia (Miller et al., 2006, 2004). In agreement, a recent study by Sellgren et al. from patients with bipolar disorder experiencing psychosis, exquisitely show how a genetic variation, linked to the expression of sorting nexin 7, regulates the processing and secretion of IL-1β, subsequently leading to increased TDO expression and, as a result, increased KYNA (Sellgren et al., 2016). In a similar manner the gene encoding for G-protein coupled receptor kinase (GRK) 3 has been implicated in both schizophrenia and bipolar disorder (Bychkov et al., 2011; Shaltiel et al., 2006), where data presented in this thesis proposes that reduced expression of GRK3 is associated to increased KYNA and psychosis, through increased IL-1β formation.

Taken together, evidence for the involvement of KYNA in the pathophysiology of schizophrenia, as well as psychotic features in other disorders (e.g., bipolar disorder), is abundant. Although the underpinnings for centrally elevated KYNA levels are not fully explored, a reoccurring and common denominator appears to be brain immune activation.

1.3 IMMUNOLOGICAL ASPECTS

Several major psychiatric disorders, including schizophrenia, has been proposed to involve an inflammatory component (Müller, 2018). Indeed, some of the strongest associated genes in schizophrenia appears to be related to the immune system (Aberg et al., 2013) and clinical studies have revealed an elevation of the pro-inflammatory cytokines IL-1β and IL-6 in CSF of patients with schizophrenia (Sasayama et al., 2013; Schwieler et al., 2015; Söderlund et al., 2009). Moreover, post-mortem studies have revealed that patients exhibit increased mRNA levels of IL-1β, IL-6, IL-8 and tumor necrosis factor (TNF)-α in the frontal cortex (Fillman et al., 2013; Rao et al., 2013). Furthermore, expression of toll-like receptor-4, known to induce the kynurenine pathway, is increased in the post-mortem brains of patients with schizophrenia (MacDowell et al., 2017). Due to the limited access to CSF and post-mortem material, the number of studies is limited. However, studies have pointed towards a peripheral immune activation in schizophrenia as well, although conflicting results exists (Rodrigues-Amorim et al., 2018). An immune activation can be seen already in the early stages of schizophrenia (Upthegrove et al., 2014) and in individuals with a clinically high risk of developing psychosis (Khoury and Nasrallah, 2018). Interestingly, individuals receiving the tetracyclic antibiotics minocycline or doxycycline during adolescence seem to run a lower risk of developing schizophrenia later in life (Sellgren et al., 2019). Furthermore, epidemiological studies have shown that prenatal and early-life infections are associated with an increased risk of developing schizophrenia later in life (Canetta and Brown, 2012; Karlsson, 2003; Yolken and Torrey, 2008). Interestingly, maternal elevation of IL-8 has been associated with the risk of developing schizophrenia, regardless of infection (Brown et al., 2004), indicating that the crucial factor is not infection per se, but the resulting immune activation.

1.4 ANIMAL MODELS OF SCHIZOPHRENIA

Experimental studies using animals have provided vital insight into the etiology and pathophysiology of schizophrenia, including the role of immune activation and the kynurenine pathway. Undeniably, correct and valid modeling is fundamental to accurately evaluate new potential treatment strategies.

1.4.1 Modulation of the kynurenine pathway

Several strategies to influence the activity of the kynurenine pathway and production of KYNA exists, mainly through pharmacological or genetic manipulation. Pharmacological

manipulation includes administration of kynurenine, cyclooxygenase (COX) inhibitors, and drugs targeted at specific kynurenine pathway enzymes, such as KMO or KAT II.

1.4.1.1 Kynurenine treatment

Administration of kynurenine, especially in a subchronic manner, has proven a reliable method to elevate brain KYNA levels. Since the production of KYNA is mainly dependent on substrate and a substantial portion of kynurenine originates from the periphery (see section 1.2.2) this appears, dependent on dosage, as a seemingly natural elevation of KYNA production. Notably, subchronic administration of kynurenine augments the response to amphetamine in rats, reflected as increased locomotor activity and increased dopamine firing and release in response to amphetamine challenge compared to controls (Olsson et al., 2009, 2012a). This is in analogy to what is observed in patients with schizophrenia (Laruelle et al., 1996; Laruelle and Abi-Dargham, 1999). In addition, a single administration of kynurenine to rats disrupts prepulse inhibition (PPI), an acoustic startle reflex test measuring disrupted sensorimotor gating (Geyer et al., 2001; Geyer and Swerdlow, 1998), an effect that can successfully be reversed by treatment of antipsychotic drugs (Erhardt et al., 2004). Additionally, acute kynurenine treatment causes cognitive deficits, such as impaired spatial memory and contextual learning (Chess et al., 2009, 2007). Intriguingly, kynurenine treatment during adolescence causes disturbances in social behavior in the adult rat (Trecartin and Bucci, 2011), indicating that the effect goes beyond that of the initial acute effect and may influence brain development during critical periods.

1.4.1.2 Cyclooxygenase inhibitors

Interestingly, COX-1 and -2 inhibitors appear to produce opposite effects on brain KYNA levels. In this regard, COX-1 inhibitors increases, while COX-2 inhibitors reduces brain KYNA levels (Schwieler et al., 2005). Accordingly, COX-1 inhibitors causes an increase in dopamine cell activity, while COX-2 inhibitors decrease the activity in rodents as a result of altered KYNA levels (Schwieler et al., 2008, 2006). The exact action by which COX inhibitors modulate the kynurenine pathway and KYNA levels is still unclear, although hints have recently emerged. For instance, COX-2 inhibitors has been shown to inhibit IDO (Basu et al., 2006; Lee et al., 2009), and, recently, the COX-2 inhibitor parecoxib, was characterized as a KAT II-inhibitor (Zakrocka et al., 2019). Moreover, the COX-1 inhibitor diclofenac was recently identified as an inhibitor of KMO (Shave et al., 2018).

1.4.1.3 Targeted inhibition and deletion of KMO

Similar to kynurenine treatment or COX-1 inhibitors, specific inhibitors of KMO, such as PNU 156561A, reliably increases brain KYNA levels. Thus, administration of PNU 156561A increases dopamine cell activity (Erhardt et al., 2001b; Erhardt and Engberg, 2002) and causes deficits in PPI in rats (Erhardt et al., 2004). Accordingly, targeted deletion of KMO (KMO K/O) in mice produces elevated levels of KYNA (Giorgini et al., 2013), and schizophrenia-like behaviors (Erhardt et al., 2017a). The KMO K/O mice show increased sensitivity to amphetamine, deficits in social interaction, anxiety-like behavior, and cognitive impairments. The model is anchored to clinical data, which have shown reduced expression and genetic variation in the gene encoding for KMO in psychosis (Aoyama et al., 2006; Ekelund et al., 2004; Holtze et al., 2011; Lavebratt et al., 2014; Sathyasaikumar et al., 2011; Wonodi et al., 2011). Interestingly, inhibition or deletion of KMO does not notably affect the levels of QUIN in the brain. Thus, KMO K/O mice show a reduction of QUIN levels of about 20% compared to wild-type (WT), likely due to increased production of anthranilic acid which can be converted to QUIN, surpassing the KMO step and compensating for the loss of KMO (Clark et al., 2005; Giorgini et al., 2013).

1.4.2 Models of inflammation

Animal models of inflammation have aided substantially in understanding the mechanisms by which immune activation leads to activation of the kynurenine pathway, and behavioral disturbances relevant to psychiatric disorders. In addition, these models have provided further insight into early-life exposure to infection or inflammation as well as how it affects the adult animal (Zuckerman and Weiner, 2005). For example, neonatal infection with influence A virus leads to schizophrenia-like symptoms in the adult mouse, where both disruptions in PPI and enhanced locomotor response to amphetamine has been observed (Asp et al., 2010; Liu et al., 2014). Interestingly, treatment with kynurenine during the neonatal period produces the same phenotype (Liu et al., 2014), suggesting a role of the kynurenine pathway and elevated KYNA during development. Furthermore, maternal treatment of poly I:C, used to mimic a viral infection, causes enhanced response to the NMDA receptor antagonist MK-801 in the adult rat offspring (Zavitsanou et al., 2014). This effect appeared abolished by treatment of COX-2 inhibitors during early adolescence, again indicating a role for the kynurenine pathway during critical times of development.

Furthermore, inflammation induced by LPS has been well characterized to induce behavioral disturbances lasting beyond the initial sickness-behavior (Dantzer et al., 2008; Remus and

Dantzer, 2016). Normally, the sickness-behavior declines after 2-6 hours, while depressive-like behavior can be observed at least 24 hours after a single administration of LPS. The depressive-like behavior appears to be caused by activation of the kynurenine pathway, where induction of IDO has been proposed as a potential mechanism (O'Connor et al., 2009; Salazar et al., 2012). In this regard, activation of the kynurenine pathway by a single LPS challenge leads to elevation of QUIN, which through its agonistic effect on the NMDA receptor is thought to produce the depressive-like phenotype in mice (Cui et al., 2019; Murrough et al., 2017; O'Connor et al., 2009; Salazar et al., 2012; Walker et al., 2013). Intriguingly, dual administration of LPS, rather than a single, induces the kynurenine pathway in a different manner, causing a robust and lasting increase in brain KYNA levels (Larsson et al., 2016). Moreover, dual administration of LPS induce neurochemical changes such as increased dopamine and serotonin turn-over (Larsson et al., 2016), and induces neurogranin phosphorylation in the PFC, consistent with findings from mice with a pharmacological elevation of brain KYNA (Oliveros et al., 2017b). Mice receiving dual administration of LPS also show lasting cognitive deficits associated with learning (Oliveros et al., 2017b; Peyton et al., 2019). Although further studies are needed to fully characterize the dual administration LPS model, it offers an exciting opportunity for studying the inflammatory component leading to increased brain KYNA levels and aberrant behavior.

2 AIMS

Overall aim of the thesis

Provide a basis for the development of new treatments for patients with schizophrenia, with focus on the kynurenine pathway.

Specific aims

1) Characterize putative animal models with regards of behavior and electrophysiological properties.

2) Investigate the impact of immune activation on the kynurenine pathway in the brain.

3) Understand how the kynurenine pathway interacts with existing antipsychotic drugs with regards to dopaminergic neurotransmission.

4) Characterize putative antipsychotic drugs targeting the kynurenine pathway with regards of dopaminergic neurotransmission.

5) Identify metabolomic changes in patients that may indicate the underlying processess leading to psychosis.

6) Identify a metabolomic fingerprint that may aid diagnosis and predict efficacy of antipsychotic treatment in patients with schizophrenia.

3 MATERIAL AND METHODS

3.1 ANIMALS

All animals were group housed with water and food available ad libitum. Environmental conditions were checked daily and maintained with a constant temperature (25°C) and humidity between 40%-60% in a room with a regulated 12 h light/dark cycle (lights on at 06:00). Experiments were approved by and performed in accordance with the guidelines of the Ethical Committee of Northern Stockholm, Sweden, and University of Maryland, Baltimore Institutional Animal Care and Use of Laboratory Animals. All efforts were made to minimize the number of animals used and to optimize their well-being.

For experiments involving mice adult FVB/N, c57bl/6J, KMO K/O and GRK3 K/O were used and were breed at our animal facility. For experiments involving rats, adult Sprague-Dawley rats were obtained from Janvier labs.

3.1.1 Transgenic mice

Mice with a targeted deletion of the gene encoding KMO (KMO K/O; Giorgini et al., 2013) on a FVB/N background were received from Maryland Psychiatric Research Center, University of Maryland, Baltimore, MD, USA.

Mice with a targeted deletion of the gene encoding for Grk3 (GRK3 K/O) were obtained from the Jackson Laboratory (Bar Harbor, ME, USA) with a c57Bl/6J background.

The breeding of transgenic mice was upheld at our animal facility.

3.2 DRUGS AND CHEMICALS

The following drugs were used: Chloral hydrate (Merck, Darmstadt, Germany), PF-04859989 (Kindly donated by Pfizer, USA), CGP-52432 (kindly donated by Dr Olpe, Novartis Pharma Inc.), methyllycaconitine (MLA, Tocris, Avonmouth, UK), isoflurane (Forene®, Abbott Scandinavia, Sweden), KYNA, D-amphetamine, Probenecid, Picrotoxin and D-cycloserine (Sigma, St. Louis, MO, USA) clozapine, minocycline (Sigma, St. Louis, MO, USA), haloperidol (Janssen Pharmaceutical, Beerse, Belgium), parecoxib (Pharmacia, Buckinghamshire, UK), Bupivacain (Marcain®, Astra Zeneca, Södertälje, Sweden). LPS (Escherichia coli serotype O111:B4, Sigma-Aldrich, lot no.: 091M4031V) was prepared fresh daily in vehicle (sterile saline) and stored at 4 °C before injection as well as Interleukin-1β, diluted in PBS (phosphate buffered saline; Sigma-Aldrich, St Louis, MO, USA).

The following chemicals were used: Zinc acetate (Sigma, St. Louis, MO, USA), sodium acetate (Riedelde Haen, Germany), perchloric acid (Kebo Lab, Stockholm, Sweden) and acetonitrile (Labasco, Partille, Sweden). [5-^{3}H]-KYN (7.1 Ci/mmol; Moravek Inc.). Lysis buffer (100 mg/ml; 150 mM NaCl, 20 mM Tris pH 7.5, 1 mM EDTA, 1 mM EGTA, 1% triton X-100), Protease inhibitor (Roche, Cat. No. 1 836 170), Phosphatase Inhibitor Cocktail 3 (Sigma, Cat. No. P0044), Phosphatase Inhibitor 2 (Sigma, cat. No. P5726), acetonitrile, calcium chloride, EDTA (ethylenediaminetetraacetate), magnesium chloride, methanol, PBS, potassium chloride, acetic acid, sodium acetate, sodium chloride, sodium metabisulfite, Tris, zinc acetate, (Sigma-Aldrich).

3.2.1 LPS treatment protocol

Animals treated with LPS received two injections i.p. (0.5 mg/kg + 0.5 mg/kg or 0.83 mg/kg + 0.83 mg/kg, for rats and mice, respectively) with 16 hours between the first and second injection. Control groups received two injections of sterile saline in equivalent doses as vehicle, with the same time schedule.

Experiments were carried out 40 hours after the first dose. Complete schedule for each experiment can be seen in figure 2. During treatment with LPS, the animals were closely monitored with regards of body weight and signs of sickness. Animals were excluded if more

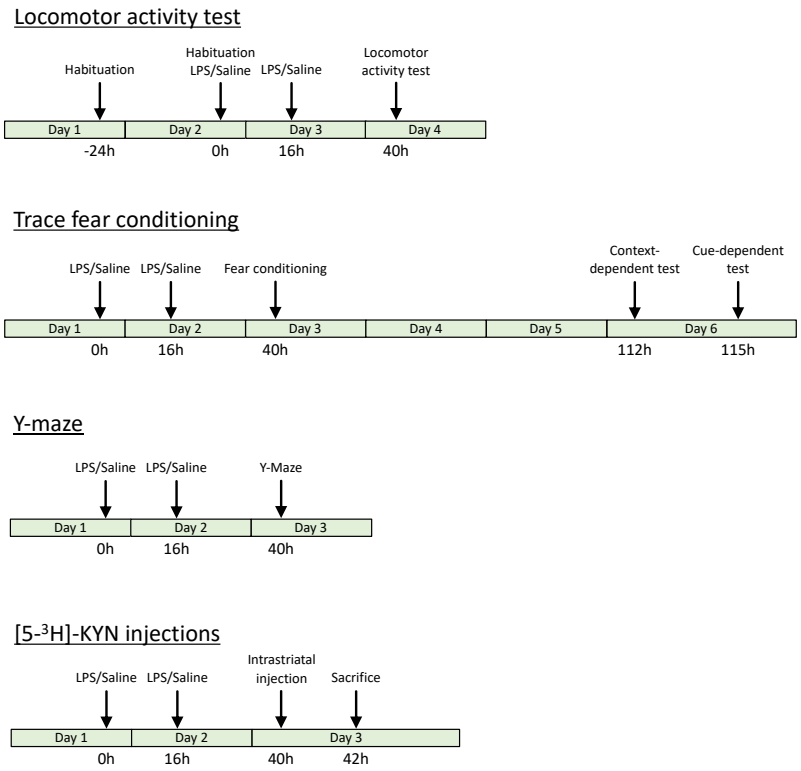

Figure 2. Schematic drawing of LPS treatments in relation to testing.

3.2.2 Radiolabeled kynurenine purification

Radiolabeled kynurenine ([5-^{3}H]-KYN) was purified using HPLC before use, as previously described (Guidetti et al., 1995). In short, [5-^{3}H]-KYN was applied to a C_{18} reverse-phase column (ESA, Bedford, MA, USA) and the radiotracer was eluted isocratically at a rate of 1 ml/min with mobile phase consisting of 0.3% glacial acetic acid and 10% acetonitrile. Kynurenine was detected using a UV detector (Applied Biosystems 785A Absorbance Detector) at 340 nm with a retention time of about 5-6 min. Fractions containing kynurenine were manually collected, aliquoted and dried under vacuum. Aliquots were stored at -80°C until use and tested for purity before each use.

3.3 IN VIVO ELECTROPHYSIOLOGY (PAPER I, II, IV)

3.3.1 Surgery

Rats and mice were anesthetized using chloral hydrate (400 mg/kg, i.p.) or, in a few control experiments (paper I), pentobarbital (60 mg/kg, i.p.). Fully anesthetized animals were mounted onto the ear bars of a stereotaxic frame (David Kopf Instruments, USA) with the head aligned horizontally in a flat-skull position. A cannula was inserted into the lateral tail vein for i.v. administration of drugs as well as additional administration of anesthesia. Throughout the experiments, body temperature was maintained at 37°C using a thermostatic heating pad and the depth of anesthesia was routinely controlled by hind paw pinching and additional anesthesia was administered if needed. The surface of the skull was exposed and hole was drilled with its center located approximately 3.0 mm anterior to the lambda and 0.7 mm lateral to the midline for rats, or 3.1 mm posterior to the bregma and 0.5 mm lateral to the midline for mice.

3.3.2 Preparation of electrode

Electrodes were produced by pulling glass capillaries (1.16 mm inner diameter; Harvard Apparatus) in a heated vertical electrode puller (Narishige, Japan). The electrode was filled with 0.5M sodium acetate saturated with Chicago Sky Blue and the tip was carefully broken under a microscope, causing an opening of approximately 1-2 μm, yielding an in vitro impedance of about 6-8 MΩ, measured in 0.9% saline at 135 Hz. For track recordings (section 3.3.5), the in vitro impedance was always between 6.5 and 7.5 MΩ in order to reduce bias caused by electrode sensitivity.

3.3.3 Extracellular single unit recording

Following surgery, an electrode was lowered using a hydraulic drive (David Kopf Instruments, USA) just above the VTA. The electrode was subsequently moved slowly down into the VTA (7.5-8.5 mm and 4.0-4.7 mm below the brain surface for rats and mice, respectively) in search of dopamine neurons. Single unit potentials were passed through a high input-impedance amplifier and filters and discriminated from background noise. Impulses were simultaneously displayed on digital storage oscilloscope, monitored on a strip chart recorder (Gould) and fed into a computer for analysis (section 3.3.6).

3.3.4 Identification of dopaminergic neurons

Putative dopamine neurons were exclusively recorded within the VTA, according to the stereotaxic coordinates of rat and mouse brain atlas (Franklin and Paxinos, 2008; Paxinos and Watson, 2005) and fulfilled the neurophysiological characteristics of dopamine cells (i.e. triphasic action potentials with a duration >2.0 ms, basal firing frequency between 1-10 Hz and with the occurrence of burst firing with a progressive decrease of spike amplitude) previously described (Grace and Bunney, 1984a, 1984b). In addition, to further confirm that recordings had been made exclusively from dopaminergic neurons, the inhibitory action of a single dose of apomorphine (0.1 mg/kg i.v.) or amphetamine (6 mg/kg, i.v.) was verified at the end of the experiment, whenever the experiment allowed.

3.3.5 Track recording

In order to determine the number of spontaneously active dopamine neurons and their firing characteristics, an electrode was lowered into the VTA as described above. The electrode was subsequently moved in a pre-determined grid-pattern (between 2.8-3.6 mm anterior to lambda and 0.7-0.9 mm lateral to the midline for rats and 3.2-2.8 mm posterior to bregma and 0.4-0.6 mm lateral to the midline) with each track separated by 200 or 100 μm for rats and mice, respectively. For each animal a minimum of three tracks were assessed.

3.3.6 Data analysis

The distribution of spikes was analyzed on line using the Spike II software. In order to avoid artifacts during sampling, the program was set to ignore time intervals below 20 ms. The onset of a burst was defined to have an inter-spike interval <80 ms and termination of a burst by the next interval >160 ms (Grace and Bunney, 1984a, 1984b). Cells were considered to be bursting if at least one inter-spike interval of a 100-spike sample was below 80 ms. The

intervals were analyzed with regards of the number of bursts occurring over a sample of 100-500 spikes and assessed as a percentage of spikes fired in bursts. Depolarization block was defined as a sudden loss of spikes followed by an unstable recovery within one minute, as a result of drug administration.

3.3.7 Drug administration and experimental protocol

In paper I, rats received a pretreatment of either methyllycaconitine (MLA; 4 mg/kg, i.p.), CGP-52432 (10 mg/kg, i.p.), picrotoxin (4.5 mg/kg, i.p.) or D-cycloserine (30 mg/kg, i.p.) before the start of the experiment. The effect of PF-04859899 (5 or 10 mg/kg) was evaluated 15-50 min after administration of pretreatment and was administered i.v. through the lateral tail vein once a dopamine neuron had been identified and baseline characteristics recorded. The firing of the dopamine cell was recorded for up to 45 min after administration of PF-04859899. In a separate set of experiments, rats were given PF-04859899 (5 mg/kg i.p.) or saline and the number of spontaneously active dopamine neurons and their firing characteristics were assessed 4-6 h after administration, through track recording.

In paper II, mice received increasing doses of haloperidol (0.05, 0.05, 0.1 and 0.2 mg/kg, i.v.) and clozapine (0.625, 1.25, 2.5 and 5.0 mg/kg, i.v.) acutely and the firing characteristics of dopamine neurons was evaluated at each dose. Parecoxib (25 mg/kg, i.v.) and minocycline (50 mg/kg, i.v.) was administered acutely in a single dose and the dopamine cells were monitored for up to 45 min. For both paper II and IV, track recordings were performed on K/O mice and compared to its respective WT mice. Following electrophysiological recordings, animals were sacrificed by an overdose of chloral hydrate and decapitation and the brains were taken out and frozen for analysis of brain kynurenine and KYNA levels (section 3.8.1).

3.4 BEHAVIOR TESTS

Behavior experiments were carried out on 3-4 months old mice. Mice were habituated to transport to the testing room and to handling by the experimenter for at least 2 days prior to the start of testing and brought to the testing room at least 30 mins prior to the test. All testing occurred between 08:30 and 16:00. In paper IV, mice were subject to multiple testing in the following order: cohort 1 - spatial novel object recognition, light-dark box, and elevated plus-maze, cohort 2 – novel object recognition, T-maze, Y-maze, locomotor activity test, cohort 3 - novel object recognition, Y-maze, T-maze, locomotor activity test. cohort 4 – Prepulse inhibition with a subset also used for microdialysis (section 3.5). A minimum of 3 days was

allowed between the tests. For paper IV, an additional separate cohort was run for locomotor activity test and one for novel object recognition. Otherwise, separate cohorts were used for each test.

3.4.1 Open-field and locomotor activity test (paper III, IV)

Open-field behavior and locomotor activity test was assessed in a Plexiglas open field arena (50×50×21.6 cm) within a solid, sound-dampened chamber. Movement was detected with two rows of infrared photocells equipped within the chamber, forming a two-layer grid over the arena (16 cells/row on each side, 3.1 cm apart) where the second layer served as a means to assess rearing activity. The breakage of a photocell beam was registered as one count by the computer. Locomotion (in cm, counted as number of consecutive beams broken in a series), horizontal activity (total count of beam breaks in the lower level), rearing activity (number of beam breaks in upper level), corner time (accumulated time, in seconds, when two peripheral beams are broken simultaneously) and central activity (number of breams of the 8x8 central beams) were analyzed. Mice were habituated to the arena for three sessions of 60 min with about 24 hours apart. During the first habituation session of the first day novelty open-field behavior was assessed (paper IV) and for the last habituation session open field behavior was used to assess anxiety-like behavior. Immediately following the third and last habituation session, d-amphetamine (5 mg/kg, i.p.) or vehicle (sterile saline in equivalent volumes) was administered, and the same parameters, as described above, were observed during a 90 min test session in order to assess the sensitivity to d-amphetamine.

3.4.2 Trace fear conditioning (paper III)

Trace fear conditioning was carried out using a fear conditioning chamber (Med Associates Inc., St. Albans, VT, USA). During training, individual mice were allowed to explore the chamber for 100 s before a tone cue (20 s, 90 dB) was presented. After an interval of 18 s following tone cue, an inescapable foot shock (2 s, 0.5 mA) was delivered through the stainless-steel rods constituting the floor of the chamber. A second tone cue-foot shock pairing was presented after a 100 s inter-trial interval and the mouse was removed from the chamber 30 s after the second shock. Three days after training, mice were return to the chamber in order to assess context and cue-dependent memory. For context-dependent memory assessment, mice were again placed in the chamber, without the presence of tone-cue or foot-shock, and the time spent freezing, defined as the absence of movement except that required for respiration, was counted automatically by the Med Associate software. Three hours after the context-test, mice were again placed in the chamber and their freezing

was recorded in a novel environment (a plastic floor covered the metal grid and a pyramidal shape was inserted in the rectangular box) but in the presence of the tone-cue. After 100 s exploration, the auditory cue was presented for 20 s followed by a 120 s inter trial interval, then another 20 s cue presented.

For this test, freezing was considered a presentation of fear and thus, the amount of freezing in the same context or after presentation of the cone-cue, a measure of their memory function.

3.4.3 Y-maze (paper III, IV)

In order to assess working memory, the continuous alternation paradigm in a Y-maze (PanLab) was used. Mice were placed in one of the arms of the Y-maze and allowed to explore freely for 5 min and their movement was recorded using a camera placed directly above the maze. Using the video, the number of spontaneous alternations was calculated as number of alternations (entering into three different arms consecutively) x 100 divided by the total number of arm entries minus 2. In addition, the number of same arm returns, alternate arm returns and total number of arm entries were calculated. As mice are curious and explorative by nature, entering already explored arms was used as a measure of working memory deficits.

3.4.4 T-maze (paper IV)

Working memory was also assessed using the rewarded alternations protocol for T-maze. Mice were placed in the starting arm (the bottom of the "T") and had the choice of going into the right or left arm, each modified to include different visual and tactile stimuli. At the end of each arm a food-cup was placed containing a reward in the form of a small cocoa puff. On the first day, mice were habituated and allowed to freely explore the maze for 5 min with unlimited rewards (one cup at a time). On day 2-4, each animal received training for 10 min where one arm was blocked and the animal need to consume the reward in the open arm before restarting and repeat the procedure with the other arm blocked off. On day 5, each animal underwent 3 trial of the test procedure, with first one arm is blocked off, followed by a free trial where the animal needs to choose the non-visited arm, containing another reward. On the sixth and last day, each animal received 10 of these trials with a delay of 60 s between sample and free phase and 15 min between each trial.

3.4.5 Spatial novel object recognition (paper IV)

Mice were habituated to an open-field arena (similar to described in 3.4.1) covered with bedding with a spatial cue presented on one of the walls in order to provide orientation for three consecutive days for 5 min per session. Two identical yellow cubes (A1 and A2) were then placed on two sides of the maze and mice were allowed to investigate both objects freely during a sample phase of 10 min. Object A2 was then moved twice 1 h and 24 h after the sample phase and mice were again allowed to investigate the objects for 5 min after the move. Time spent interacting with the object (sniffing and head dips within 5cm of the object, but not jumping or digging around the object) was calculated by through a video recording by a blinded observer using the JWatcher 1.0 software. The percent interaction time was defined as the time spent investigating the shifted object divided by the total time spent interacting with both objects (A2×100)/(A1+A2). The percent of total visits was calculated in a similair way (visits to object A2×100)/total visits (A1+A2). The test was used as a measure of spatial memory function where mice with normal function would spent more time investigating the shifted objected.

3.4.6 Novel object recognition (paper IV)

Mice were habituated to the same open-field environment as previously described (section 3.4.5). Two green wooden cylinders (A1 and A2) were placed in a similar manner and mice were allowed to investigate both objects for 5 min during a sample phase. Object A2 was then changed to a novel object (B, blue triangle) 1 hour after the sample phase and then again changed again to a novel object (C, yellow cube) 4 hours after sample phase. Animals were reintroduced to the arena after the switches for 5 min and the time spent investigating the novel object was calculated as previously described (section 3.4.5). The percent time of interaction was defined as the time spent investigating the novel object divided by the total time spent interacting with both objects (B (or C)×100)/(B+A) and the percent of total visits was calculated in the same way (visits to new object×100)/total visits (A+B (or C)).

3.4.7 Morris water maze (paper IV)

In order to assess long-term memory, the morris water maze was used. A platform (10 cm in diameter, Ugo Basile was placed 1-1.5 cm below the water surface of a round water pool (120 cm in diameter, Ugo Basile) filled with opaque water (temp. 24 ±1°C) and equipped with visual cues surrounding the pool. Mice were given 60 s to find the platform and their performance was recorded using a video camera suspended directly above the pools center.

Each mouse received 4 training trial sessions per day with the experimenter being blinded to their identities (WT or K/O). The time to reach the platform was recorded for 5 days (memory acquisition) with the starting quadrant being altered each day. During day 6, the platform was removed and the time each animal spent in the quadrant were the platform used to be was measured as compared to other quadrants (probe 1). The platform was subsequently moved to 180° to the other side of the pool and mice had to relearn its location during 3 days (reverse learning phase). On the last day, the platform was again removed and time spent in each quarter was recorded (probe 2).

3.4.8 Light-dark box (paper IV)

For evaluating an anxiety-like phenotype in mice, the light-dark box was used, consisting of a Plexiglass box (50×25×25 cm) divided equally into a black and a white compartment, separated by a partition with an opening in its center. The black compartment was covered by a lid and completely dark while the white part was open and bright. Each mouse was placed at the center, in the light part, facing away from the partition and allowed to freely explore the box for 5 min. Their movements were recorded from above using a digital video camera and time spent in the light vs. dark part and total number of transitions were scored using the JWatcher 1.0 software. It was considered that more anxious mice would prefer to stay in the dark part as it might be thought of as safer, rather than giving in to their explorative nature and spend time in the light part.

3.4.9 Elevated-plus maze (paper IV)

Anxiety-like behaviors were further evaluated using the elevated-plus maze. The maze was elevated above the ground and consisted of two open arms and two arms enclosed with walls in a plus-shape. Mice were put in the center of the maze and allowed to freely explore the maze for 5 min. The movement of the animals were recorded through a video camera mounted above the center of the maze and the time spent and number of entries into each part (open arm, closed arm and center) was analyzed using the TopScan Lite tracking software (Clever Systems, Inc., Reston, VA, USA). Here, more anxious mice were thought to prefer to stay in the closed arms instead of exploring.

3.4.10 Prepulse inhibition (paper IV)

Startle response and PPI were tested in a dual setup of ventilated and sound-attenuating commercial startle chambers (35×33×46 cm, SR-LAB™ system, San Diego Instruments, CA, USA). Within each chamber, a Plexiglas cylinder (3.7 cm in diameter) was mounted where

the mouse was placed. A piezoelectric accelerometer attached below the cylinder which detected sudden movements caused by the mouse. A loudspeaker provided the broadband background noise and acoustic stimuli while a standard computer controlled the presentations of the acoustic stimuli. The experimental session consisted of a 10-min acclimatization period with a 65 dB background noise (continuous throughout the session), followed by presentation of four trial types: a 40 ms, 120 dB startle pulse (PULSE ALONE), and three 20 ms prepulse+pulse combinations (69, 73 or 81 dB prepulses followed 100 ms later by a 120 dB stimulus (PREPULSE+PULSE). There were 12 presentations of the PULSE ALONE trial and 10 presentations of each PREPULSE+PULSE combination. Throughout the session, hidden NOSTIM trials (i.e. no acoustic stimulus) were presented in between each trial. Trial types were presented in a pseudo-random order with an average inter-trial interval of 15 s, not including the hidden NOSTIM trials. In addition, six PULSE ALONE trials were presented at the beginning to assess startle reactivity before appreciable habituation, and the end of the acoustic test session. For experiments including IL-1β injections, a brief session (20 min) was conducted every hour for 6 hours post-infusion as previously described (Gresack and Risbrough, 2011). Briefly, a 2 min acclimation period was followed by presentation of four 120 dB pulse trials and then two blocks of PREPULSE+PULSE trials. In the first block, prepulse trials varied by their prepulse intensity (69, 73, 77 dB above background; 10 of each); whereas, in the second block, prepulse trials had a constant prepulse of 73 dB but varied interstimulus intervals of 20, 120, 360 ms (four trials of each). Percent acoustic PPI from the prepulse intensity block of the test was calculated using the following formula: 100 – (avg startle of prepulse + pulse trial/avg startle pulse alone)*100.

3.5 MICRODIALYSIS (PAPER IV)

3.5.1 Surgery

Mice were anesthetizes using an induction chamber continuously ventilated with 4% isoflurane using a vaporizer (Univentor 400 Anesthesia Unit; Univentor Ltd, Zejtun, Malta). Once full anesthesia was achieved, animals were quickly transferred to a stereotaxic frame equipped with a nose-cone delivering isoflurane (2-3%) in order to maintain anesthesia. Body temperature was monitored and maintained at 37°C by means of a thermometer and a heating pad and the depth of anesthesia was routinely controlled by controlled by hind paw pinching and eye reflexes. Mice were mounted onto ear bars of the stereotaxic frame and put in a flat-skull position. The skull was exposed and a hole was drilled above the ventral hippocampus (2.9 mm posterior to the bregma and 3.2 mm lateral to the midline). A guide cannula

(AT4.7.IC, Agntho's, Sweden) containing a dummy probe with an outer diameter of 0.2 mm, was lowered 1.5 mm below the skull surface into the striatum or ventral hippocampus, according to the stereotaxic coordinates of Franklin and Paxinos (2008), and secured to the skull with acrylic dental cement (Dentalon® plus, Heraeus, Hanau, Germany). The wound was then swabbed with bupivacaine (5 mg/ml), sutured and mice were allowed to recover single-housed for 48 hours.

3.5.2 Microdialysis

Two days following surgery, the dummy was replaced with a microdialysis probe (AT4.7.2.PES, shaft length 7 mm, probe length 2 mm, 6kD cut-off, PES membrane) and connected to a liquid swivel to allow free movement for the animal. A microinfusion pump (Univentor 864, Univentor Ltd) perfused Ringer solution (148 mM NaCl, 4 mM KCl, 0.8 mM $MgCl_2$, 1.4 mM $CaCl_2$) at a constant rate of 1 µl/min through the probe and the dialysate was collected by every 30 min in plastic tubes. The first three samples were taken for determination of basal levels of extracellular KYNA or dopamine (determined through HPLC, see section 3.8). The mice then received i.p. injections of probenecid (200 mg/kg), blocking the efflux of KYNA and causing an accumulation, or amphetamine (2 mg/kg) in order to evaluate dopaminergic sensitivity. The subsequent samples were collected for up to 300 min and the results calculated as a percent of baseline for each animal. Following microdialysis, animals were sedated with isoflurane and sacrificed by cervical dislocation and tissues were frozen for later analysis and verification of probe placement.

3.6 INTRASTRIATAL INJECTIONS

3.6.1 Intrastriatal injection of radiolabeled kynurenine

Animals were anesthetized with isoflurane (~5% for induction, ~2% for maintain) using an induction chamber. Once full anesthesia was achieved, animals were quickly transferred to a stereotaxic frame (David Kopf Instruments, USA) equipped with a nose-cone delivering isoflurane in order to maintain anesthesia. Animals were mounted onto the ear bars of the stereotaxic frame and put in a flat-skull position. The skull was exposed and two holes were drilled above each striata at 0.8 mm anterior and 2.7 mm lateral from bregma for rats, or 0.7 mm anterior and 1.6 mm lateral to the bregma for mice. An injection needle, coupled to an automatic injector, was lowered 4.5 or 3.0 mm down into the striatum for rats and mice, respectively. 5 µCi of purified [5-^{3}H]-KYN was slowly injected over 10 minutes in volumes of 5 µl or 2 µl for rats and mice, respectively, first in the left and then the right striatum. The

coordinates were confirmed by the appearance of injection site and, in a few test animals, injection of crystal violet as well as quantification of radioactivity in the striatum compared the remaining brain tissue. Two hours after the first intrastriatal injection, animals were sacrificed using CO_2 and decapitated. The brain was rapidly taken out and the striata were carefully dissected out on ice and immediately put on dry ice and stored at -80°C until analysis (section 3.7.4 and 3.8.2).

3.6.2 Intracerebroventricular injection of IL-1β (paper IV)

The procedure was carried out on mice as described above for rats (section 3.6.1). The needle was inserted into the lateral ventricle (0.34 mm posterior to the bregma, 1 mm lateral to the midline and 2 mm below the skull surface). For biochemical measurements, 0.5, 1, 5 and 5 ng of IL-1β, dissolved in PBS to a volume of 4 µl, was slowly injected over 10 min. Animals were sacrificed 6 hours after the start of the infusion and tissues were collected.

Mice used for PPI, a stainless-steel cannula was implanted above the ventricle, similar to that of animals going through microdialysis surgery, and were allowed to recover for 5 days before the start of PPI experiments. IL-1β, or vehicle, was infused in volumes of 0.5 µl directly before the start of the experiment.

3.7 TISSUE PREPARATION

3.7.1 Preparation for KYNA and kynurenine analysis (paper I, II, IV)

Rat and mouse brains were homogenized in 1:3 (w/v) 0.4M perchloric acid containing 0.1% sodium metabisulfite and 0.05% EDTA with the aid of a disperser (Ultra-Turrax®, IKA, Germany) and subsequently centrifuged (18 400 rcf for 5 min). The resulting supernatant was mixed with 1/10 (v/v) 70% PCA and centrifuged one additional time (18 400 rcf for 5 min). The supernatant was saved and used for analysis with HPLC (section 3.8).

3.7.2 Label-free neuroproteomics (paper IV)

WT and GRK3 K/O mice were fully anesthetized with isoflurane, decapitated and the brains were rapidly removed and washed in ice-cold 1x PBS. The prefrontal cortex was subsequently dissected and frozen on dry ice and stored in -80°C awaiting further analysis. In order to extract the total protein from the PFC samples, an individual biological replicate was combined with 0.5 mm zirconium oxide beads and 50 µL of ice-cold lysis buffer (containing CelLytic™ MT lysis reagent (Sigma-Aldrich), Complete protease inhibitor cocktail (Roche) and phosphatase inhibitor cocktails II and III (Sigma-Aldrich)). The tissues were

homogenized using a Storm 24 Bullet Blender (Next Advance Inc.). Homogenates were centrifuged (16 400 RPM for 15 min at +4°C) and the resulting supernatant was collected and analyzed with regards of protein concentrations using Bradford Reagent (Bio-Rad). The proteins were denaturated using in NuPAGE® LDS Sample Buffer (Invitrogen, Carlsbad, CA) for 10 min at 70°C for SDS-PAGE. The lysates were loaded in triplicates of 15 µg and resolved on a 4-12% Bis-Tris Gel. Gels were fixed using a 50% methanol and 10% acetic acid solution, washed with ultra-pure H_2O and stained with BioSafe Coomassie Stain (Bio-Rad) per the supplier's instructions. Sections of the gel were destained, trypsin-digested (140ng of trypsin dissolved in 25mM Tris pH 8.2), reduced using dithiothreitol and alkylated with iodoacetamide. Peptides were extracted from gel sections with 50% acetonitrile in 4% trifluoroacetic acid, followed by two additional extractions using acetonitrile. Extracts were dried under vacuum and stored at in -80°C for further analysis (section 3.12).

3.7.3 Preparation of membrane fractions (paper IV)

WT and GRK3 K/O mice were fully anesthetized using isoflurane, decapitated and the brains were rapidly isolated and stored at -80°C until further use. The brain tissue was homogenized in complete hypotonic buffer (10 µM, sodium bicarbonate, 1:1000, protease inhibitor cocktail (Sigma-Aldrich) and 1:1000, phosphatase inhibitor cocktail I and II (Sigma-Aldrich)) and centrifuged (1 200 rcf for 10 min at +4°C). The resulting supernatant was further centrifuged (21 600 rcf for 10 min at +4°C) and the resulting pellet containing internal membranes was resuspended in extraction buffer (EB: 0.5% Triton X-100, 50 mM Tris-HCl pH 7.5, 150 mM NaCl, 1 mM EDTA, 1% sodium dodecyl sulfate, protease inhibitor cocktail and phosphatase inhibitor cocktail I and II), while the remaining supernatant was centrifuged one additional time (150 000 rcf for 10 min at +4°C). The pellet, containing the plasma membranes was dissolved in EB. Finally, the protein content of the internal and plasma membrane fractions was determined using BCA protein assay kit (Pierce, Thermo Scientific) in accordance with the supplier's recommendations.

3.7.4 Preparation of radiolabeled tissue

For samples from animals receiving intrastriatal injections of [5-^{3}H]-KYN, each striatum was weighed and diluted with 4x or 10x H2O for rats and mice, respectively. The samples were homogenized using sonication and deproteinated with ¼ (v/v) of 6% perchloric acid. The resulting solution was quickly vortexed followed by centrifugation (18 400 rcf for 10 min) and the supernatant was collected for HPLC analysis (section 3.8.2).

In order to validate successful tissue processing, the pellet was resuspended and radioactivity was measured using scintillation counter. Through this it was determined that only traces of radioactivity were present in the pellet and the main portion of radioactivity was found in the supernatant.

3.8 HIGH PERFORMANCE LIQUID CHROMATOGRAPHY

3.8.1 Fluorescent detection (paper I, II, IV)

For analysis of KYNA and kynurenine in microdialysis samples, an isocratic reversed-phase HPLC system was used, with a Shimadzu LC-10AD dual piston, high pressure liquid delivery pump (Shimadzu Corporation, Kyoto, Japan), and a ReproSil-Pur C_{18} column (4×150mm, Dr. Maisch GmbH, Ammerbuch, Germany) coupled to a Shimadzu SPD-10A UV detector (Shimadzu Corporation, Kyoto, Japan) followed by a Jasco FP-2020 Plus fluorescence detector (Jasco Ltd, Hachioji City, Japan). 20 µl samples were manually injected through a Rheodyne 7725i injector (Rheodyne, Cotati, CA, USA) and eluted isocratically with mobile phase (50 mM sodium acetate, pH 6.2, adjusted with acetic acid, 7% acetonitrile) at a flow rate of 0.5 ml/min. Zinc acetate (0.5 M, not pH adjusted) was delivered after the UV-detector, and before the fluorescence detector, at a flow rate of 10 ml/h through a syringe pump (P-500, Pharmacia, Uppsala, Sweden). Kynurenine was measured through UV-detection at an absorption wavelength of 360 nm, while KYNA was measured through fluorescence detection with a and excitation and emission wavelengths of 344 nm and 398, respectively. The signals from the detectors were transferred to a computer for analysis utilizing Datalys Azur (Grenoble, France). The retention time of kynurenine and KYNA was about 4 and 7 min, respectively.

3.8.2 Electrochemical detection (paper IV)

Brain perfusate from microdialysis experiments (section 3.5) were separated using reversed-phase liquid chromatography with a mobile phase consisting of 55 mM sodium acetate buffer (pH 4.1, 10 % methanol) containing 1.16 mM octanesulfonic acid and 0.01 mM Na_2EDTA. The mobile phase was delivered by a HPLC pump (Bischoff Chromatography, Leonberg, Germany) and passed through a Agilent Eclipse XDB-C_{18} column (4.6×150 mm, Agilent Technologies, Inc., CA, USA) at a rate of 0.7 ml/min. Samples were subsequently quantified through sequential oxidation and reduction in a high-sensitivity analytical cell (ESA 5011; ESA Inc., Chelmsford, MA, USA) controlled by a potentiostat (Coulochem III; ESA Inc.) with an applied potential of -350 mV for the detection of dopamine. The signals from the

detector were transferred to a computer for further analysis (Datalys Azur, Grenoble, France). The retention time of dopamine was approximately 7 min.

3.8.3 Radiodetection

Analysis of radiolabeled kynurenine pathway metabolites were based on previously described methods (Guidetti et al., 1995). To the radiolabeled samples, 15 µl standard (containing 500 µM of unlabeled kynurenine, kynurenic acid, 3-hydroxykynurenine, anthranilic acid, 3-hydroxyanthranilic acid, xanthurenic acid, picolinic acid and quinolinic acid) was added and the samples were diluted with mobile phase (100mM ammonium phosphate (11.5 g/L), 100mM glacial acetic acid (5.75 mL/L = 6.03 g/L), 1.5mM 1-octanesulfonic acid (0.34 g/L), 4% acetone nitrile at pH 3.2 adjusted with 1:1 H3PO4/acetic acid) to a final volume of 210 µl. Samples were applied to a YMC-Pack Pro C_{18} (250×4.6 mm) column through a Rheodyne 7725i manual injector (Rheodyne, Cotati, CA, USA) and eluted isocratically with mobile phase at a flow rate of 1.2 ml/min using a HPLC coupled with a UV detector (Applied Biosystems 785A Absorbance Detector) followed by a radiodetector (Berthold Technologies FlowStar LB514). Scintillation fluid (FlowLogic U, LabLogic) was delivered at a flow of 2.7 ml/min after the UV detector and before the radiodetector. Standards were detected through UV spectrometry at an absorption wavelength of 254 nm with an approximate retention time of 2.8 min for QUIN, 3.6 min for picolinic acid, 11.5 min for xanthurenic acid, 12.7 min for 3-HK, 14.5 min for KYNA, 22.5 min for 3-HANA, 33.0 min for kynurenine and 38.0 min for anthranilic acid. Retention time of the peaks from the standard was matched with peaks detected by the radiodetector to identify radiolabeled metabolites. The signals from the detectors were transferred to a computer and analyzed using Radiostar.

3.9 BIOCHEMICAL ANALYSIS (PAPER IV)

3.9.1 Western blot

Internal and plasma membrane fractions (section 3.7.3) were separated using a NuPAGE 4-12% Bis-Tris gel electrophoresis (Invitrogen) and subsequently transferred onto nitrocellulose membranes (Invitrogen). Non-specific binding sites were blocked by incubation in Tris buffer (50 mM Tris-Cl, 6 mM NaCl) containing 5% low-fat dried milk and 0.1% Tween 20 for 1 hour at room temperature. Membranes were subsequently incubated with a primary antibody agains P2RX7 (1:10 000, Cat # APR-004, Almone Labs) overnight at 4 °C. Following three washes (Tris buffer containing 0.1% Tween 20) for 5 min each, the blots were probed with horseradish peroxidase-conjugated secondary antibodies (Cat # 7076

and # 7074, Cell signaling Technology) for 1 hour at room temperature. The specific protein bands were visualized utilizing chemiluminescent detection reagents (Supersignal West Pico and West Femto, Thermo Scientific). Antibody against β-actin (1:10 000, Cat # 3700, Cell Signaling Technology) was used as a control for protein-loading. All signal intensity measurements were made using Quantity One software (Bio-Rad Laboratories) and the obtained data of P2X7R was normalized to β-actin.

3.9.2 qPCR

RNA was isolated from hippocampal tissue from WT and GRK3 K/O mice using Isol-RNA Lysis Reagent (5 PRIME) in accordance to the manufacturer's instructions. From each sample, 1 μg RNA was treated with Amplification Grade DNase I (Life Technologies) and 500 ng of that was used for preparation of cDNA utilizing the Applied Biosystem Reverse Transcription Kit (Life Technologies). SYBR Green PCR Master Mix (Applied Biosystems) was added and quantitative Real-Time PCR was carried out using a ViiA 7 Real-Time PCR system thermal cycler (Applied Biosystems). Subsequently, gene expression was analyzed using the ΔΔCt method and relative gene expression was calculated normalized to mRNA levels of hypoxanthine phosphoribosyltransferase.

3.9.3 Cytokine measurements

Mice were euthanized (isoflurane followed by cervical dislocation) and their brains removed and put on ice. From the brains, the hippocampus was rapidly dissected and stored in -80°C until time of analysis. Samples were then put in ice-cold lysis buffer, including protease inhibitor, phosphatase Inhibitor Cocktail 3 and phosphatase Inhibitor 2, and homogenized using a Bullet Blender® (Next Advance, Inc. Averill Park, NY, USA). The resulting homogenate was subsequently centrifuged (16 000 rcf for 10 min) and 50 μl of the supernatant was used for cytokine measurements, where IL-1β, IL-6, KC/GRO (IL-8), IL-10, IL-12p70, IFN-γ, and TNF-α were detected using a multiplex sandwich enzyme-linked immunosorbent assay, in duplicates. To this means, we employed Discovery assays (Meso Scale, Gaithersburg, MD, USA) using the protocol provided by the manufacturer, on a SECTOR® Imager 2400 instrument (Meso Scale Diagnostics, LLC). Due to high inter-individual variation coefficients and levels below our limit of detection, only IL-1β could be reliably measured.

3.10 HISTOLOGICAL ANALYSIS (PAPER IV)

Mice were anesthetized and perfused through the ascending aorta with Tyrode's Ca^{2+}-free solution, followed by a 4% paraformaldehyde solution containing 0.4% picric acid in a 0.16 M phosphate buffer (pH 6.9) as a fixative. The brains were rapidly taken out and submerged and stored in ice-cold paraformaldehyde with picric acid for 90 min, followed by an overnight rinse in phosphate buffered 10% sucrose solution (pH 7.4). The brains were then frozen on dry-ice and cut in 14 μm thick sections using a cryostat (Microm, Heidelberg, Germany) and thaw-mounted on SuperFrost plus slides (VWR, Radnor, PA). For subsequent analysis, sections spanning approximately 0.98 mm anterior and 2.30 mm posterior to the bregma were used, including areas such as the thalamus, hippocampus and caudate putamen.

Results were quantified using the Image J Software (National Institutes of Health). In brief, the area of interest was selected on micrographs, and the sum of labeling, with intensity above a set threshold, was calculated (raw integrated density).

3.10.1 [^{3}H]-PBR28 autoradiography

Sections were thawed in room temperature and and pre-incubated for 20 min in a 50 mM Tris-HCl buffer (pH 7.4) containing 120 mM NaCl, 5 mM KCl, 2 mM $CaCl_2$, 1 mM $MgCl_2$, followed by incubation with 1.5 nM [^{3}H]-PBR28, (specific activity 50 Ci/mmol; produced in-house by Karolinska Institutet, Department of Clinical Neuroscience, Sweden) for 1 hour. PBR28 is a radiotracer for translocator protein, which is used as a marker for inflammation, and have been used for studying neuroinflammation using positron emission tomography (Collste et al., 2017).

In order to determining non-specific binding, 10 μM PK11195 (Sigma-Aldrich) was added to parallel sections, thus block specific bindings. After incubation, sections were washed in ice-cold 50 mM Tris-HCl (pH 7.4; 3×3 min) followed by a brief wash with distilled water. The slides containing the sections were dried and underwent quantification of the binding density using phosphor imaging plates (Fujifilm Plate BAS-TR2025, Fujifilm, Tokyo, Japan), together with micro scales standards (American Radiolabeled Chemicals Inc.) for calibration purposes. Phosphor imaging plates were scanned and processed in a Fujifilm BAS-5000 phosphor imager (Fujifilm, Tokyo, Japan). Mean pixel values of the hippocampus was transformed into radioactivity values and to binding density (pmol/mg tissue, tissue wet weight) using the micro scale standards and a quantitative analysis was performed using the Multi Gauge 3.2 phosphorimager software (Science Imaging Scandinavia, Sweden). Specific binding, indicating receptor density, were calculated by subtracting the levels of non-specific

binding from the total bound amount for each section. A few slides processed using this method were later reused for immunohistochemistry (section 3.10.2)

3.10.2 Immunohistochemistry

Sections were pretreated with 0.03% H_2O_2 followed by incubation with antiserum against markers of glial activation, including glial fibrillary acidic protein (1:4000, Sigma-Aldrich), Aldh1L1 (1:3000, Abcam, Cambridge, UK), ionized calcium-binding adapter 1 (1:4000, Wako Pure Chemical Industries, Osaka, Japan), or Cd11b (1:2000, Serotec, Kidlington, UK) at 4˚C overnight. Prior to pretreatment, sections used for the detection of Aldh1L1 underwent antigen retrieval using sodium citrate buffer, in order to reveal the epitope.

Sections were subsequently washed in TNT buffer (0.1 M Tris-HCl, pH 7.5; 0.15 M NaCl; 0.05 % Tween 20; Sigma-Aldrich), incubated with TNB buffer (0.1 M Tris-HCl, pH 7.5; 0.15 M NaCl; 0.5 % blocking reagent) for 30 min at room temperature, followed by incubation with anti-rabbit horseradish-peroxidase conjugated secondary antibody (Dako A/S), diluted 1:200 in TNB buffer, for 30 min. Sections were then washed in TNT buffer and incubated in biotinyl tyramide fluorescein conjugate (PerkinElmer Life Science) diluted 1:200 in amplification diluent for 10 min at room temperature, in accordance to the protocol of the TSA-plus Fluorescein System (PerkinElmer Life Science).

3.11 HUMAN SUBJECTS

All studies involving human subjects were approved by the Regional Ethics Committee in Stockholm and were conducted in accordance to the Helsinki Protocol. All participants received both verbal and written information and were only included after providing written consent before inclusion.

3.11.1 Bipolar cohort and human data (paper IV)

Data used in this study was collected from euthymic patients suffering from bipolar disorder enrolled in a long-term follow-up program (St. Göran Bipolar Project) at an outpatient unit of the Northern Stockholm psychiatric clinic. The patients were characterized and CSF samples were collected as previously outlined (Olsson et al., 2012b). Healthy controls were randomly selected from the general population by Statistics Sweden and underwent the same clinical characterization as the patients. As part of enrollment, all subjects underwent genotyping using the Affymetrix 6.0 array (Santa Clara, CA, USA) at the Broad Institute in Boston, MA (Bergen et al., 2012).

3.11.2 Karolinska Schizophrenia Project (KaSP) cohort (paper V)

Drug-naïve first-episode psychosis (FEP) patients were recruited as a part of Karolinska Schizophrenia Project (KaSP) from four clinics in Stockholm, Sweden (Psykiatri Nordväst, Norra Stockholms Psykiatri, Södra Stockholms Psykiatri and PRIMA Vuxenpsykiatri) at their first clinical presentation of psychosis. At recruitment, all patients were fully naïve to antipsychotic medication and met the diagnostic criteria of DSM-IV for schizophrenia, schizophreniform psychosis, psychosis not-otherwise-specified (NOS) or brief psychotic episode. Patients underwent a comprehensive battery of psychiatric and cognitive evaluations, including characterization of symptomatic severity using the Positive and Negative Syndrome Scale for schizophrenia (PANSS), Global Assessment of Function (GAF) and the Clinical Global Impression (CGI) scale as well as cognitive assessments using the Measurement and Treatment Research to Improve Cognition in Schizophrenia (MATRICS) Consensus Cognitive Battery (MCCB). At the end of the testing battery (conducted under 1 week), blood and CSF samples were collected. CSF was collected through standards lumbar puncture procedure (L4/L5) on the morning (between 07:45 and 10:00) following a night of fasting. CSF samples were centrifuged (3 500 rpm for 10 min) separating cells and supernatant. The resulting supernatant was aliquoted and stored at -80°C. Blood was collected in conjunction with lumbar puncture through standard venipuncture from the cephalic or medial cubital vein. Blood samples were centrifuged (2 900 rcf for 15 min) in order to isolate cell-free serum which was subsequently aliquoted and stored at -80°C until analysis.

Due to the naturalistic setting of the study, antipsychotic treatment was started in 52% of patients prior to CSF and blood sampling (maximum 30 days). Patients were excluded if they suffered from severe somatic or neurological illness, as well as neurodevelopmental disorders, e.g. autism spectrum disorder, or current, or history of, drug abuse.

In parallel, healthy controls were recruited and underwent the sampling procedure as FEP patients. Healthy controls were deemed healthy based on medical history, clinical examination, routine blood and urine, and brain MRI. In addition, the Mini International Neuropsychiatric Interview was used to exclude current or previous psychiatric illness, and subjects were excluded if they had first-degree relatives suffering from any psychotic disorder or if they had any history or current use of illegal drugs. Eighteen months following recruitment, patients and healthy controls returned for a follow-up evaluation where the same testing and sampling procedures was repeated. In total, CSF and serum samples of 25 patients and 21 healthy controls were analyzed using metabolomics (section 3.13).

3.12 PROTEOMIC ANALYSIS (PAPER IV)

3.12.1 Liquid chromatography tandem mass spectrometry

Peptide extracts (section 3.7.2) were reconstituted in H_2O containing 0.2% formic acid and loaded on a OptiPak trap (Optimize Technologies, Oregon City, Oregon) for analysis by liquid-chromatography tandem mass spectrometry (LC-MS/MS), using a Dionex UltiMate® 3000 RSLC liquid chromatography system (Thermo-Fisher Scientific, Waltham, MA) coupled with a QExactive mass spectrometer (Thermo-Fisher Scientific, Waltham, MA), as described in details previously (Oliveros et al., 2017a).

3.12.2 Data processing

Proteins differentially expressed between groups were identified using a label-free peptide MS1 intensity-based method. The raw data was processed using the MaxQuant (version 1.5.1) software (Cox et al., 2014), identifying protein groups and their corresponding intensities using UniProt mouse reference proteome. Identified peptides and proteins were filtered using a 2% false-discovery rate (FDR), grouped and reported as protein group intensities.

3.13 METABOLOMIC ANALYSIS (PAPER V)

3.13.1 Liquid chromatography time-of-flight mass spectrometry

Large-scale and untargeted metabolomic analysis was performed by the Mayo Metabolomic Core at Mayo Clinic in Rochester, Minnesota. Serum and CSF samples from FEP patients and healthy controls at baseline and follow-up were analyzed using ultra-high pressure liquid chromatography (1200, Agilent Technologies Inc, Santa Clara, CA, USA) coupled with time-of-flight mass spectrometry (UPLC/ToF-MS; 6550, Agilent Technologies Inc, Santa Clara, CA, USA). For maximum coverage of metabolites, duplicate injections were made for each sample using positive and negative electrospray ionization as well as using both polar hydrophilic interaction liquid chromatography and nonpolar reverse phase C18 chromatography columns. Moreover, pooled quality control samples were used.

3.13.2 Data processing

Metabolites were identified using the METLIN metabolomics database with a detection window of 10 ppm and verified based on analysis of MS/MS output. The obtained data was analyzed using Mass Profiler Professional (MPP, Agilent Technologies Inc, Santa Clara, CA, USA) and normalized to an internal standard (250 ng of 13C6-phenylalanine).

Disease-associated metabolites were defined as those differing between patients and HCs at baseline, or distinguished patients from HCs at both baseline and follow-up, if the difference between patients and HCs at follow-up compared to baseline was not approximately equal to the difference between follow-up and baseline.

Treatment-associated metabolites were defined as those metabolites differing between patients at follow-up and baseline, but also included metabolites differing between patients and HCs only at baseline or only at follow-up.

3.14 DATA ANALYSIS

3.14.1 Statistical analysis

All statistical analysis was carried out using Prism® (GraphPad Software Inc.) and data is reported as mean ± SEM, unless otherwise specified. All tests were two-tailed with alpha set to 0.05.

For paper I and II, differences in change of firing rate were determined using Mann-Whitney U test with Bonferroni correction while differences in burst firing were determined using Wilcoxon signed rank test. Whole brain levels of kynurenine and KYNA was analyzed by Kruskal-Wallis test followed by Dunn's multiple comparison test for drug treatment, and Mann-Whitney U test between groups.

For paper IV, animal behaviors were analyzed with repeated measures two-way ANOVA followed by Fisher's least significant difference (LSD) post-hoc test. For PPI experiments, two-way ANOVAs with Tukey's post-hoc tests were used while startle magnitude differences were calculated with the Mann-Whitney U test. Analyses of P2X7R protein levels and hippocampal IL-1β concentrations, were performed using Wilcoxon signed-rank test. For KYNA and with-in group comparisons, one-way ANOVA with Bonferroni post-hoc test was used. For microdialysis experiments, repeated measure two-way ANOVA with Bonferroni post-hoc test was used. Histological differences were calculated using unpaired two-tailed *t*-tests. The results from proteomic analysis were analyzed using an in-house script written in

R. The protein group intensities were normalized and log2 transformed and analyzed using an ANOVA test to detect differential expression between experimental groups (WT vs. GRK3 K/O). Results were corrected for FDR using Benjamini-Hochberg-Yekutieli procedure. Protein groups with an FDR < 0.05 and an absolute log2 fold change ≥0.5 were considered statistically significant in terms of differential expression and subsequently used for pathway analysis (section 3.14.2).

Human data in paper IV was analyzed using SPSS Statistics (IBM, Inc.). The effect of rs478655 allele frequency on history of psychosis in BD patients was analyzed using a logistic regression model, while allele frequency effect on CSF KYNA levels was evaluated using a linear regression model. Here, age was shown to have a significant effect on CSF KYNA levels and as a result, residuals from a linear regression of age vs. CSF KYNA levels was used as outcome variable.

For paper V, disease- and treatment-associated metabolites were analyzed using an in-house script written in R. Disease associated metabolites were identified by matched analysis reporting fold change and FDR while treatment associated metabolites were identified using an unmatched analysis. A cut-off of FDR < 0.05 and minimum fold-change value of 0.075 was applied. Results were subsequently used for pathway analysis (section 3.14.2). Clinical outcomes were analyzed using Prism, using one- or two-way ANOVA followed by Tukey's and Bonferroni post-hoc analysis, respectively. Moreover, student's t-test was used when appropriate.

3.14.2 Ingenuity pathway analysis (paper IV, V)

Ingenuity pathway analysis (IPA; Qiagen, redwood City, CA) was used to identifying network interactions with results obtained from proteomic (paper IV) and metabolomic (paper V) analyses. IPA used Fisher's exact test to determine statistical significance and results are shown with significance, ratio ([number of proteins/metabolites from data set]/[total known proteins/metabolites in pathway]), and/or z-score (number of standard deviations above or below the mean) when applicable.

For paper IV, proteins identified as significantly different between WT and GRK3 K/O mice by the MaxQuant bioinformatic analysis were analyzed using IPA, restricted to select tissues and cells primarily involved in the nervous and immune system. Results were further restricted to only analyze only those proteins with ≥1.5-fold change.

For paper V, metabolomics analysis was carried out using default settings, but excluding pathways specific to cancer cell lines, and with a corrected confidence interval value of $p < 0.05$ (Fischer's exact test).

4 RESULTS AND DISCUSSION

4.1 INHIBITION OF KYNURENINE AMINOTRANSFERASE II REDUCES THE ACTIVITY OF MIDBRAIN DOPAMINE NEURONS (PAPER I)

In the first study, we investigated the potential of a specific KAT II-inhibitor, PF-04859989, as a treatment strategy for schizophrenia utilizing *in vivo* electrophysiology. Previous studies on this compound found that PF-04859989 effectively reduces brain levels of KYNA and ameliorates ketamine-induced cognitive deficits in rats and non-human primates (Kozak et al., 2014). Here, we aimed to investigate its effect on dopaminergic transmission in the VTA.

4.1.1 Acute effects of PF-04859989 on VTA dopamine neurons

Acute administration of PF-04859989 (5 or 10 mg/kg, i.v.) to anesthetized rats caused a time-dependent decrease in firing frequency and burst firing rate of VTA dopamine neurons (Figure 3). The effect of PF-04859989 (5 mg/kg) could be prevented by pretreatment with either D-cycloserine (30 mg/kg, i.p., 21-50 min), a partial NMDA receptor agonist on the glycine-site, or CGP-52432 (10 mg/kg, i.p., 20-55 min), a selective $GABA_B$ receptor inhibitor. Furthermore, pretreatment with the non-competitive $GABA_A$ receptor antagonist picrotoxin (4.5 mg/kg, i.p., 20-55 min) was able to partially block the effect of PF-04859989, while pretreatment with the α7nACh antagonist MLA (4 mg/kg, i.p., 15-32 min) was without effect. Taken together, these results suggest that the effect of PF-04859989 is related to the activation of NMDA receptors on GABAergic interneurons, likely as a result of reduced endogenous KYNA. These findings are in line with studies showing that mesolimbic dopamine cells are tightly regulated by GABAergic interneurons (Tan et al., 2012; Van Zessen et al., 2012) and in particular via the $GABA_B$ receptor (Erhardt et al., 2002; Xi and Stein, 1999). Importantly, our electrophysiological results are in line with previous studies showing reduced dopamine activity following administration of parecoxib, a COX-2 inhibitor which reduces brain KYNA levels (Schwieler et al., 2008, 2006) and was recently shown to be an inhibitor of KAT II (Zakrocka et al., 2019).

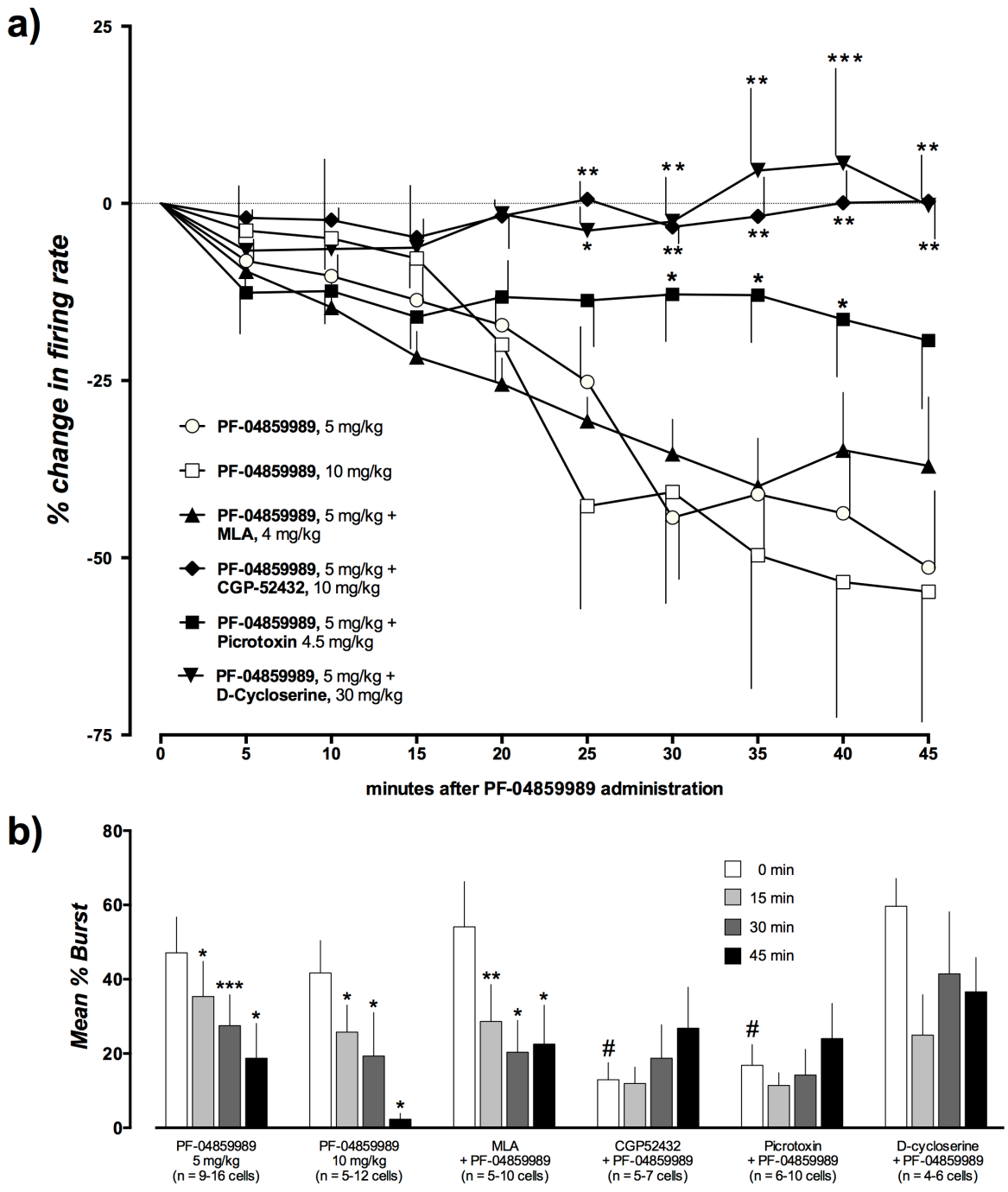

Figure 3. Effect of the KAT II-inhibitor PF-04859989 (5 or 10 mg/kg, i.v.) on a) firing rate and b) burst activity of VTA DA neurons in controls (n = 9-15) and in rats pretreated with MLA (4 mg/kg, i.p., 15-32 min, n = 5-10), CGP-52432 (10 mg/kg, i.p., 21-33 min, n = 5-7), picrotoxin (4.5 mg/kg, i.p., 20-55 min, n = 5-8) or D-cycloserine (30 mg/kg, i.p., 21-50 min, n = 4-6). In a) comparisons were made versus corresponding value from PF-04859989 treated control rats (5 mg/kg; *P < 0.05, **P < 0.01, ***P < 0.001, Mann-Whitney U test). In b) changes in burst firing activity for each treatment group were compared to basal value and control value prior to the administration of PF-04859989 (5 mg/kg; *P < 0.05, **P < 0.01, ***P < 0.001 vs. corresponding value before administration of PF-04859989, Wilcoxon matched-pairs sign ranked test. #P < 0.05 vs. controls, Mann-Whitney U test). Each value represents mean ± SEM.

4.1.2 KYNA concentrations following PF-04859989 administration

Whole-brain analysis of KYNA levels revealed no change 45 min after intravenous administration of PF-04859989 (5 mg/kg) compared to saline control rats (Figure 4). In contrast, KYNA levels were robustly reduced 5 hours after intraperitoneal administration (2.7 ± 0.31 nM) compared to saline-treated rats (10.7 ± 1.3 nM). The results seem contradictory to the relative fast reduction of brain KYNA levels seen in previous microdialysis studies (Kozak et al., 2014). This discrepancy may be explained by the fact that whole-brain analysis includes a considerable amount of intracellular KYNA that may not be detected by microdialysis (Herédi et al., 2019; Schwarcz et al., 2012; Wu et al., 1992). Nevertheless, we observed a considerable and rapid effect on the firing of dopaminergic neurons, indicating that the functional extracellular levels indeed decrease quite rapidly, whereas an effect in whole-brain occurs much later.

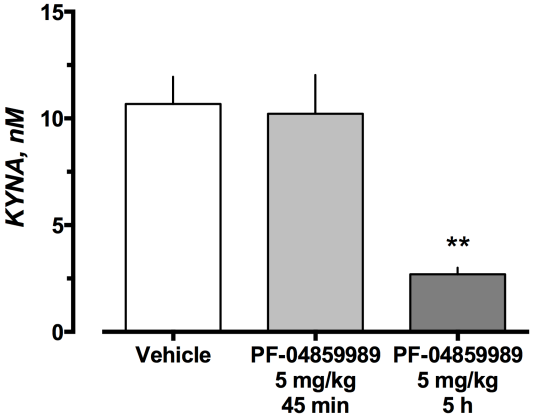

Figure 4. Whole-brain KYNA levels after administration of PF-04859989, (5 mg/kg) at 45 min, (i.v.) or 5 h (i.p). Bars represent mean ± SEM, **P < 0.01 vs. controls, Mann-Whitney U test.

4.1.3 Effect of PF-04859989 pretreatment on VTA dopamine neurons

Intrigued by the findings that PF-04859989 caused such a robust decrease in whole-brain KYNA after 5 hours, we set out to investigate its effect on basal VTA dopamine cell characteristics following a 5-hour pretreatment. Rats receiving PF-04859989 (5 mg/kg, i.p. 4-6 h, n = 5, 16 cells) showed a marked reduction in number of spontaneously active dopamine cells found per track (0.69 ± 0.08 cells/track) compared to saline-treated rats (n = 5, 41 cells, 2.4 ± 0.32 cells/track; Figure 5A). However, there was no significant change in firing rate or burst firing (Figure 5B and C).

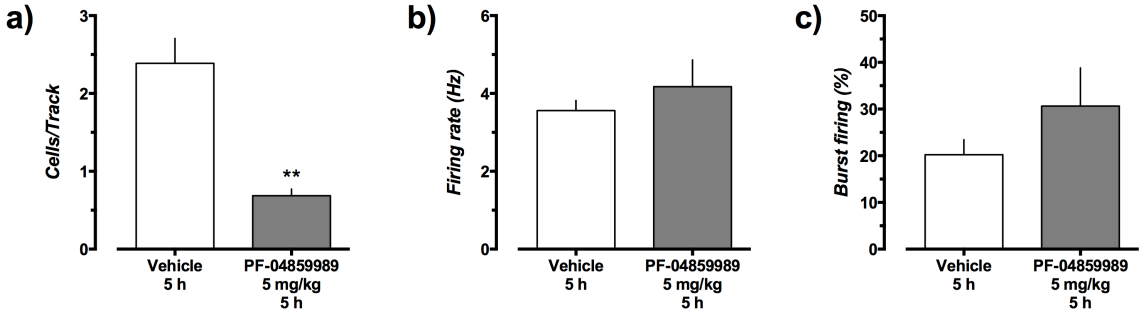

Figure 5. Effect of pretreatment with PF-04859989 (5 mg/kg, i.p, 4-6 h) on VTA DA cell activity compared to vehicle. a) Numbers of spontaneously active cells found per electrode track, b) firing rate and c) burst activity. Bars represent mean ± SEM, **P < 0.01 vs. controls, Mann-Whitney U test.

4.2 ELECTROPHYSIOLOGICAL CHARACTERIZATION OF DOPAMINE CELL ACTIVITY AND PHARMACOLOGICAL RESPONSE IN KMO K/O MICE (PAPER II)

Previous studies have identified the KMO K/O mice as a valuable tool for investigating the effects of chronic elevation of KYNA (Giorgini et al., 2013). Thus, KMO K/O mice show behavioral abnormalities resembling the symptoms of schizophrenia (Erhardt et al., 2017a). The present study builds upon these findings by characterizing dopaminergic activity at baseline as well as the response of VTA dopamine neurons to traditional antipsychotic drugs, and drugs known to affect the levels of brain KYNA.

4.2.1 Baseline characteristics of VTA dopamine cells in KMO K/O mice

KMO K/O mice (n = 6, 44 cells) showed a significantly higher number of spontaneously active VTA dopamine cells per track (2.3 ± 0.09 cells/track) compared to WT mice of the same genetic background (n = 7, 37 cells; 0.75 ± 0.07 cells/track; Figure 6A). In addition, dopamine cells in KMO K/O had a higher firing rate (5.5 ± 0.45 Hz) and burst firing rate (40.0 ± 4.7 %) compared to WT (4.1 ± 0.30 Hz, 19.5 ± 3.2 %, respectively; Figure 6B, C). The results show that KMO K/O display an overall enhanced dopamine cell activity, in line with previous studies analyzing pharmacologically increased KYNA levels in rats (Erhardt et al., 2001b; Erhardt and Engberg, 2002; Schwieler et al., 2006) and studies showing that systemic administration of NMDA receptor antagonists is associated with increased VTA dopamine activity (French, 1994; French et al., 1993; Murase et al., 1993).

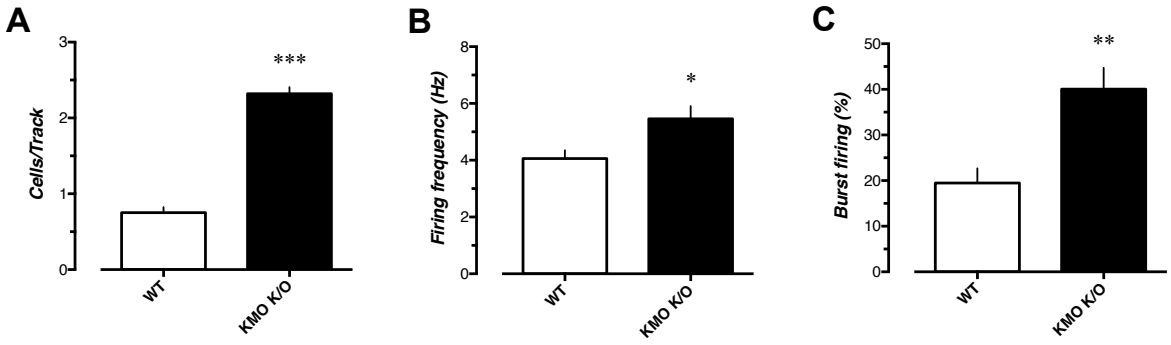

Figure 6. Basal VTA DA cell activity in WT mice (n = 7 mice, 37 cells) compared to KMO K/O mice (n = 6, 44 cells). A) Numbers of spontaneously active cells found per electrode track, B) firing rate (Hz) and C) percent of action potentials fired in bursts. Bars represent the mean ± SEM. ***p < 0.001, **p < 0.01, *p < 0.05 vs. WT, Mann-Whitney U test

4.2.2 Effect of antipsychotic drugs on VTA dopamine cells in KMO K/O mice

Acute administration of the typical antipsychotic drug haloperidol (0.05-0.4 mg/kg, i.v.) produced a dose-dependent increase in firing rate of VTA dopamine cells in KMO K/O mice (n = 2-6; Figure 7). In contrast, WT mice showed no significant effect of haloperidol (n = 6). Notably, in KMO K/O mice, acute administration of haloperidol caused depolarization block in 4 out of 6 VTA dopamine neurons, reflected as a sudden loss of firing followed by an unstable recovery. This effect was not observed in WT mice. The increase in firing rate may be explained by blockade of somatodendritic D_2 autoreceptors, causing a disinhibition of dopamine cells to the point where it causes a depolarization blockade (Pucak and Grace, 1996, 1994). However, as no effect was seen by haloperidol in WT mice, this suggests that a secondary control mechanism is able to compensate for the disinhibition caused by haloperidol, likely involving GABAergic control via the NMDA receptor (Linderholm et al., 2016) that is disrupted by excessive brain KYNA levels (Schwieler and Erhardt, 2003).

In contrast to haloperidol, acute administration of the atypical antipsychotic drug clozapine (0.625-10 mg/kg, i.v.) caused a dose-dependent decrease of VTA dopamine cell firing in KMO K/O mice (n = 8-9; Figure 8). In WT mice (n = 4-8), however, clozapine produced an increase in firing of VTA dopamine cells in a dose-dependent manner. The opposite effect of clozapine on the two genotypes might be explained by clozapine's interaction with the glycine-site of the NMDA receptor (Millan, 2005), where it appears to have a partial agonistic effect, in line with previous studies, showing different effect of clozapine on VTA dopamine firing dependent on brain KYNA levels in rats (Schwieler et al., 2008, 2004).

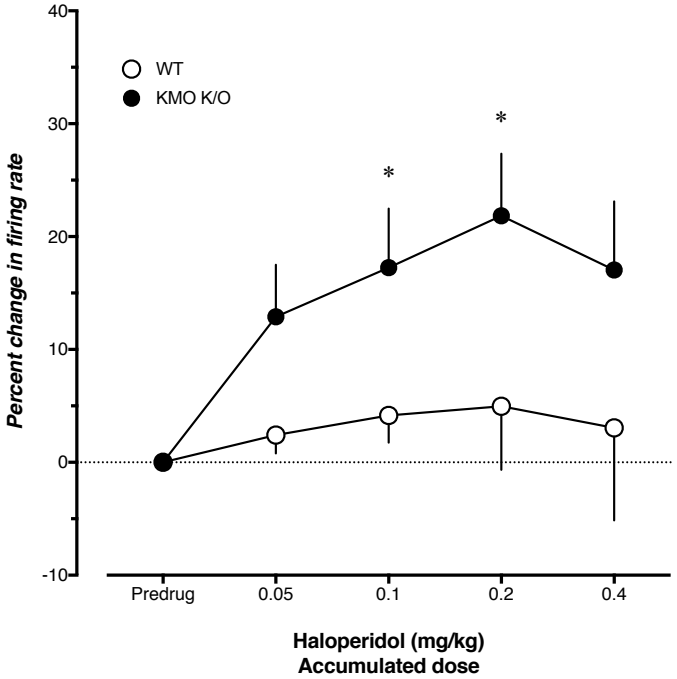

Figure 7. Effect of haloperidol (0.05-0.4 mg/kg, i.v.) on firing rate of VTA DA neurons in WT (n = 6) and KMO K/O (n = 2-6) mice. In A, the percent change was compared to the corresponding pre-drug value (*p < 0.05; Mann-Whitney U test) and between WT and KMO K/O mice at corresponding doses (no significance, Mann- Whiney U test). Each value is the mean ± SEM. All values were corrected for repeated measure (Bonferroni correction).

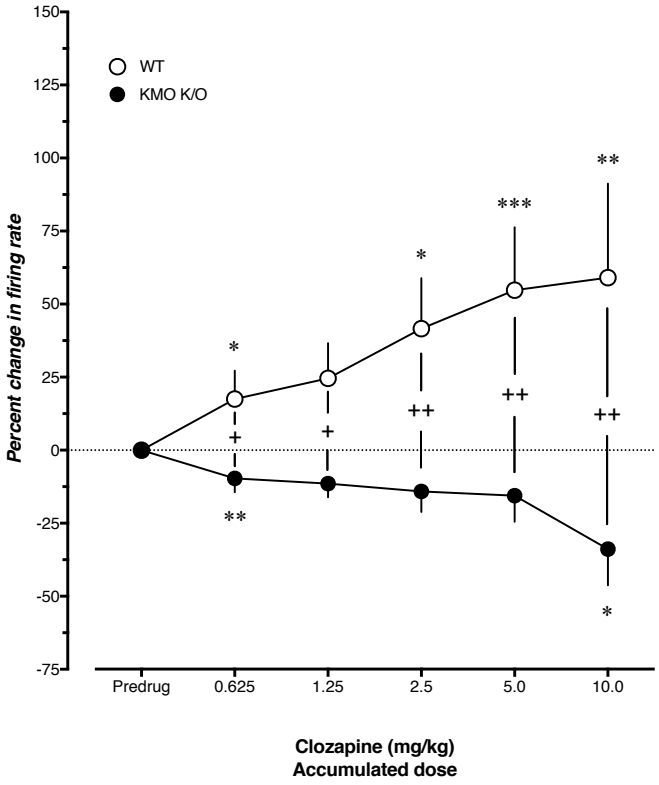

Figure 8. Effect of clozapine (0.625-10.0 mg/kg, i.v.) on firing rate of VTA DA neurons in WT (n = 4-8) and KMO K/O (n = 8-9) mice. The percent change was compared to corresponding pre-drug values (***p < 0.001, **p < 0.01, *p < 0.05, Mann-Whitney U test) and between WT and KMO K/O mice at corresponding doses ($^{++}$p < 0.01, $^{+}$p < 0.05, Mann-Whitney U test). Each value is the mean ± SEM. All values were corrected for repeated measure (Bonferroni correction).

4.2.3 Effect of parecoxib on VTA dopamine cell activity in KMO K/O mice

In WT mice (n = 6-7), acute administration of parecoxib (25 mg/kg, i.v.), a selective COX-2 inhibitor and anti-inflammatory drug, did not alter the firing of VTA dopamine neurons during the 45 min recording period (Figure 9). However, parecoxib produced a robust decrease in firing of VTA dopamine neurons in KMO K/O mice (n = 6-8). Most notably, 2 out of 8 recorded cells in KMO K/O mice completely ceased firing within 30 min following administration. This effect might be related to the ability of COX-2 inhibitors to inhibit IDO, thus limiting the amount of available kynurenine for the production of KYNA (Basu et al., 2006; Lee et al., 2009). In addition, it was recently discovered that parecoxib acts as an inhibitor of KAT II (Zakrocka et al., 2019), although the contribution of this effect needs further investigation as previous studies suggests that parecoxib's effect can be counteracted by pretreatment of kynurenine (Schwieler et al., 2006).

In similarity to the haloperidol experiments, we saw no effect of parecoxib in WT mice, which is not entirely in agreement with similar *in vivo* electrophysiology experiments done with parecoxib in rats (Gessa et al., 2000; Schwieler et al., 2008, 2006; Schwieler and Erhardt, 2003). Clearly, a difference between species could explain this discrepancy. Notably, rats produce KYNA to a higher degree than mice (see section 4.3). Thus, VTA dopamine neurons in control rats may at baseline be under a more substantial control by KYNA, thereby showing a greater response to both parecoxib and haloperidol compared to WT mice.

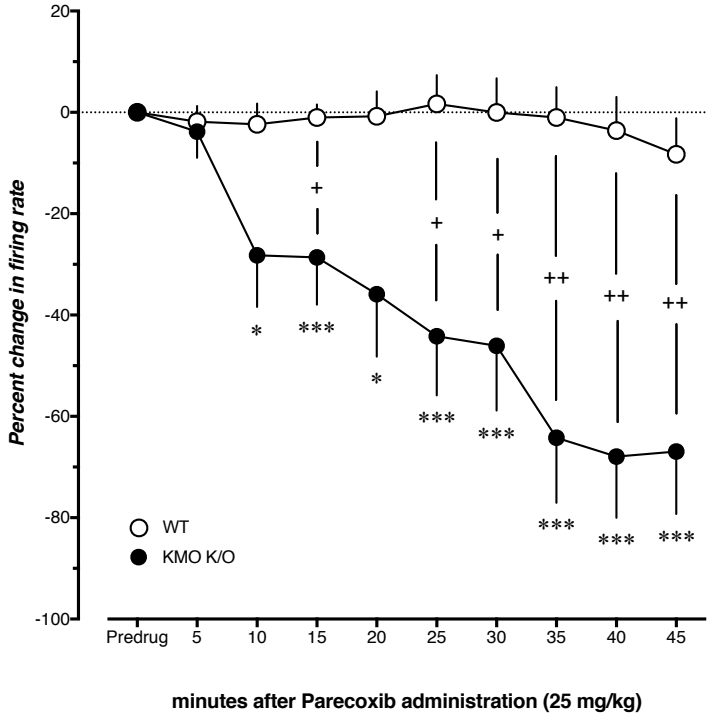

Figure 9. Effect of parecoxib (25 mg/kg, i.v.), administered over 45 min, on firing rate of VTA DA neurons in WT (n = 6-7) and KMO K/O (n = 6-8) mice. The percent change in firing rate at different timepoints was compared to the corresponding value before the administration of parecoxib (***p < 0.001, *p < 0.05, Mann-Whitney U test). The change in firing rate between WT and KMO K/O mice was compared at corresponding timepoints ($^{++}$p < 0.01, $^{+}$p < 0.05, Mann-Whitney U test). Each value is the mean ± SEM. All values were corrected for repeated measure (Bonferroni correction).

Furthermore, the largely different, and in some cases, opposite effect of drugs in this study highlights the importance of proper modeling when investigating new potential antipsychotic drugs. Taken together with the distinct schizophrenia-like behavioral phenotype previously described (Erhardt et al., 2017a), the KMO K/O model may provide exciting opportunities and serve as a valuable tool for investigation of novel treatment options for schizophrenia.

4.3 INDUCTION OF THE KYNURENINE PATHWAY IN RATS AND MICE FOLLOWING IMMUNE CHALLENGE (PRELIMINARY RESULTS)

An important factor for the development of a proper animal model is the choice of species. In this regard, KYNA production, and the activity of the kynurenine pathway appears to differ between species (Allegri et al., 2003a, 2003b; Fujigaki et al., 1998). However, the difference in brain kynurenine metabolism between species is not that well described, and even less so the influence of immune activation. In order to gain some clarity in this matter, we injected radiolabeled [5-^{3}H]-kynurenine into the striatum of rats and mice and measured the percentage of formed metabolites. In addition, rats and mice received dual administration of LPS (0.83 mg/kg or 0.5 mg/kg, respectively) or sterile saline.

We found that rats (n = 7) showed an overall increased metabolism of [5-^{3}H]-kynurenine compared to mice (n = 7). LPS treatment increased the metabolism additionally in both rats (n = 5) and mice (n = 6), but significantly more in rats (Figure 10A; 2-way ANOVA, effect of

treatment p=0.0299, $F_{(1, 21)} = 5.424$, effect of species p = 0.0028, $F_{(1, 21)} = 11.43$). From the metabolism of [5-^{3}H]-kynurenine, rats generally produced more KYNA compared to mice, while LPS treatment caused an increased production of KYNA in both species (Figure 10B; 2-way ANOVA, effect of treatment p < 0.0001, $F_{(1, 21)} = 27.52$, effect of species p < 0.0001, $F_{(1, 21)} = 47.74$, interaction p = 0.0227, $F_{(1, 21)} = 6.050$). Although no significant differences could be observed in 3-HK production (Figure 10C, the ratio between KYNA and 3-HK was elevated in rats compared to mice in both treatment groups and LPS caused a robust increase (Figure 10D; 2-way ANOVA, effect of treatment p < 0.0001, $F_{(1, 21)} = 32.74$, effect of species p < 0.0001, $F_{(1, 21)} = 45.85$, interaction p = 0.0005, $F_{(1, 21)} = 17.00$). Notably, the largest increase in KYNA:3HK ratio was observed in LPS treated rats, which was the only group with a ratio above 1, indicating a preference towards KYNA production.

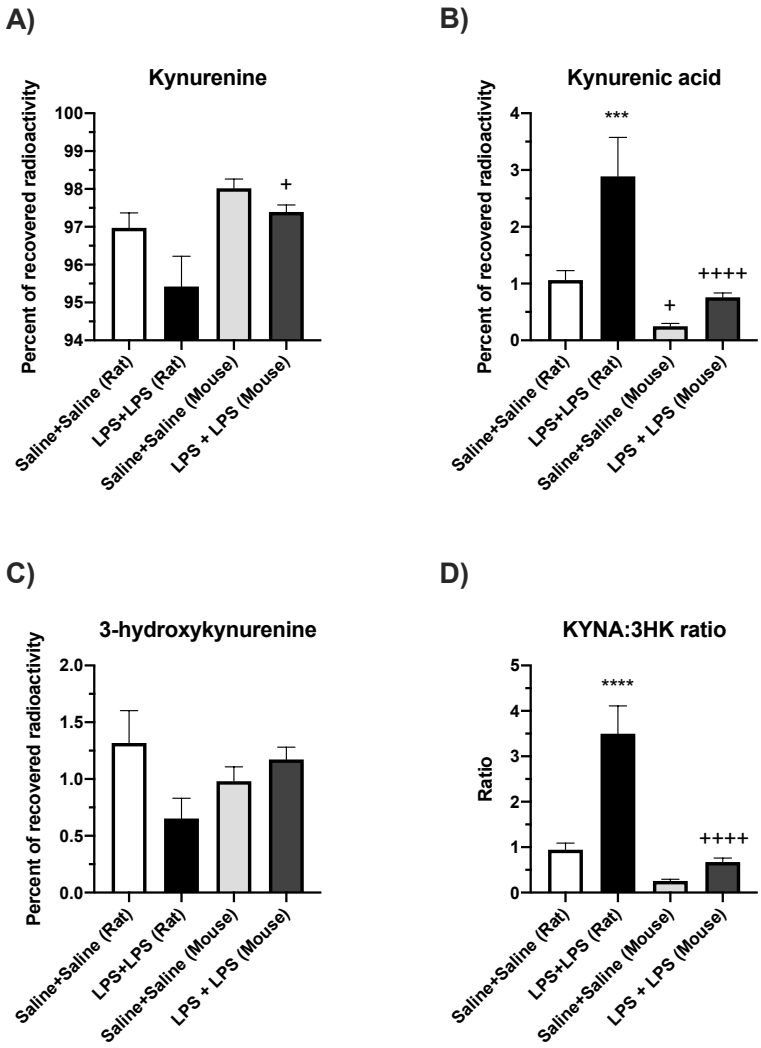

Figure 10. Percent of total recovered radioactivity identified as A) kynurenine, B) KYNA and C) 3-hydroxykynurenine and D) KYNA:3HK ratio in rats and mice treated with dual administration of either sterile saline or LPS. Effect of treatment, species and interaction was analyzed using 2-way ANOVA with Tukey's multiple comparisons test *post-hoc*. $p^{***}<0.001$, $p^{****}<0.001$ vs. corresponding Saline+Saline group, $p^{+}<0.05$, $p^{++++}<0.0001$ vs. corresponding rat group

Our results highlight the differences in brain kynurenine metabolism in two species often used to investigate mechanisms for psychiatric disorders and the evaluation of drugs. As such, it is essential to carefully consider the model of choice based on the question at hand. For instance, for testing a drug aimed at reducing KYNA, rats would be preferable to mice, while investigations on the QUIN producing branch of the kynurenine pathway might be better suited in mice. The observation that mice to a larger extent produce 3-HK compared to rats is in line with previous observations of increased activity of KMO in the periphery in mice compared to rats (Allegri et al., 2003b). Possibly, this difference in basal KYNA production could explain our previous electrophysiological results, where we see differences in response to parecoxib and haloperidol in control mice compared to what has previously been described in rats (see section 4.2)

Furthermore, previous studies have shown increased brain KYNA levels following dual-LPS challenge (Larsson et al., 2016; Oliveros et al., 2017b). However, the origin of this phenomenon has been unclear. The increased kynurenine pathway activity following LPS has previously been thought to mainly depend on activation of the initial enzymes IDO (O'Connor et al., 2009) or possibly TDO as a result of increased cytokine signaling (Sellgren et al., 2016). Although the contribution of the initial enzymes should not be disregarded, the present result indicates that kynurenine metabolism beyond this step is of high relevance. In addition, present results show that kynurenine metabolism is still affected 24 hours after the last LPS administration, demonstrating that prolonged increase in brain KYNA levels after a dual-LPS challenge is not exclusively a result of a robust initial increase that slowly declines. Although the dual-LPS model produced similar effects in both rats and mice in this study, LPS-treated rats were the only group preferentially producing KYNA rather than 3-HK, strongly arguing for important species differences.

4.4 EFFECT ON BEHAVIOR FOLLOWING DUAL ADMINISTRATION OF LPS (PAPER III)

Immune challenge by LPS has previously been shown to produce anxiety- and depressive-like phenotype in mice (Dantzer et al., 2008; Remus and Dantzer, 2016) as well as cognitive deficits (Imbeault et al., 2019). The origin of these behavioral abnormalities is thought to be caused by activation of the kynurenine pathway with increased production of QUIN (Connor et al., 2008; O'Connor et al., 2009; Salazar et al., 2012; Walker et al., 2013). Indeed, increased QUIN has been proposed to produce symptoms of depression through its action as a NMDA receptor agonist (Bay-Richter et al., 2015; Cui et al., 2019; Erhardt et al., 2013; Murrough et al., 2017; Walker et al., 2013). However, dual, rather than single, administration of LPS increases brain KYNA and produces long-lasting cognitive deficits in mice (Larsson et al., 2016; Oliveros et al., 2017b; Peyton et al., 2019). As KYNA is known to produce schizophrenia-like symptoms, we decided to investigate the effect of dual LPS administration (0.83 + 0.83 mg/kg, i.p.) on behaviors relevant for schizophrenia in mice.

4.4.1 Effect of LPS in locomotor activity test

During the last habituation session, we measured baseline locomotor activity and open-field behavior. LPS treated mice (n = 19) showed reduced locomotion (Figure 11A, $F_{(1,36)} = 27.44$, $p < 0.0001$) and time spent in the corners (Figure 11B, $F_{(1,36)} = 12.52$, $p = 0.0011$) while time spent in the center of the arena was reduced (Figure 11C, $F_{(1,36)} = 18.82$, $p = 0.0001$) compared to saline-treated mice (n = 19). Taken together, these observations point to a reduced willingness to explore and anxiety-like behaviors in LPS treated mice.

Mice treated with LPS (n = 9) showed an increased response to D-amphetamine (5 mg/kg, i.p.) with a stronger elevation of locomotion, horizontal activity, vertical activity and centre activity from baseline compared to saline-treated mice (n = 11; Figure 12). The increased sensitivity to D-amphetamine is indicative of a psychosis-like behavior, and is in line with clinical findings showing enhanced dopamine release and increased locomotion in response to amphetamine (Laruelle et al., 1996; Laruelle and Abi-Dargham, 1999; Perry et al., 2009). In addition, enhanced dopamine release has previously been found as a result of LPS treatment in both mice and humans (Petrulli et al., 2017; Van Heesch et al., 2014). Although not measured here, we have previously shown that LPS treatment increases brain dopamine metabolism, and that this effect was more pronounced following dual administration (Larsson et al., 2016).

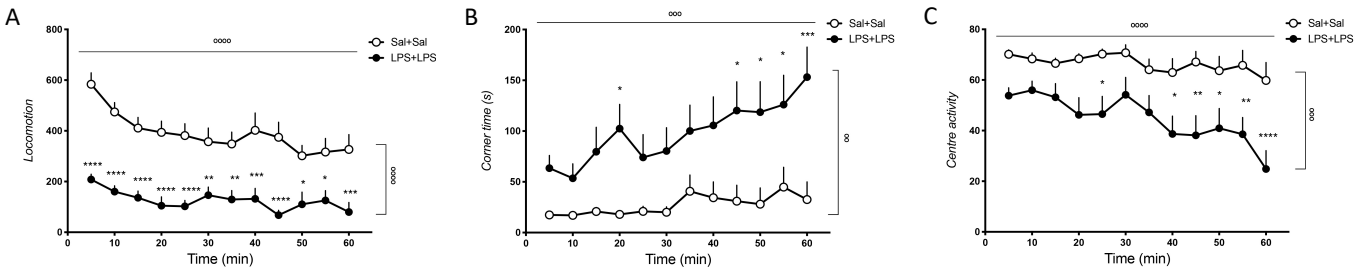

Figure 11. Base locomotor activity in the open-field for dual-LPS and saline treated mice. A) Locomotion, B) Corner time, C) Centre activity. n=19 per group. $^{ooo}p < 0.001$, $^{oooo}p < 0.0001$ repeated measures two-way ANOVA. *p < 0.05, **p < 0.01, ***p < 0.001, ****p < 0.0001 vs. saline treated group. Bonferroni *post-hoc*

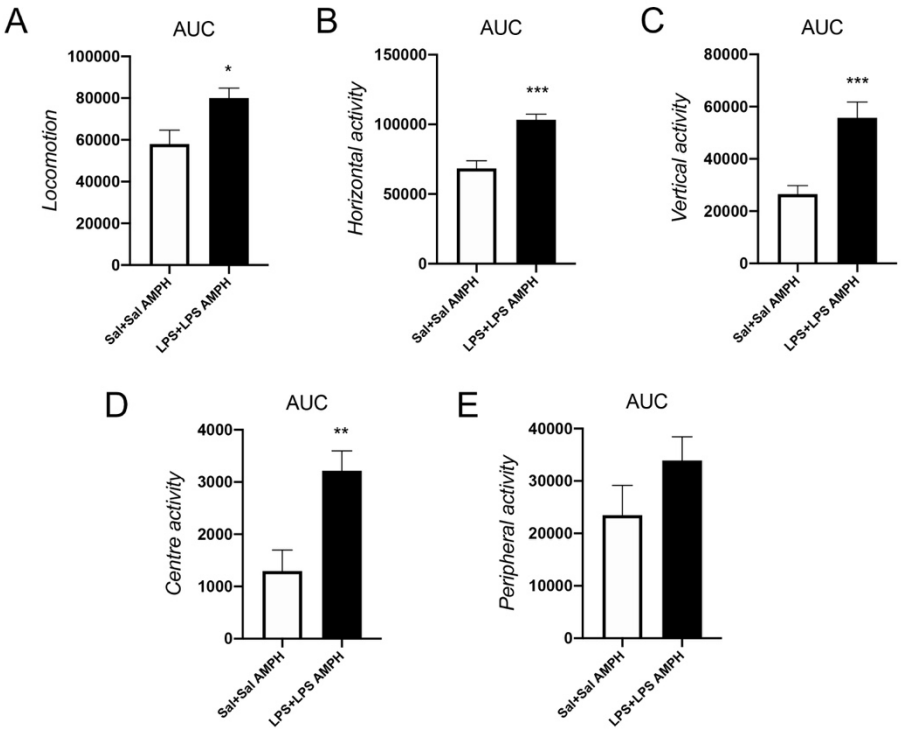

Figure 12. Area under the curve (AUC) of A) locomotion, B) horizontal activity, C) vertical activity, D) centre activity, and E) peripheral activity in response to D-amphetamine administration. n = 11 Sal+Sal, n = 9 LPS+LPS. *p<0.05, **p<0.01, ***p<0.001 unpaired t-test.

4.4.2 Effect of LPS on learning and memory

The effect of LPS on learning and memory formation was assessed using the trace fear conditioning paradigm. Mice receiving dual administration of LPS (n = 11) exhibited decreased freezing both in the context- (Figure 13A, $F_{(1,13)} = 5.279$, $p = 0.0388$) and cue-dependent test (Figure 13B, $F_{(1,13)} = 7.668$, $p = 0.0159$) 72 hours after learning compared to saline-treated mice (n = 9). These results indicate cognitive dysfunctions associated with learning in mice receiving dual-LPS, in line with previous studies (Oliveros et al., 2017b; Peyton et al., 2019). However, no differences between treatments were seen in spatial working memory using the Y-maze paradigm, with the exception of the number of total arm entries, potentially indicating a reduced will to explore or reduced motility. Thus, the cognitive deficits caused by dual-LPS are subject to further investigations.

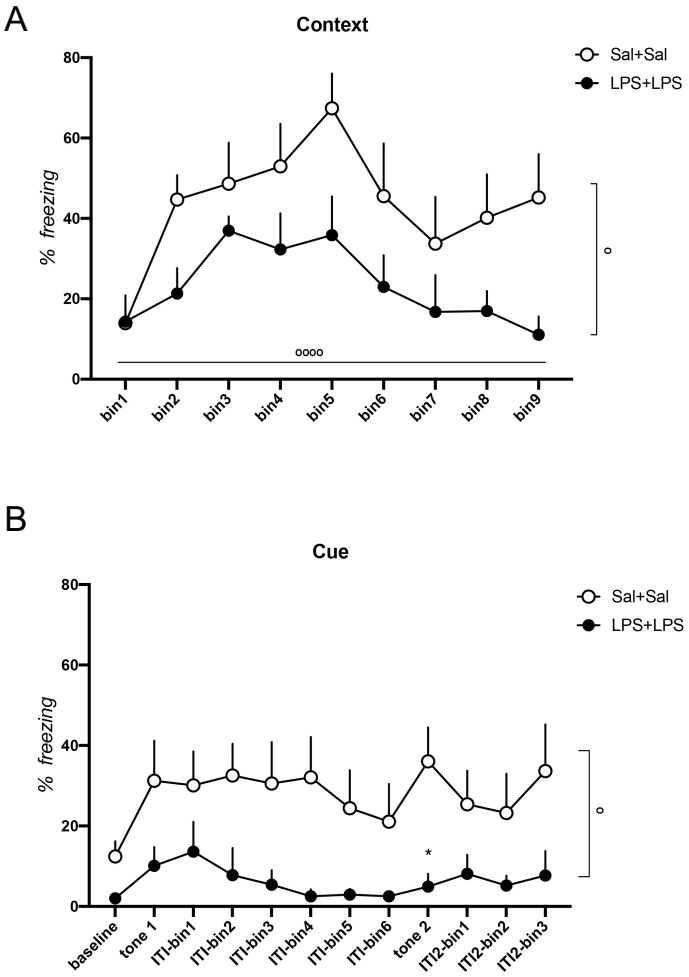

Figure 13. Percent of time spent freezing during A) contextual memory testing and during B) testing for tone-cued memory. n = 11 Sal+Sal, n = 9 LPS+LPS. ºp < 0.05, repeated measures two-way ANOVA. *p < 0.05, *post-hoc* Bonferroni.

4.5 FUNCTIONAL ASPECTS OF GRK3 (PAPER IV)

A primary trigger for the kynurenine pathway and production of KYNA in the brain is the immune system. However, the specific pathways leading to this phenomenon in patients is shrouded. One possibility is genetic variations that in one way or another converge in the activation of pro-inflammatory cytokines, activating glial cells to produce KYNA in the brain (Sellgren et al., 2016). Here we propose another such pathway, where expression of GRK3 regulates brain KYNA levels through immune activation and induce behavioral deficits and biochemical alterations associated with psychosis.

4.5.1 Attentional deficits and psychosis-like behavior in Grk3$^{-/-}$ mice

In the Y-maze paradigm, Grk3$^{-/-}$ mice showed the same number of spontaneous alternations as WT (+/+), but increased same arm returns (Figure 14A-B) indicating attentional deficits. However, Grk3$^{-/-}$ mice showed no other cognitive deficits and only subtle signs of anxiety in the open-field test. Furthermore, Grk3$^{-/-}$ mice displayed sensorimotor gating deficits in PPI (Figure 14C) without a difference in startle magnitude compared to WT (Figure 14D). In addition, Grk3$^{-/-}$ mice were more sensitive to the effects of D-amphetamine in the locomotor activity test (Figure 14E), and with regard to striatal dopamine release (Figure 14F). In line with these results, Grk3$^{-/-}$ mice showed an increased number of spontaneously active VTA dopamine neurons with faster firing frequency, but unchanged burst firing rate (Figure 14G-I). Taken together, these results primarily indicate a psychosis-like phenotype with an increased dopaminergic tone, similar to what has previously been described in psychosis.

4.5.2 Kynurenine pathway activity in Grk3$^{-/-}$ mice

Only a significant elevation of hippocampal kynurenine levels was observed in Grk3$^{-/-}$ mice compared to WT (Figure 15B). However, microdialysis revealed an increased accumulation of KYNA after administration of probenecid (200 mg/kg, i.p.; Figure 15E), blocking the efflux of KYNA from the brain, indicating a higher turn-over rate of KYNA. This effect could be mediated through endogenous IL-1β, which was found to be robustly increased in Grk3$^{-/-}$ mice (Figure 16A). Thus, intracerebroventricular injections of IL-1β (0.5 ng) produced an increase of hippocampal KYNA in WT mice within 6 hours (Figure 16B), as well as deficits in PPI (Figure 16C). Hence, the disrupted PPI seen in Grk3$^{-/-}$ mice could likely arise as a result of increased IL-1β, subsequently leading to increased KYNA (Erhardt et al., 2004).

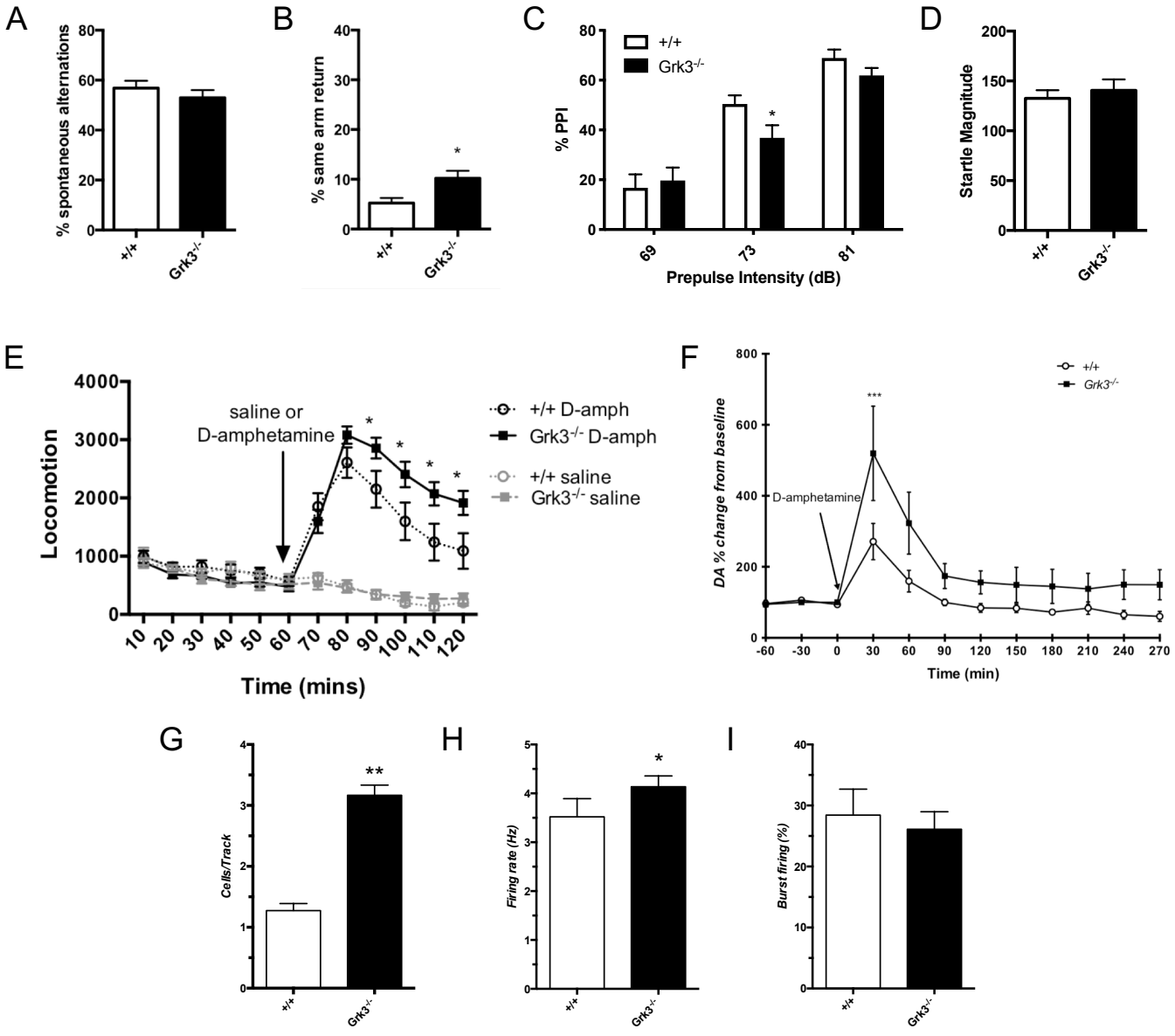

Figure 14. Working memory was assessed by calculating the A) % spontaneous alternations (p=0.37, Mann-Whitney) and B) the % same arm return (p=0.011, Mann-Whitney) in Grk3$^{-/-}$ (n=20) and +/+ (n=19) mice. C) Deficits in prepulse inhibition are observed in Grk3$^{-/-}$ mice (effect of prepulse intensity $F_{(2,74)}$=134.9, p<0.0001; effect of genotype $F_{(1, 37)}$=1.271, p=0.27; prepulse intensity x genotype interaction $F_{(2,74)}$=4.20, p=0.019; *p<0.05 *post-hoc* LSD, +/+ n=19, GRK3$^{-/-}$ n=20) but startle magnitude is similar (D +/+ 132.5 ± 8.2, GRK3$^{-/-}$ 140.6 ± 11.0, p=0.56, t-test). Grk3$^{-/-}$ mice show higher sensitivity to the locomotor effects of D-amphetamine (5mg/kg) (effect of time post-amphetamine $F_{(5,140)}$=18.54, p<0.0001; effect of genotype $F_{(1,28)}$=4.94, p=0.034; interaction $F_{(5,140)}$=2.95, p=0.014, +/+ n=13 amphetamine, Grk3$^{-/-}$ n=17 amphetamine, *p<0.05 *post-hoc* LSD). F) Accumulation of striatal dopamine induced by amphetamine (2 mg/kg) in Grk3$^{-/-}$ mice (n = 5) and wildtype controls (n = 5) measured by *in vivo* microdialysis. (effect of time $F_{(11,88)}$=13.52, p<0.0001; effect of genotype $F_{(1,8)}$=4.079, p=0.078, time x genotype interaction $F_{(11,88)}$=2.21, p=0.020 repeated measures 2-way ANOVA, *** p<0.001 *post-hoc* Bonferroni). *In vivo* electrophysiology of dopaminergic cells in the VTA shows increased G) number of detectable cells per track (Grk3$^{+/+}$ 1.27 ± 0.31 n=7 mice, Grk3$^{-/-}$ 3.17 ± 0.17 n=6 mice, p=0.0012 Mann-Whitney) and H) firing rate (Grk3$^{+/+}$ 3.52 ± 0.37 n=35 cells, Grk3$^{-/-}$ 4.13 ± 0.22 n=78 cells, p=0.043, Mann-Whitney) but no change in I) burst firing (Grk3$^{+/+}$ 28.42 ± 4.27 n=35, Grk3$^{-/-}$ 26.08 ± 2.87 n=78, p=0.56, Mann-Whitney)

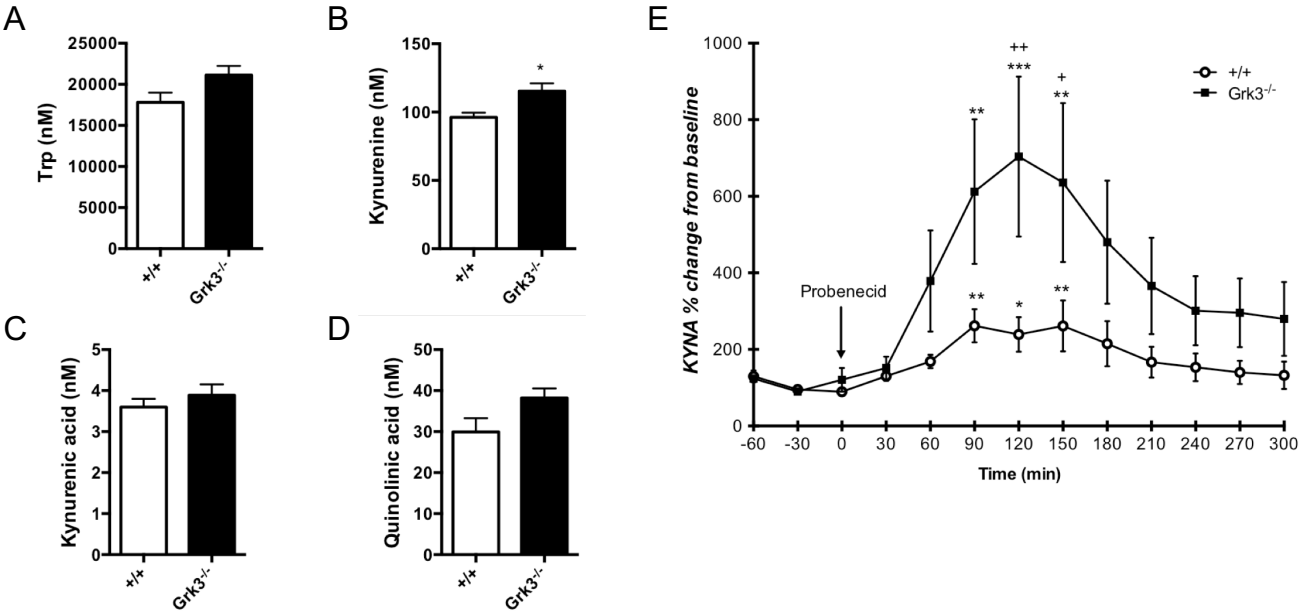

Figure 15. Levels of A) tryptophan (+/+ 17806 ± 1193 nM, -/- 21116 ± 1113 nM, p = 0.07 t-test) B) kynurenine (+/+ 96.1 ± 3.3 M, -/- 115.2 ± 5.7 nM, p = 0.01 t-test) C) kynurenic acid (+/+ 3.6 ± 0.2 nM, -/- 3.9 ± 0.3 nM, p = 0.40 t-test) D) quinolinic acid (+/+ 30.0 ± 3.3 nM, -/- 38.2 ± 2.3 nM, p = 0.07 t-test) E) increased accumulation in hippocampal KYNA over time. n = 8 Grk3$^{+/+}$, n = 7 Grk3$^{-/-}$

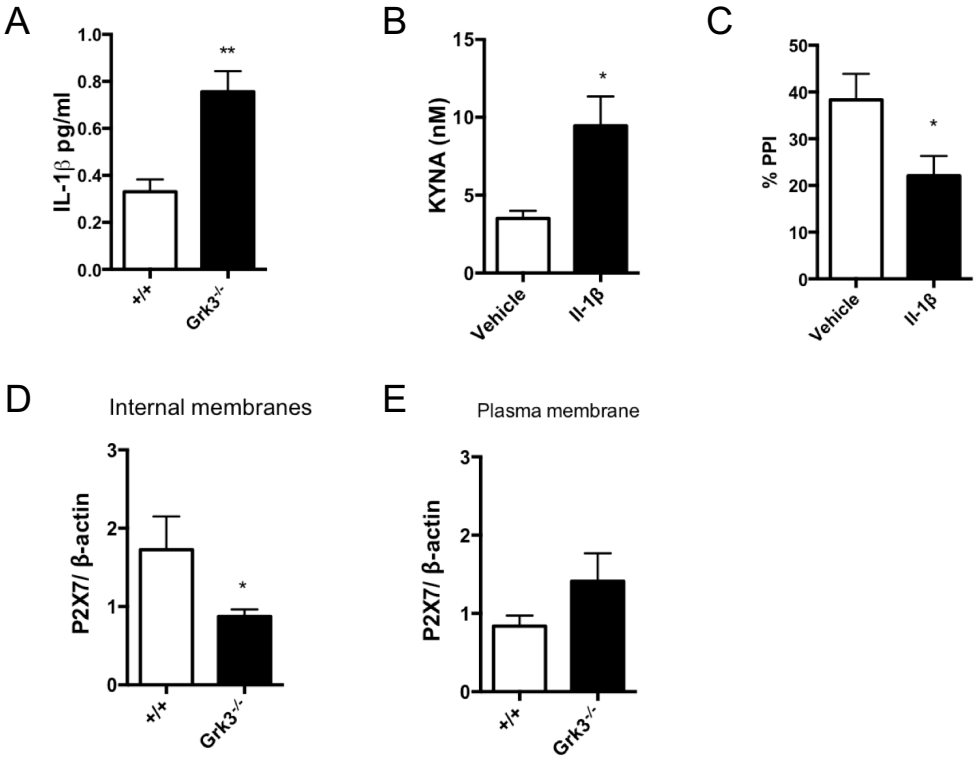

Figure 16. A) Increased levels of IL-1β are detected in hippocampus of Grk3$^{-/-}$ compared to controls (+/+ 0.33 ± 0.05 pg/mL -/- 0.76 ± 0.09 pg/mL, p = 0.0031, n = 5 per group, t-test) B) ICV administration of IL-1β increases KYNA levels (+/+ 3.5 ± 0.5 nM n = 8 vs. -/- 9.5 ± 1.9 nM n = 7 , p = 0.019, t-test) C) Administration of IL-1β leads to PPI deficits (veh 38.3 ± 5.2 %, n = 8, Il 22.1 ± 4.0 %, n = 9, p = 0.02, t-test) D) Decreased P2X7R expression on internal membranes (+/+ 1.73 ± 0.43 n = 5, -/- 0.87 ± 0.09 n = 6, p = 0.017 Mann-Whitney) and a non-significant increase in plasma membrane (+/+ 0.84 ± 0.13 n = 5, -/- 1.41 ± 0.36 n = 6).

To further elucidate the connection between GRK3 and IL-1β we studied a possible involvement of the purinergic P2X7 receptor, mainly expressed in glial cells and known to interact with GRK3 (Feng et al., 2005). We observed a significant reduction of P2X7 receptor expression in the internal membrane fraction compared to WT in brain (Figure 16D), indicating reduced internalization of the receptor. Interestingly, the P2X7 receptor is involved in the release of IL-1β, through activation of caspase-1 (Giuliani et al., 2017; Solle et al., 2001). Based on these findings, a reasonable hypothesis for the psychosis-like phenotype seen in Grk3$^{-/-}$ mice is that reduced GRK3 expression results in reduced internalization of the P2X7 receptor, leading to activation of caspase-1 and, in turn, increased production of IL-1β, activating the kynurenine pathway and producing symptoms related to psychosis.

4.5.3 Human genetic studies

Based on that hypothesis, we looked at human genetic data. Specifically, a SNP located in the *GRK3* promotor gene was used to assess human GRK3 expression. In a sample of 48 healthy individuals who underwent lumbar puncture, an association between low predicted GRK3 expression and high CSF KYNA was observed (Figure 17A). Moreover, in a sample of 70 patients suffering from bipolar disorder, decreased predicted GRK3 expression was associated with increased KYNA and a history of psychosis (Figure 17B).

Taken together, our data reveal an essential role for GRK3 in psychosis, which is supported both by experimental and human data.

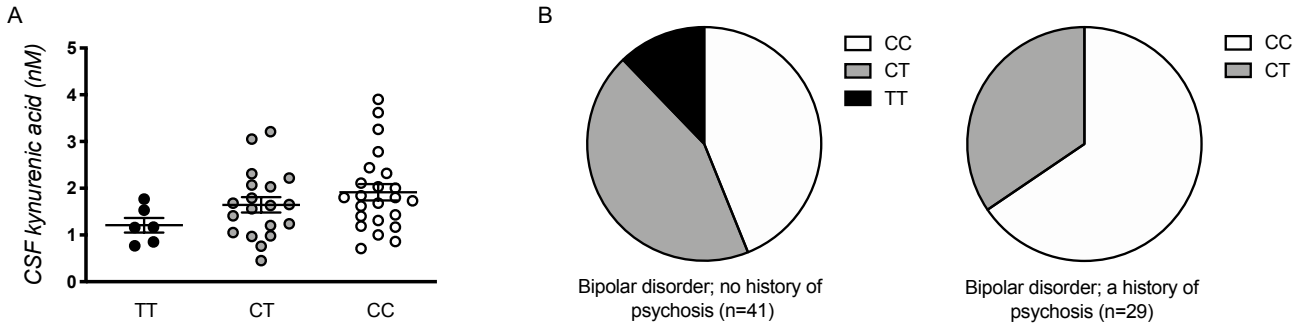

Figure 17. The SNP rs478655 (MAF: 0.29) was used to represent a *cis* acting eQTL in the *Grk3* promoter with TT genotype denoted as high *GRK3* RNA expression (black circle), CT as medium *GRK3* RNA expression (grey circle), and CC as low *GRK3* RNA expression (white circle). A) CSF levels of KYNA, in a sample of 48 healthy individuals, as a result of genetically predicted *GRK3* RNA expression (β = 0.051, *P* = 0.026). B) Distribution of subjects with high, low, and medium prediction scores for *GRK3* RNA expression in a sample of 70 bipolar disorder subjects. Subjects with a history of psychosis also had higher predicted *Grk3* RNA expression (OR = 2.6; 95% CI: 1.09-6.16).

4.6 METABOLIC BIOMARKERS ASSOCIATED WITH DISEASE AND TREATMENT IN PSYCHOSIS (PAPER V)

In an effort to elucidate disease mechanisms and provide biological biomarkers for diagnosis and treatment response prediction, serum and CSF from 25 FEP patients and 21 healthy controls included in KaSP were analyzed at baseline and 1.5-year follow-up using global untargeted metabolomics. We used Ingenuity Pathway Analysis (IPA) to connect metabolic differences to canonical pathways and mechanisms.

Patients and healthy controls did not significantly differ with regards to gender, age or body mass index (Table 1). However, nicotine consumption was different between the groups.

As expected, we found that at follow-up patients improved with regards to their psychotic symptoms, whereas they showed little or no improvement of the negative symptom domain and cognitive function.

4.6.1 Disease-associated metabolites

Disease-associated metabolites were considered as those differing between patients and healthy controls at baseline. In total, we identified 92 disease-associated metabolites in serum and 22 in the CSF. For serum, IPA analysis revealed canonical pathways, including tryptophan degradation and phenylalanine degradation. Pathological analysis revealed that the identified metabolites and associated canonical pathways are implicated in cell-to-cell signaling, small molecule biochemistry, the cell cycle, and gene expression (Figure 18A-B).

In the CSF, IPA demonstrated roles for identified metabolites in multiple canonical pathways, including acetyl-CoA synthesis, serotonin synthesis and signaling, and calcium signaling. Comprehensive network and pathological analysis revealed that these disease-associated metabolomic differences and canonical pathways are related to the function of multiple proteins and molecules associated with nervous system function, including multiple serotonin receptor subtypes and inflammation, including immune-related receptors, TNF, as well as kynurenic acid and the endocannabinoid 2-arachidonylglycerol (Figure 18C-E). Serotonin was identified as the metabolite with the strongest association to psychosis, in line with several findings implicating serotonin in schizophrenia (Eggers, 2013; Li et al., 2013).

Table 1: Demographic and Clinical Characteristics of Subjects at Baseline and 1.5 Year Follow-Up.

Characteristic	MEAN ± SD			
	Healthy Controls	FEP Patients	Healthy controls at 15y follow-up	Patients at 1.5y follow-up
	(n=21)	(n=25)	(n=21)	(n=25)
Demographic Characteristics				
Age	25.4 ± 5.9	31.4 ± 9.8	26.9 ± 5.9	32.9 ± 9.8
Gender (M/F)	9/12	13/12	9/12	13/12
Years of education		13.5 ± 3.2		13.8 ± 3.4
Basic Clinical Characteristics				
BMI (kgm^{-2})	23.0 ± 3.3	23.0 ± 2.6	23.0 ± 3.1	23.9 ± 2.9
Nicotine %	4.8%	24.0%	9.5%	28.0%
Smoking %	0.0%	8.0%	0.0%	12.0%
DUP (months)		14.5 ± 11.0		
Under antipsychotic treatment %	0.0%	52.0%	0.0%	60.0%
Under antidepressive treatment %	0.0%	20.0%	0.0%	32.0%
Psychiatric Characteristics				
PANSS				
Positive		19.7 ± 6.2		11.7 ± 3.6*
Negative		17.5 ± 8.5		13.9 ± 6.0
General		38.0 ± 11.6		28.8 ± 7.9*
Total		75.2 ± 23.2		54.4 ± 14.2*
Level of Functioning				
GAF Symptom		32.6 ± 8.7		59.2 ± 18.8*
GAF Function		39.8 ± 12.3		65.2 ± 17.0*
CGI Scores		4.5 ± 1.2		2.6 ± 1.5*
Cognitive Characteristics				
Speed of Processing				
TMT, Part A (sec)		35.7 ± 14.9		35.4 ± 24.2
Fluency Test (# named)		21.6 ± 5.8		21.7 ± 6.8
BACS-SC (# correct)		44.2 ± 11.8		47.5 ± 14.3
Attention/Vigilance				
CPT-IP (detectability)		2.1 ± 0.7		2.4 ± 0.6
Working Memory				
LNS (# correct trials)		12.8 ± 3.3		12.9 ± 2.9
WMS-III SS (Sum forward and backward scores)		16.3 ± 3.2		15.5 ± 3.3
Verbal Learning				
HVLT-R (Total number words recalled over 3 trials)		22.8 ± 5.4		22.0 ± 6.1
Visual Learning				
NAB (3-trial total learning score)		18.4 ± 6.7		19.6 ± 5.6
BVMT-R (3-trial total recall score)		21.8 ± 7.0		24.4 ± 6.7
Social Cognition				
MSCEIT-ME (branch score)		90.0 ± 11.7		90.6 ± 10.4

Note: SD, standard deviation; BMI, body mass index; DUP, duration of untreated psychosis; PANSS, Positive and Negative Syndrome Scale Score; GAF, Global Assessment of Function; CGI, Clinical Global Impression; TMT, Trail Making Test; BACS-SC, Brief Assessment of Cognition in Schizophrenia-Symbol Coding Subtest; CPT-IP, Continuous Performance Test-Identical Pairs version; LNS, Letter Number Span test; WMS-III SS, Wechsler Memory Scale-3rd ed. Spatial Span subtest; HVLT-R, Hopkins Verbal Learning Test-Revised; NAB, Neuropsychological Assessment Bat.; BVMT-R, Brief Visuospatial Memory Test-Revised; MSCEIT-ME, Mayer-Salovey-Caruso Emotional Intelligence Test-Managing Emotions branch.
$p^* < 0.05$, t-test

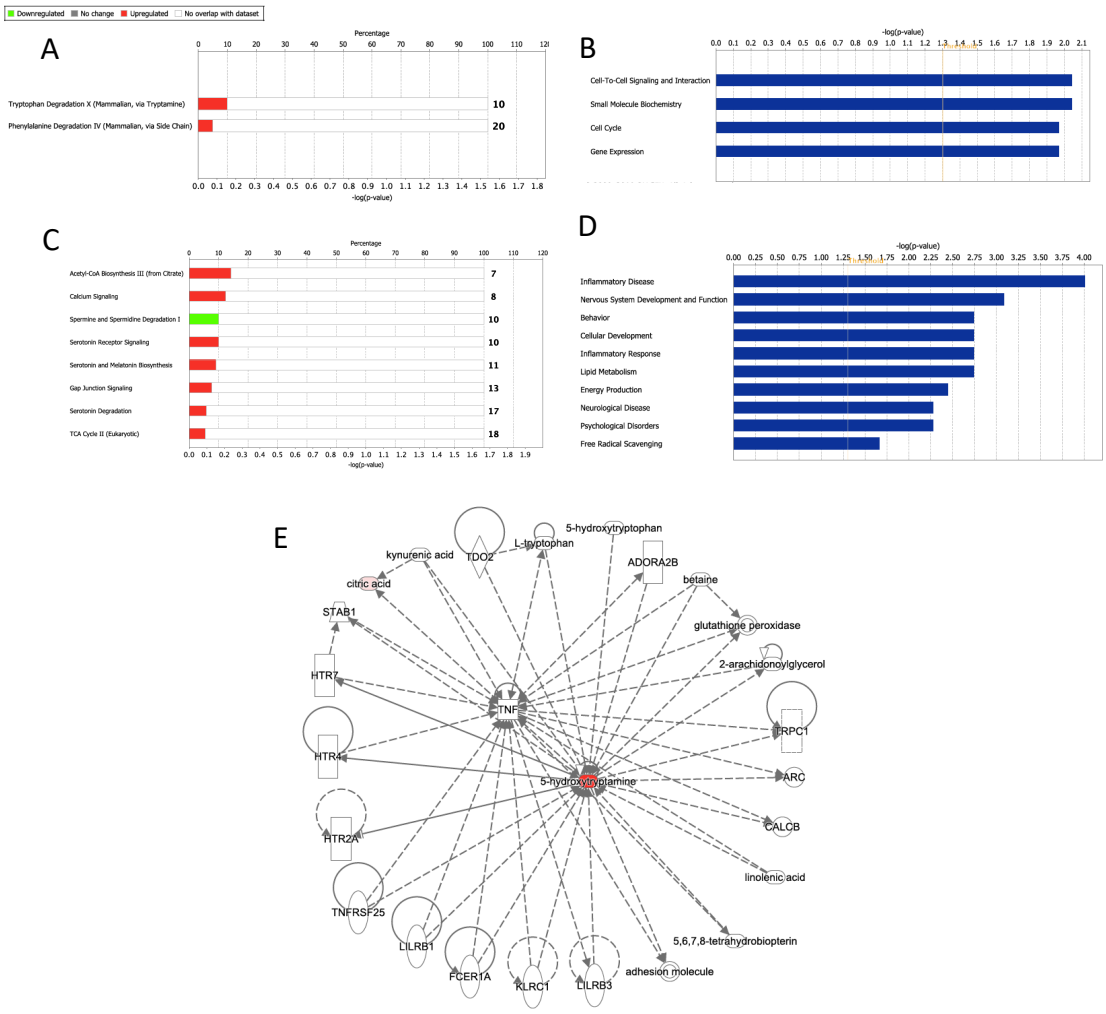

Figure 18. Ingenuity Pathway Analysis revealed canonical pathway and disease mechanisms for which disease-associated metabolites in A-B) serum and C-D) CSF were associated with. E) Network analysis of metabolites and proteins from CSF.

4.6.2 Treatment-associated metabolites

Metabolites found to differ in patients at follow-up compared to baseline were considered treatment-associated metabolites. In total, 87 treatment-associated metabolites were found in serum and 229 in CSF. In serum, IPA implicated these metabolites to be involved in pathways such as protein degradation and biosynthesis, tRNA charging, nNos signaling in neurons and PI3K/Akt signaling. Further, the metabolites and pathways were implicated in molecular networks associated with proinsulin, EGFR, and nitric oxide, and linked to physiological and pathological functions such as amino acid metabolism, organismal development, inflammation, behavior, nervous system function and development, as well as neurological diseases (Figure 19A-B, E). The association with insulin- and growth-factor signaling may, atleast in part, account for the metabolic side-effects that are associated with antipsychotic treatment.

With regards to the metabolites found in CSF, IPA found these to be involved in tRNA charging as well as several pathways associated with amino acid metabolism. Network and pathological analysis revealed that the metabolites, and their associated canonical pathways are implicated in protein synthesis, amino acid metabolism, inflammation and nervous system function, mediated via the relationship of identified metabolites to important signaling networks including Akt/PI3K, NFκB, ERK1/2, TNF, insulin, and the kynurenine pathway (Figure 19C-D).

In conclusion, we lay the foundation for further work to associate metabolites to clinical parameters, which may reveal metabolites that can predict treatment outcome, give prognosis, and characterize disease-types based on the symptomatic picture. Interestingly, the main pathways implicated in our analyses involved immune signaling and tryptophan degradation, in line with our previous findings (Erhardt et al., 2017b).

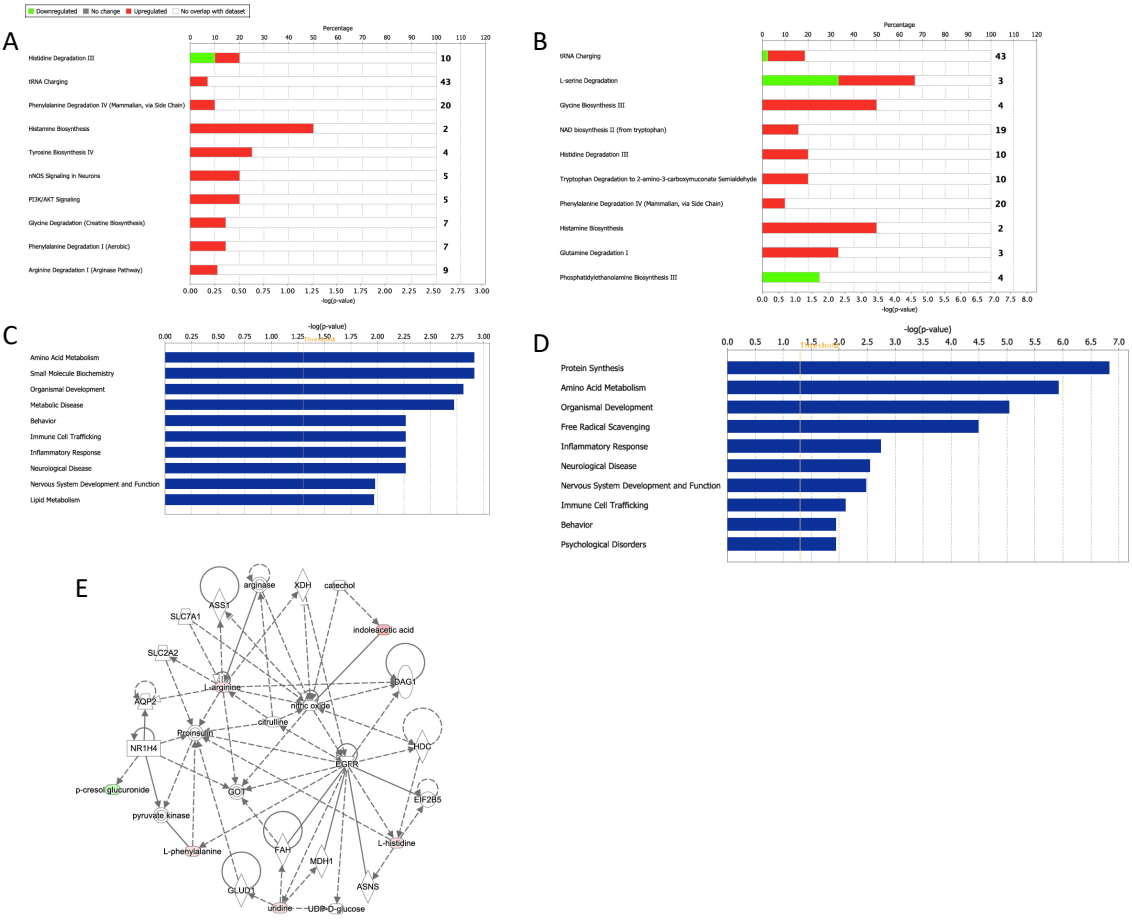

Figure 19. Ingenuity Pathway Analysis revealed canonical pathway and disease mechanisms for which treatment-associated metabolites in A+C) serum and B+D) CSF were associated with. E) Network analysis of metabolites and proteins from serum.

5 GENERAL DISCUSSION

The etiology of schizophrenia seems nothing less than multifactorial, where several factors may converge into creating the symptomatic picture seen in patients. Through-out this thesis, I suggest how different mechanisms converge into a common denominator, the kynurenine pathway, resulting in increased brain KYNA levels and schizophrenia-like symptoms.

Thus, genetic deletion of the gene encoding for KMO, can directly affect central levels of KYNA and produce symptoms associated with schizophrenia in mice (**Paper II**; Erhardt et al., 2017a; Giorgini et al., 2013). The model is anchored to findings in humans, were genetic variation and expression of KMO is associated with increased CSF KYNA levels and schizophrenia and psychotic features in bipolar disorder (Aoyama et al., 2006; Ekelund et al., 2004; Holtze et al., 2012, 2011; Lavebratt et al., 2014; Sathyasaikumar et al., 2011; Wonodi et al., 2011). However, complete deletion of KMO is a more severe form of what is seen in humans, which is also reflected by the greatly elevated levels of brain KYNA seen in the KMO K/O mice. Nevertheless, the KMO K/O model proves an important principle by which chronically elevated levels of brain KYNA can produce a schizophrenia-like phenotype. Moreover, our electrophysiological studies on KMO K/O mice, showing that the response of midbrain dopamine neurons to antipsychotic drugs is dependent on endogenous KYNA levels, proves a critical concept with regards to drug discovery and evaluation of new treatment options for schizophrenia.

One short-coming of the KMO K/O model is the lack of direct involvement of the immune system, a key influencer of the kynurenine pathway. As such, for testing of drugs acting on the immune component of schizophrenia, such as minocycline, a model of inflammation would be more appropriate. Thus, we evaluated whether a dual administration of LPS, previously shown to produce a lasting increase in brain KYNA levels (Larsson et al., 2016), could also produce schizophrenia-like behaviors in mice (**Paper III**). We confirmed previous studies showing cognitive dysfunctions associated with learning in the dual-LPS model (Oliveros et al., 2017b) and found behaviors associated with positive and negative symptoms in this model as well. Although further characterization and validation are needed, the dual-LPS model offers exciting opportunities to investigate inflammatory components of elevated brain KYNA and schizophrenia. The main advantage of the dual-LPS model over the KMO K/O model is the more naturalistic induction of the kynurenine pathway, with a more realistic increase in brain KYNA, about 2-3 times more than saline-treated mice, compared to the very large increase seen in KMO K/O. Further, the KMO K/O model lacks an inflammatory

component, which has become increasingly apparent in schizophrenia (Müller, 2018). However, the dual-LPS model is limited as a rather acute induction of immune activation and brain KYNA, whereas the KMO K/O represents a more chronic setting.

As a middle-ground, we tested whether the $Grk^{-/-}$ mice could represent a chronic deficit causing an elevation in brain KYNA through inflammatory mechanisms (**Paper IV**). Based on our data, and available literature, we hypothesized that reduced GRK3 expression would reduce internalization of the P2X7 receptor, in turn causing increased activation of caspase-1 and production of IL-1β (Giuliani et al., 2017; Solle et al., 2001) to activate the kynurenine pathway (Zunszain et al., 2012). Although we were unsuccessful in finding increased brain KYNA levels in the $Grk^{-/-}$ mice, we found an elevated KYNA production, suggesting an increased turn-over rate of KYNA. Moreover, the $Grk^{-/-}$ mice showed an apparent psychosis-like phenotype, with deficits in PPI, and increased sensitivity to amphetamine, similar to what is seen in patients (Geyer et al., 2001; Laruelle and Abi-Dargham, 1999; Perry et al., 2009; Young et al., 2016). Human data further strengthened these findings, where we observed associations with GRK expression and CSF KYNA levels, and psychotic features in patients with bipolar disorder. However, the $Grk^{-/-}$ mice fail to present any other relevant symptoms of schizophrenia, e.g., negative symptoms or cognitive deficits.

The fact that the phenotype of $Grk^{-/-}$ mice appeared specific to psychosis-like behaviors, putatively caused by IL-1β, while the dual-LPS model shows behaviors indicative of negative symptoms and cognitive dysfunctions as well, points to the complex nature of the interaction between the immune system and the kynurenine pathway. This is also evident when considering the effect of LPS, where a single LPS challenge causes depressive-like behaviors associated with an increase in brain QUIN (Parrott et al., 2016; Remus and Dantzer, 2016; Walker et al., 2013), whereas a dual administration causes a more schizophrenia-like phenotype with increased brain KYNA (**Paper III**; Larsson et al., 2016; A. Oliveros et al., 2017). Notably, the effect does not appear to be related to the dose per se, but rather to the dual administration as larger single doses of LPS only causes modest changes in brain KYNA (Larsson et al., 2016), and dual administration causes cognitive deficits even at smaller doses (Peyton et al., 2019). The exact mechanism that distinguishes the dual from the single administration model, and how a single administration can lead to elevated QUIN, and dual to elevated KYNA, is still unclear. It has been shown that immune challenge leads to disruption of the blood-brain barrier, which theoretically would cause subsequent immune challenges to produce a more substantial effect in the brain (Erickson and Banks, 2011). Moreover, the level and duration of inflammation caused by single or dual-LPS might be

different, causing different cytokine-profiles to be produced, which may affect the kynurenine pathway differently. The questions and theories are numerous, and, clearly, further investigations are needed, and answering these questions would provide a more detailed understanding of the interaction between the immune system and the kynurenine pathway.

Nevertheless, the main effect of LPS on the kynurenine pathway is thought to be related to its ability to induce the initial and rate-limiting enzymes. In particular, the induction of IDO appears responsible for producing the depressive-like phenotype seen after a single administration (O'Connor et al., 2009; Salazar et al., 2012). However, results presented in this thesis suggest that alterations in kynurenine pathway metabolism following immune activation are rather related to metabolism after the initial step. Thus, intrastriatal injected kynurenine, thereby bypassing the initial step, was metabolized to a greater extent in animals receiving dual administration of LPS. Here, LPS caused an increase in KYNA formation comparable to whole-brain levels following LPS (i.e., 2-3 times increased KYNA levels; Larsson et al., 2016). These findings suggest that KMO and KAT might play a more significant role in kynurenine pathway activation following immune stimulation than previously thought.

It is important to note, that even though we see effects on the kynurenine pathway in the models tested in this thesis, we did not directly test whether KYNA was solely responsible for producing these phenotypes. For example, GRK3 is widely expressed in the brain and involved in many important functions that could influence our results, i.e. desensitization of a variety of receptors, including dopamine receptors (Gurevich et al., 2016). Further, LPS produces a broad systemic inflammation that does not solely affect the kynurenine pathway. Nevertheless, it seems reasonable to assume that elevation of KYNA can, at least in part, contribute to producing our phenotype.

One of the perhaps most important findings of the present thesis is that the dopaminergic response to existing and novel antipsychotic drugs is dependent on endogenous KYNA levels, indicating that the model of choice is crucial for investigating novel drugs. An example highlighting the importance of proper modeling and consideration of KYNA levels for studying schizophrenia, is the effects of COX-2 inhibitors such as parecoxib on dopaminergic neurotransmission. In rats, parecoxib effectively reduces brain KYNA levels and decreases the activity of VTA dopamine cells (Schwieler et al., 2008, 2006), while no effect in this regard was observed in WT mice (**Paper II**). This discrepancy is possibly explained by a different baseline production of KYNA in rats and mice, as shown in this thesis. Tentatively, in a situation of low endogenous KYNA levels, as seen in WT mice,

KYNA would have less influence in controlling dopamine firing, whereas higher levels may impact spontaneous dopamine firing to a larger extent. Accordingly, mice with elevated brain KYNA levels showed a marked reduction in VTA dopamine activity following the administration of parecoxib. Through its ability to lower brain KYNA, parecoxib can also alter the dopaminergic response to antipsychotic drugs (Schwieler et al., 2008), an interaction that ought to be of critical importance in clinical situations. Interestingly, COX-2 inhibitors have been tested clinically as an add-on therapy to conventional antipsychotics with varying results (Zheng et al., 2017). However, given the assumption that increased brain KYNA levels are the underlying cause of the symptoms, and that the COX-2 inhibitors are effective in lowering these, the addition of antipsychotics might, in this case, perhaps rather be negative, masking the true effect of COX-2 inhibitors. Accordingly, drugs aimed at lowering brain KYNA levels, such as COX-2 inhibitors, should be evaluated as a monotherapy first and foremost.

With regards to novel therapeutic strategies for schizophrenia, one of the most exciting prospects, in particular in the context of the present thesis, lies within specific inhibitors of KAT II, such as the PF-04859989. The drug has previously been shown to lower brain KYNA and improve cognitive functions (Kozak et al., 2014). In the present thesis, we show that PF-04859989 efficiently reduces the activity of VTA dopamine neurons through an action on the glycine-site of the NMDA receptor (**Paper I**). Although specific KAT II inhibitors have shown promising results in experimental studies in animals, it remains to be elucidated whether these drugs show antipsychotic actions in humans. Clearly, a prerequisite for a success in this regard, is that the elevated brain KYNA levels seen in patients contributes to causing the symptoms of schizophrenia (Erhardt et al., 2017b).

Although schizophrenia is generally considered a heterogenous disorder, one must bear in mind that specific NMDA receptor antagonists are able to reproduce the full scale of schizophrenia symptoms in healthy individuals (see section 1.1.1.3). On this basis, although the symptomatic picture might be heterogenous, one may argue that the pathophysiology of schizophrenia is relatively narrow where multiple factor may converge in a common mechanism, i.e., NMDA receptor hypofunction. Nevertheless, it may be naïve to assume elevation of brain KYNA as the pathophysiological cause for the entire population of patients with schizophrenia, and a KAT II inhibitor might not be advantageous for all patients. Thus, another challenge in the search for novel treatment strategies in schizophrenia is to distinguish patient groups. In order to do this, new tools must be developed, which rely on a biological basis rather than the subjective diagnostic tools available today, based on

interviews and patient experience. Here, metabolomics emerges as a valuable approach for the discovery of biomarkers to predict the outcome of a particular treatment, and to aid diagnosis. In this thesis, we start this work with a limited explorative study, and larger sample sizes are obviously needed to implement such a strategy in clinical settings. Similar efforts have previously been able to identify biomarkers and metabolomic fingerprints for predicting the outcome of acamprosate and sertraline treatment for alcohol use disorder, and depression, respectively (Hinton et al., 2017; Kaddurah-Daouk et al., 2011). In schizophrenia, a small preliminary study identified changes in lipids that correlated to acute effects of atypical antipsychotic treatment (Kaddurah-Daouk et al., 2007) while another identified metabolites associated to the response of risperidone (Xuan et al., 2011). However, these studies analyzed blood samples in more progressed patients who previously had received treatment, and only after a short period of treatment. In our analysis, we used a similar approach but in FEP patients with both serum and CSF at baseline and following 1.5 years of treatment (**Paper V**).

Interestingly, in our metabolomic analysis we found tryptophan metabolism along the kynurenine pathway as well as inflammatory processes to be implicated in the pathophysiology of schizophrenia as well as its treatment. However, although samples from very well-characterized patients, engaged in The Karolinska Schizophrenia Project were analyzed, our study, in similarity with previous metabolomics studies in schizophrenia, had an explorative and preliminary approach. Further validation with a larger sample size is needed to confirm our findings and to correlate the metabolites to clinical parameters.

One of the most common critiques against the role of KYNA in schizophrenia is that the levels measured in patients, although elevated, are too low to produce any significant neurological actions. However, one has to consider that the concentrations of KYNA that occur locally directly upon efflux are lowered vastly by diffusion. In addition, KYNA is produced mainly in astrocytes, which are tightly connected to synaptic sites and serve as crucial regulators of synaptic transmission. Thus, it seems likely that concentrations of KYNA are high enough to affect receptors within the vicinity of its release (Schwarcz and Stone, 2017).

In conclusion, the present thesis provides new information regarding how different mechanisms, such as genetic variations and immune activation, converge at the kynurenine pathway and causes schizophrenia-like phenotypes in animals as a result of increased brain KYNA. Our results are anchored in clinical findings where similar genetic variations and pathophysiological processes, like increased brain KYNA and immune activation, are associated with psychosis. The models used here may provide valuable tools for evaluating

novel treatment options for schizophrenia, and offer exciting opportunities for studying its pathophysiology. In addition, we provide an unbiased confirmation for the involvement of inflammation and the kynurenine pathway in schizophrenia through metabolomics.

6 ACKNOWLEDGEMENTS

Through-out my time as a student I have had the good fortune to meet and work with many wonderful and distinguished people.

First and foremost, I would like to thank my supervisors,

Professor **Göran Engberg**, for his broad knowledge, stress-free attitude and always taking the time to sit down and listen to my ideas and discuss everything from science to life in general. I have little doubt in my mind that I have him to thank for much of my development as a scientist and that a better supervisor is hard to find.

Professor **Sophie Erhardt**, a true inspiration for anyone in science, for her openness and always willing to discuss and listen, despite her busy schedule.

Dr. **Lilly Schwieler**, for always taking the time to answer my questions, no matter how small and stupid they may be, and running between her office and the lab to help me identifying dopamine neurons.

Dr. **Simon Cervenka**, for his always kind attitude, inspiring talks and all help with everything related to clinical research.

Dr. **Kristian Sandberg**, a brilliant scientist whom I unfortunately was not able to work with as much as originally planned.

To my mentor, Dr. **Sophie Imbeault**, for all our long talks about everything related to science and life in general and help with explaining everything related to animal research.

To my colleagues, both in the past and present,

Dr. **Michel Goiny**, for all the help with HPLC and microdialysis and being a constant happy presence in the lab.

Dr. **Funda Orhan**, for being one of the kindest persons I have ever met, always taking time to sit down and discuss anything and helping to develop ideas.

Anthi Faka, for her encouragement and always bringing a smile to everyone.

Ada Trepci, for being a great colleague and companion those long days of running locomotor activity test.

Dr. **Markus Larsson**, for always lending a helping hand and all the fun conversations.

Dr. **Xicong Liu**, for her easy-going attitude and moon-cake inspirations.

Alexandra Andersson, for always being happy and full of energy

Chengui Xu, for her innocent and playful attitude and always caring about everyone

Yiran Zheng, for being a happy presence in the animal house and a great student.

Neda Khanlarkhani, for being a good desk-neighbor and not complaining about my incredibly messy desk.

Mikael Hedberg and **Anna Malmqvist** for giving me important perspectives regarding the clinical side of schizophrenia

I would like to thank Dr. **Kent Jardemark** for our inspiring conversations and guidance in teaching and science, as well as **Oscar Jungholm** for being a great friend during my time as a student.

I would like to thank Dr. **Carl Sellgren**, for all the work in paper IV and his inspiring talks, and everyone in his group, **Jessica Gracias**, for bringing me beers when I need it the most, **Sravan Goparaju**, **Eleonora Moroncini**, and **Hayley French** for being a welcome presence around the office.

I would also like to thank everyone involved in KaSP, in particular **Maria Lee**, who helped out a lot with patient information for paper V.

As part of my education, I have also had the opportunity to go abroad and visit other universities, where I have met a lot of incredible people and eminent scientists.

I would like to thank Dr. **Doo-Sup Choi** and everyone in his group at Mayo Clinic, Rochester, for welcoming me with open arms and for a fruitful collaboration. In particular, Dr. **Daniel Lindberg**, **Lee Peyton** and **Caroline Grant**.

I would also like to thank Prof. **Robert Schwarcz** for welcoming me to his lab at Maryland Psychiatric Research Center at University of Maryland, Baltimore, and for being open and kind and giving me new perspectives when it comes to the kynurenine pathway. I would also like to thank everyone in his group, in particular **Tonali Blanco Ayala** and **Alex Klausing**, for all the help with the labeled kynurenine data and for welcoming me with open arms.

In addition, I would like to thank Dr. **Leon Brown** and Dr. **Paul Shepard**, for allowing me to run electrophysiology using their equipment at Maryland Psychiatric Research Center.

This work was made possible by several funding agencies:

Swedish Medical Research Council S. Erhardt (ML 2018-02653, GE 2009-3068; 2011-4789, SE 2017-00875, 2013–2838 and Dr. Svensson 2009-3068), the Swedish Brain Foundation, Åhlén-stiftelsen, the Swedish Foundation for Strategic Research (KF10-0039), The KI-AstraZeneca Joint Research Program, Torsten Söderbergs Stiftelse, the Swedish Brain Foundation, Petrus och Augusta Hedlunds Stiftelse, Märta Lundqvists Stiftelse, Svenska sällskapet för medicinsk forskning, the Stanley Medical Research Institute, the regional agreement on medical training and clinical research between Stockholm County Council and the Karolinska Institutet (ALF 20170019 and KID); the Broad Institute, Knut och Alice Wallenbergs Stiftelse, grant P50-MH103222 from the U.S. National Institutes of Health, the Mayo Clinic-Karolinska Institutet Collaborative Grant Foundation, and the Mayo Clinic Metabolomics Core Pilot Grant, Samuel C. Johnson Genomics of Addiction Program at Mayo Clinic, the Ulm Foundation, the Godby Foundation, and the National Institute on Alcohol Abuse and Alcoholism (AA017830, AA018779).

Finally, I would like to express my gratitude to my loved ones,

Victoria, for her loving support through-out my time as a student, and in particular during the time of writing this thesis.

To my entire family, for always encouraging me to pursue my dreams with nothing but love and support.

7 REFERENCES

Aberg, K.A., Liu, Y., Bukszár, J., McClay, J.L., Khachane, A.N., Andreassen, O.A., Blackwood, D., Corvin, A., Djurovic, S., Gurling, H., Ophoff, R., Pato, C.N., Pato, M.T., Riley, B., Webb, T., Kendler, K., O'Donovan, M., Craddock, N., Kirov, G., Owen, M., Rujescu, D., St Clair, D., Werge, T., Hultman, C.M., Delisi, L.E., Sullivan, P., Van Den Oord, E.J., 2013. A comprehensive family-based replication study of schizophrenia genes. JAMA Psychiatry. https://doi.org/10.1001/jamapsychiatry.2013.288

Abi-Dargham, A., Laruelle, M., 2005. Mechanisms of action of second generation antipsychotic drugs in schizophrenia: Insights from brain imaging studies. Eur. Psychiatry. https://doi.org/10.1016/j.eurpsy.2004.11.003

Agudelo, L.Z., Femenía, T., Orhan, F., Porsmyr-Palmertz, M., Goiny, M., Martinez-Redondo, V., Correia, J.C., Izadi, M., Bhat, M., Schuppe-Koistinen, I., Pettersson, A.T., Ferreira, D.M.S., Krook, A., Barres, R., Zierath, J.R., Erhardt, S., Lindskog, M., Ruas, J.L., 2014. Skeletal muscle PGC-1α1 modulates kynurenine metabolism and mediates resilience to stress-induced depression. Cell. https://doi.org/10.1016/j.cell.2014.07.051

Alberati-Giani, D., Ricciardi-Castagnoli, P., Köhler, C., Cesura, A.M., 1996. Regulation of the kynurenine pathway by IFN-γ in murine cloned macrophages and microglial cells. Adv. Exp. Med. Biol. https://doi.org/10.1007/978-1-4613-0381-7_28

Allegri, G., Bertazzo, A., Biasiolo, M., Costa, C.V.L., Ragazzi, E., 2003a. Kynurenine pathway enzymes in different species of animals, in: Advances in Experimental Medicine and Biology. https://doi.org/10.1007/978-1-4615-0135-0_53

Allegri, G., Costa, C.V.L., Bertazzo, A., Biasiolo, M., Ragazzi, E., 2003b. Enzyme activities of tryptophan metabolism along the kynurenine pathway in various species of animals. Farmaco. https://doi.org/10.1016/S0014-827X(03)00140-X

Andreasen, N.C., 1995. Symptoms, signs, and diagnosis of schizophrenia. Lancet. https://doi.org/10.1016/S0140-6736(95)91325-4

Andreasen, N.C., Olsen, S., 1982. Negative v Positive Schizophrenia: Definition and Validation. Arch. Gen. Psychiatry. https://doi.org/10.1001/archpsyc.1982.04290070025006

Angrist, B., Sathananthan, G., Wilk, S., Gershon, S., 1974. Amphetamine psychosis: Behavioral and biochemical aspects. J. Psychiatr. Res. https://doi.org/10.1016/0022-3956(74)90064-8

Aoyama, N., Takahashi, N., Saito, S., Maeno, N., Ishihara, R., Ji, X., Miura, H., Ikeda, M., Suzuki, T., Kitajima, T., Yamanouchi, Y., Kinoshita, Y., Yoshida, K., Iwata, N., Inada, T., Ozaki, N., 2006. Association study between kynurenine 3-monooxygenase gene and schizophrenia in the Japanese population. Genes, Brain Behav. https://doi.org/10.1111/j.1601-183X.2006.00231.x

Arvanov, V.L., Liang, X., Schwartz, J., Grossman, S., Wang, R.Y., 1997. Clozapine and haloperidol modulate N-methyl-D-aspartate- and non-N- methyl-D-aspartate receptor-mediated neurotransmission in rat prefrontal cortical neurons In Vitro. J. Pharmacol. Exp. Ther.

Arvanov, V.L., Wang, R.Y., 1999. Clozapine, but not haloperidol, prevents the functional

hyperactivity of N-methyl-D-aspartate receptors in rat cortical neurons induced by subchronic administration of phencyclidine, in: Journal of Pharmacology and Experimental Therapeutics.

Asp, L., Holtze, M., Powell, S.B., Karlsson, H., Erhardt, S., 2010. Neonatal infection with neurotropic influenza A virus induces the kynurenine pathway in early life and disrupts sensorimotor gating in adult Tap1-/- mice. Int. J. Neuropsychopharmacol. https://doi.org/10.1017/S1461145709990253

Badawy, A.A.B., 2017. Kynurenine pathway of tryptophan metabolism: Regulatory and functional aspects. Int. J. Tryptophan Res. https://doi.org/10.1177/1178646917691938

Balu, D.T., 2016. The NMDA Receptor and Schizophrenia. From Pathophysiology to Treatment., in: Advances in Pharmacology. https://doi.org/10.1016/bs.apha.2016.01.006

Balu, D.T., Coyle, J.T., 2015. The NMDA receptor "glycine modulatory site" in schizophrenia: D-serine, glycine, and beyond. Curr. Opin. Pharmacol. https://doi.org/10.1016/j.coph.2014.12.004

Baran, H., Schwarcz, R., 1990. Presence of 3-Hydroxyanthranilic Acid in Rat Tissues and Evidence for Its Production from Anthranilic Acid in the Brain. J. Neurochem. https://doi.org/10.1111/j.1471-4159.1990.tb04553.x

Basu, G.D., Tinder, T.L., Bradley, J.M., Tu, T., Hattrup, C.L., Pockaj, B.A., Mukherjee, P., 2006. Cyclooxygenase-2 Inhibitor Enhances the Efficacy of a Breast Cancer Vaccine: Role of IDO. J. Immunol. https://doi.org/10.4049/jimmunol.177.4.2391

Bay-Richter, C., Linderholm, K.R., Lim, C.K., Samuelsson, M., Träskman-Bendz, L., Guillemin, G.J., Erhardt, S., Brundin, L., 2015. A role for inflammatory metabolites as modulators of the glutamate N-methyl-d-aspartate receptor in depression and suicidality. Brain. Behav. Immun. https://doi.org/10.1016/j.bbi.2014.07.012

Bender, D.A., McCreanor, G.M., 1985. Kynurenine hydroxylase: A potential rate-limiting enzyme in tryptophan metabolism. Biochem. Soc. Trans. https://doi.org/10.1042/bst0130441

Beninger, R.J., Colton, A.M., Ingles, J.L., Jhamandas, K., Boegman, R.J., 1994. Picolinic acid blocks the neurotoxic but not the neuroexcitant properties of quinolinic acid in the rat brain: Evidence from turning behaviour and tyrosine hydroxylase immunohistochemistry. Neuroscience. https://doi.org/10.1016/0306-4522(94)90438-3

Bergen, S.E., O'Dushlaine, C.T., Ripke, S., Lee, P.H., Ruderfer, D.M., Akterin, S., Moran, J.L., Chambert, K.D., Handsaker, R.E., Backlund, L., Sby, U., McCarroll, S., Landen, M., Scolnick, E.M., Magnusson, P.K.E., Lichtenstein, P., Hultman, C.M., Purcell, S.M., Sklar, P., Sullivan, P.F., 2012. Genome-wide association study in a Swedish population yields support for greater CNV and MHC involvement in schizophrenia compared with bipolar disorder. Mol. Psychiatry. https://doi.org/10.1038/mp.2012.73

Birch, P.J., Grossman, C.J., Hayes, A.G., 1988. Kynurenic acid antagonises responses to NMDA via an action at the strychnine-insensitive glycine receptor. Eur. J. Pharmacol. https://doi.org/10.1016/0014-2999(88)90367-6

Breier, A., 1999. Cognitive deficit in schizophrenia and its neurochemical basis. Br. J. Psychiatry. https://doi.org/10.1192/s0007125000293604

Breier, A., Buchanan, R.W., Kirkpatrick, B., Davis, O.R., Irish, D., Summerfelt, A.,

Carpenter, W.T., 1994. Effects of clozapine on positive and negative symptoms in outpatients with schizophrenia. Am. J. Psychiatry. https://doi.org/10.1176/ajp.151.1.20

Bromet, E.J., Fennig, S., 1999. Epidemiology and natural history of schizophrenia. Biol. Psychiatry. https://doi.org/10.1016/S0006-3223(99)00153-5

Brown, A.S., Derkits, E.J., 2010. Prenatal infection and schizophrenia: A review of epidemiologic and translational studies. Am. J. Psychiatry. https://doi.org/10.1176/appi.ajp.2009.09030361

Brown, A.S., Hooton, J., Schaefer, C.A., Zhang, H., Petkova, E., Babulas, V., Perrin, M., Gorman, J.M., Susser, E.S., 2004. Elevated Maternal Interleukin-8 Levels and Risk of Schizophrenia in Adult Offspring. Am. J. Psychiatry. https://doi.org/10.1176/appi.ajp.161.5.889

Brown, S., Inskip, H., Barraclough, B., 2000. Causes of the excess mortality of schizophrenia. Br. J. Psychiatry. https://doi.org/10.1192/bjp.177.3.212

Brunello, N., Masotto, C., Steardo, L., Markstein, R., Racagni, G., 1995. New insights into the biology of schizophrenia through the mechanism of action of clozapine. Neuropsychopharmacology. https://doi.org/10.1016/0893-133X(95)00068-O

Burton, N., 2012. Living with Schizophrenia, 2nd ed.

Bychkov, E.R., Ahmed, M.R., Gurevich, V. V., Benovic, J.L., Gurevich, E. V., 2011. Reduced expression of G protein-coupled receptor kinases in schizophrenia but not in schizoaffective disorder. Neurobiol. Dis. https://doi.org/10.1016/j.nbd.2011.07.009

Bymaster, F.P., Felder, C.C., Tzavara, E., Nomikos, G.G., Calligaro, D.O., Mckinzie, D.L., 2003. Muscarinic mechanisms of antipsychotic atypicality. Prog. Neuro-Psychopharmacology Biol. Psychiatry. https://doi.org/10.1016/j.pnpbp.2003.09.008

Campbell, B.M., Charych, E., Lee, A.W., Möller, T., 2014. Kynurenines in CNS disease: Regulation by inflammatory cytokines. Front. Neurosci. https://doi.org/10.3389/fnins.2014.00012

Canetta, S.E., Brown, A.S., 2012. Prenatal infection, maternal immune activation, and risk for schizophrenia. Transl. Neurosci. https://doi.org/10.2478/s13380-012-0045-6

Cannon, T.D., Kaprio, J., Lönnqvist, J., Huttunen, M., Koskenvuo, M., 1998. The genetic epidemiology of schizophrenia in a Finnish twin cohort: A population-based modeling study. Arch. Gen. Psychiatry. https://doi.org/10.1001/archpsyc.55.1.67

Cantor-Graae, E., Selten, J.P., 2005. Schizophrenia and migration: A meta-analysis and review. Am. J. Psychiatry. https://doi.org/10.1176/appi.ajp.162.1.12

Carlsson, A., Lindqvist, M., 1963. Effect of Chlorpromazine or Haloperidol on Formation of 3-Methoxytyramine and Normetanephrine in Mouse Brain. Acta Pharmacol. Toxicol. (Copenh). https://doi.org/10.1111/j.1600-0773.1963.tb01730.x

Carlsson, A., Waters, N., Holm-Waters, S., Tedroff, J., Nilsson, M., Carlsson, M.L., 2001. Interactions Between Monoammines, Glutamate, and GABA in Schizophrenia: New Evidence. Annu. Rev. Pharmacol. Toxicol.

Carpenter, W.T., Buchanan, R.W., 1994. Schizophrenia. N. Engl. J. Med. 330, 681–690. https://doi.org/10.1056/NEJM199403103301006

Carr, D.B., Sesack, S.R., 2000. Projections from the rat prefrontal cortex to the ventral tegmental area: Target specificity in the synaptic associations with mesoaccumbens and mesocortical neurons. J. Neurosci. https://doi.org/10.1523/jneurosci.20-10-03864.2000

Catts, V.S., Lai, Y.L., Weickert, C.S., Weickert, T.W., Catts, S. V., 2016. A quantitative review of the postmortem evidence for decreased cortical N-methyl-d-aspartate receptor expression levels in schizophrenia: How can we link molecular abnormalities to mismatch negativity deficits? Biol. Psychol. https://doi.org/10.1016/j.biopsycho.2015.10.013

Chess, A.C., Landers, A.M., Bucci, D.J., 2009. L-kynurenine treatment alters contextual fear conditioning and context discrimination but not cue-specific fear conditioning. Behav. Brain Res. https://doi.org/10.1016/j.bbr.2009.03.013

Chess, A.C., Simoni, M.K., Alling, T.E., Bucci, D.J., 2007. Elevations of endogenous kynurenic acid produce spatial working memory deficits. Schizophr. Bull. https://doi.org/10.1093/schbul/sbl033

Chiarugi, A., Carpenedo, R., Molina, M.T., Mattoli, L., Pellicciari, R., Moroni, F., 1995. Comparison of the Neurochemical and Behavioral Effects Resulting from the Inhibition of Kynurenine Hydroxylase and/or Kynureninase. J. Neurochem. https://doi.org/10.1046/j.1471-4159.1995.65031176.x

Claghorn, J., Honigfeld, G., Abuzzahab, F.S., Wang, R., Steinbook, R., Tuason, V., Klerman, G., 1987. The risks and benefits of clozapine versus chlorpromazine. J. Clin. Psychopharmacol. https://doi.org/10.1097/00004714-198712000-00002

Clark, C.J., Mackay, G.M., Smythe, G.A., Bustamante, S., Stone, T.W., Phillips, R.S., 2005. Prolonged survival of a murine model of cerebral malaria by kynurenine pathway inhibition. Infect. Immun. https://doi.org/10.1128/IAI.73.8.5249-5251.2005

Collste, K., Plavén-Sigray, P., Fatouros-Bergman, H., Victorsson, P., Schain, M., Forsberg, A., Amini, N., Aeinehband, S., Erhardt, S., Halldin, C., Flyckt, L., Farde, L., Cervenka, S., 2017. Lower levels of the glial cell marker TSPO in drug-naive first-episode psychosis patients as measured using PET and [11 C]PBR28. Mol. Psychiatry. https://doi.org/10.1038/mp.2016.247

Connor, T.J., Starr, N., O'Sullivan, J.B., Harkin, A., 2008. Induction of indolamine 2,3-dioxygenase and kynurenine 3-monooxygenase in rat brain following a systemic inflammatory challenge: A role for IFN-γ? Neurosci. Lett. https://doi.org/10.1016/j.neulet.2008.06.007

Coward, D.M., 1992. General pharmacology of clozapine. Br. J. Psychiatry. https://doi.org/10.1192/s0007125000296840

Cox, J., Hein, M.Y., Luber, C.A., Paron, I., Nagaraj, N., Mann, M., 2014. Accurate proteome-wide label-free quantification by delayed normalization and maximal peptide ratio extraction, termed MaxLFQ. Mol. Cell. Proteomics. https://doi.org/10.1074/mcp.M113.031591

Creese, I., Burt, D.R., Snyder, S.H., 1996. Dopamine receptor binding predicts clinical and pharmacological potencies of antischizophrenic drugs. J. Neuropsychiatry Clin. Neurosci. https://doi.org/10.1176/jnp.8.2.223

Cui, W., Ning, Y., Hong, W., Wang, J., Liu, Z., Li, M.D., 2019. Crosstalk Between Inflammation and Glutamate System in Depression: Signaling Pathway and Molecular

Biomarkers for Ketamine's Antidepressant Effect. Mol. Neurobiol. https://doi.org/10.1007/s12035-018-1306-3

Danesch, U., Hashimoto, S., Renkawitz, R., Schutz, G., 1983. Transcriptional regulation of the tryptophan oxygenase gene in rat liver by glucocorticoids. J. Biol. Chem.

Dantzer, R., O'Connor, J.C., Freund, G.G., Johnson, R.W., Kelley, K.W., 2008. From inflammation to sickness and depression: When the immune system subjugates the brain. Nat. Rev. Neurosci. https://doi.org/10.1038/nrn2297

Davis, K.L., Kahn, R.S., Ko, G., Davidson, M., 1991. Dopamine in schizophrenia: A review and reconceptualization. Am. J. Psychiatry. https://doi.org/10.1176/ajp.148.11.1474

Desai, P.R., Lawson, K.A., Barner, J.C., Rascati, K.L., 2013. Identifying patient characteristics associated with high schizophrenia-related direct medical costs in community-dwelling patients. J. Manag. Care Pharm. https://doi.org/10.18553/jmcp.2013.19.6.468

Di Forti, M., Morgan, C., Dazzan, P., Pariante, C., Mondelli, V., Marques, T.R., Handley, R., Luzi, S., Russo, M., Paparelli, A., Butt, A., Stilo, S.A., Wiffen, B., Powell, J., Murray, R.M., 2009. High-potency cannabis and the risk of psychosis. Br. J. Psychiatry. https://doi.org/10.1192/bjp.bp.109.064220

Dostal, C.R., Gamsby, N.S., Lawson, M.A., McCusker, R.H., 2018. Glia- and tissue-specific changes in the Kynurenine Pathway after treatment of mice with lipopolysaccharide and dexamethasone. Brain. Behav. Immun. https://doi.org/10.1016/j.bbi.2017.12.006

Eggers, A.E., 2013. A serotonin hypothesis of schizophrenia. Med. Hypotheses. https://doi.org/10.1016/j.mehy.2013.03.013

Ekelund, J., Hennah, W., Hiekkalinna, T., Parker, A., Meyer, J., Lönnqvist, J., Peltonen, L., 2004. Replication of 1q42 linkage in Finnish schizophrenia pedigrees. Mol. Psychiatry. https://doi.org/10.1038/sj.mp.4001536

Ekman, M., Granström, O., Omérov, S., Jacob, J., Landén, M., 2013. The societal cost of schizophrenia in Sweden. J. Ment. Health Policy Econ.

Erhardt, S., Blennow, K., Nordin, C., Skogh, E., Lindström, L.H., Engberg, G., 2001a. Kynurenic acid levels ae elevated in the cerebrospinal fluid of patients with schizophrenia. Neurosci. Lett. https://doi.org/10.1016/S0304-3940(01)02242-X

Erhardt, S., Engberg, G., 2002. Increased phasic activity of dopaminergic neurones in the rat ventral tegmental area following pharmacologically elevated levels of endogenous kynurenic acid. Acta Physiol. Scand. https://doi.org/10.1046/j.1365-201X.2002.00962.x

Erhardt, S., Lim, C.K., Linderholm, K.R., Janelidze, S., Lindqvist, D., Samuelsson, M., Lundberg, K., Postolache, T.T., Träskman-Bendz, L., Guillemin, G.J., Brundin, L., 2013. Connecting inflammation with glutamate agonism in suicidality. Neuropsychopharmacology. https://doi.org/10.1038/npp.2012.248

Erhardt, S., Mathé, J.M., Chergui, K., Engberg, G., Svensson, T.H., 2002. GABA(B) receptor-mediated modulation of the firing pattern of ventral tegmental area dopamine neurons in vivo. Naunyn Schmiedebergs Arch Pharmacol 365, 173–180.

Erhardt, S., Öberg, H., Mathé, J.M., Engberg, G., 2001b. Pharmacological elevation of endogenous kynurenic acid levels activates nigral dopamine neurons. Amino Acids.

https://doi.org/10.1007/s007260170032

Erhardt, S., Pocivavsek, A., Repici, M., Liu, X.C., Imbeault, S., Maddison, D.C., Thomas, M.A.R., Smalley, J.L., Larsson, M.K., Muchowski, P.J., Giorgini, F., Schwarcz, R., 2017a. Adaptive and Behavioral Changes in Kynurenine 3-Monooxygenase Knockout Mice: Relevance to Psychotic Disorders. Biol. Psychiatry. https://doi.org/10.1016/j.biopsych.2016.12.011

Erhardt, S., Schwieler, L., Emanuelsson, C., Geyer, M., 2004. Endogenous kynurenic acid disrupts prepulse inhibition. Biol. Psychiatry. https://doi.org/10.1016/j.biopsych.2004.06.006

Erhardt, S., Schwieler, L., Engberg, G., 2003. Kynurenic acid and schizophrenia, in: Advances in Experimental Medicine and Biology. https://doi.org/10.1007/978-1-4615-0135-0_18

Erhardt, S., Schwieler, L., Imbeault, S., Engberg, G., 2017b. The kynurenine pathway in schizophrenia and bipolar disorder. Neuropharmacology. https://doi.org/10.1016/j.neuropharm.2016.05.020

Erickson, M.A., Banks, W.A., 2011. Cytokine and chemokine responses in serum and brain after single and repeated injections of lipopolysaccharide: Multiplex quantification with path analysis. Brain. Behav. Immun. https://doi.org/10.1016/j.bbi.2011.06.006

Farde, L., Nordström, A.L., Wiesel, F.A., Pauli, S., Halldin, C., Sedvall, G., 1992. Positron Emission Tomographic Analysis of Central D1 and D2 Dopamine Receptor Occupancy in Patients Treated with Classical Neuroleptics and Clozapine: Relation to Extrapyramidal Side Effects. Arch. Gen. Psychiatry. https://doi.org/10.1001/archpsyc.1992.01820070032005

Fazio, F., Lionetto, L., Curto, M., Iacovelli, L., Copeland, C.S., Neale, S.A., Bruno, V., Battaglia, G., Salt, T.E., Nicoletti, F., 2017. Cinnabarinic acid and xanthurenic acid: Two kynurenine metabolites that interact with metabotropic glutamate receptors. Neuropharmacology. https://doi.org/10.1016/j.neuropharm.2016.06.020

Feng, Y.H., Wang, L., Wang, Q., Li, X., Zeng, R., Gorodeski, G.I., 2005. ATP stimulates GRK-3 phosphorylation and β-arrestin-2-dependent internalization of P2X7 receptor. Am. J. Physiol. - Cell Physiol. https://doi.org/10.1152/ajpcell.00315.2004

Fillman, S.G., Cloonan, N., Catts, V.S., Miller, L.C., Wong, J., Mccrossin, T., Cairns, M., Weickert, C.S., 2013. Increased inflammatory markers identified in the dorsolateral prefrontal cortex of individuals with schizophrenia. Mol. Psychiatry. https://doi.org/10.1038/mp.2012.110

Foley, C., Corvin, A., Nakagome, S., 2017. Genetics of Schizophrenia: Ready to Translate? Curr. Psychiatry Rep. https://doi.org/10.1007/s11920-017-0807-5

Foster, A.C., Vezzani, A., French, E.D., Schwarcz, R., 1984. Kynurenic acid blocks neurotoxicity and seizures induced in rats by the related brain metabolite quinolinic acid. Neurosci. Lett. https://doi.org/10.1016/0304-3940(84)90050-8

Foster, A.C., White, R.J., Schwarcz, R., 1986. Synthesis of Quinolinic Acid by 3-Hydroxyanthranilic Acid Oxygenase in Rat Brain Tissue In Vitro. J. Neurochem. https://doi.org/10.1111/j.1471-4159.1986.tb02826.x

Franklin, K.B.J., Paxinos, G., 2008. The Mouse Brain in Stereotaxic Coordinates, third ed.

Elsevier Acadmic Press.

French, E.D., 1994. Phencyclidine and the midbrain dopamine system: Electrophysiology and behavior. Neurotoxicol. Teratol. https://doi.org/10.1016/0892-0362(94)90023-X

French, E.D., Mura, A., Wang, T., 1993. MK-801, phencyclidine (PCP), and PCP-like drugs increase burst firing in rat A10 dopamine neurons: Comparison to competitive NMDA antagonists. Synapse. https://doi.org/10.1002/syn.890130203

Fujigaki, S., Saito, K., Takemura, M., Fujii, H., Wada, H., Noma, A., Seishima, M., 1998. Species differences in L-tryptophan-kynurenine pathway metabolism: Quantification of anthranilic acid and its related enzymes. Arch. Biochem. Biophys. https://doi.org/10.1006/abbi.1998.0861

Fukui, S., Schwarcz, R., Rapoport, S.I., Takada, Y., Smith, Q.R., 1991. Blood–Brain Barrier Transport of Kynurenines: Implications for Brain Synthesis and Metabolism. J. Neurochem. https://doi.org/10.1111/j.1471-4159.1991.tb03460.x

Gál, E.M., Sherman, A.D., 1980. l-Kynurenine Its synthesis and possible regulatory function in brain. Neurochem. Res. https://doi.org/10.1007/BF00964611

Gardner, D.M., Baldessarini, R.J., Waraich, P., 2005. Modern antipsychotic drugs: A critical overview. CMAJ. https://doi.org/10.1503/cmaj.1041064

Gessa, G.L., Devoto, P., Diana, M., Flore, G., Melis, M., Pistis, M., 2000. Dissociation of haloperidol, clozapine, and olanzapine effects on electrical activity of mesocortical dopamine neurons and dopamine release in the prefrontal cortex. Neuropsychopharmacology. https://doi.org/10.1016/S0893-133X(00)00087-7

Geyer, M.A., Krebs-Thomson, K., Braff, D.L., Swerdlow, N.R., 2001. Pharmacological studies of prepulse inhibition models of sensorimotor gating deficits in schizophrenia: A decade in review. Psychopharmacology (Berl). https://doi.org/10.1007/s002130100811

Geyer, M.A., Swerdlow, N.R., 1998. Measurement of Startle Response, Prepulse Inhibition, and Habituation. Curr. Protoc. Neurosci. https://doi.org/10.1002/0471142301.ns0807s03

Giménez-Gómez, P., Pérez-Hernández, M., Gutiérrez-López, M.D., Vidal, R., Abuin-Martínez, C., O'Shea, E., Colado, M.I., 2018. Increasing kynurenine brain levels reduces ethanol consumption in mice by inhibiting dopamine release in nucleus accumbens. Neuropharmacology. https://doi.org/10.1016/j.neuropharm.2018.04.016

Giorgini, F., Huang, S.Y., Sathyasaikumar, K. V., Notarangelo, F.M., Thomas, M.A.R., Tararina, M., Wu, H.Q., Schwarcz, R., Muchowski, P.J., 2013. Targeted deletion of kynurenine 3-Monooxygenase in mice a new tool for studying kynurenine pathway metabolism in periphery and brain. J. Biol. Chem. https://doi.org/10.1074/jbc.M113.503813

Giuliani, A.L., Sarti, A.C., Falzoni, S., Di Virgilio, F., 2017. The P2X7 receptor-interleukin-1 liaison. Front. Pharmacol. https://doi.org/10.3389/fphar.2017.00123

Grace, A.A., Bunney, B.S., 1984a. The control of firing pattern in nigral dopamine neurons: Single spike firing. J. Neurosci. https://doi.org/10.1523/jneurosci.04-11-02866.1984

Grace, A.A., Bunney, B.S., 1984b. The control of firing pattern in nigral dopamine neurons: Burst firing. J. Neurosci. https://doi.org/10.1523/jneurosci.04-11-02877.1984

Gramsbergen, J.B.P., Hodgkins, P.S., Rassoulpour, A., Turski, W.A., Guidetti, P., Schwarcz, R., 2002. Brain-Specific Modulation of Kynurenic Acid Synthesis in the Rat. J. Neurochem. https://doi.org/10.1046/j.1471-4159.1997.69010290.x

Green, M.F., Kern, R.S., Braff, D.L., Mintz, J., 2000. Neurocognitive deficits and functional outcome in schizophrenia: Are we measuring the "right stuff"? Schizophr. Bull. https://doi.org/10.1093/oxfordjournals.schbul.a033430

Gresack, J.E., Risbrough, V.B., 2011. Corticotropin-releasing factor and noradrenergic signalling exert reciprocal control over startle reactivity. Int. J. Neuropsychopharmacol. https://doi.org/10.1017/S1461145710001409

Griffiths, J.J., Zarate, C.A., Rasimas, J.J., 2014. Existing and novel biological therapeutics in suicide prevention. Am. J. Prev. Med. https://doi.org/10.1016/j.amepre.2014.06.012

Guidetti, P., Eastman, C.L., Schwarcz, R., 1995. Metabolism of [5-3H]Kynurenine in the Rat Brain In Vivo: Evidence for the Existence of a Functional Kynurenine Pathway. J. Neurochem. https://doi.org/10.1046/j.1471-4159.1995.65062621.x

Guidetti, P., Okuno, E., Schwarcz, R., 1997. Characterization of rat brain kynurenine aminotransferases I and II. J. Neurosci. Res. https://doi.org/10.1002/(SICI)1097-4547(19971101)50:3<457::AID-JNR12>3.0.CO;2-3

Guillemin, G.J., 2012. Quinolinic acid, the inescapable neurotoxin. FEBS J. https://doi.org/10.1111/j.1742-4658.2012.08485.x

Guillemin, G.J., Kerr, S.J., Smythe, G.A., Smith, D.G., Kapoor, V., Armati, P.J., Croitoru, J., Brew, B.J., 2001. Kynurenine pathway metabolism in human astrocytes: A paradox for neuronal protection. J. Neurochem. https://doi.org/10.1046/j.1471-4159.2001.00498.x

Gurevich, E. V., Gainetdinov, R.R., Gurevich, V. V., 2016. G protein-coupled receptor kinases as regulators of dopamine receptor functions. Pharmacol. Res. https://doi.org/10.1016/j.phrs.2016.05.010

Gustavsson, A., Svensson, M., Jacobi, F., Allgulander, C., Alonso, J., Beghi, E., Dodel, R., Ekman, M., Faravelli, C., Fratiglioni, L., Gannon, B., Jones, D.H., Jennum, P., Jordanova, A., Jönsson, L., Karampampa, K., Knapp, M., Kobelt, G., Kurth, T., Lieb, R., Linde, M., Ljungcrantz, C., Maercker, A., Melin, B., Moscarelli, M., Musayev, A., Norwood, F., Preisig, M., Pugliatti, M., Rehm, J., Salvador-Carulla, L., Schlehofer, B., Simon, R., Steinhausen, H.C., Stovner, L.J., Vallat, J.M., den Bergh, P. Van, van Os, J., Vos, P., Xu, W., Wittchen, H.U., Jönsson, B., Olesen, J., 2011. Cost of disorders of the brain in Europe 2010. Eur. Neuropsychopharmacol. https://doi.org/10.1016/j.euroneuro.2011.08.008

Hagger, C., Buckley, P., Kenny, J.T., Friedman, L., Ubogy, D., Meltzer, H.Y., 1993. Improvement in cognitive functions and psychiatric symptoms in treatment-refractory schizophrenic patients receiving clozapine. Biol. Psychiatry. https://doi.org/10.1016/0006-3223(93)90043-D

Han, Q., Cai, T., Tagle, D.A., Li, J., 2010. Structure, expression, and function of kynurenine aminotransferases in human and rodent brains. Cell. Mol. Life Sci. https://doi.org/10.1007/s00018-009-0166-4

Harrison, P.J., 2015. Recent genetic findings in schizophrenia and their therapeutic relevance. J. Psychopharmacol. https://doi.org/10.1177/0269881114553647

Herédi, J., Berkó, A.M., Jankovics, F., Iwamori, T., Iwamori, N., Ono, E., Horváth, S., Kis, Z., Toldi, J., Vécsei, L., Gellért, L., 2017. Astrocytic and neuronal localization of kynurenine aminotransferase-2 in the adult mouse brain. Brain Struct. Funct. https://doi.org/10.1007/s00429-016-1299-5

Herédi, J., Cseh, E.K., Berkó, A.M., Veres, G., Zádori, D., Toldi, J., Kis, Z., Vécsei, L., Ono, E., Gellért, L., 2019. Investigating KYNA production and kynurenergic manipulation on acute mouse brain slice preparations. Brain Res. Bull. https://doi.org/10.1016/j.brainresbull.2018.12.014

Hilmas, C., Pereira, E.F.R., Alkondon, M., Rassoulpour, A., Schwarcz, R., Albuquerque, E.X., 2001. The brain metabolite kynurenic acid inhibits α7 nicotinic receptor activity and increases non-α7 nicotinic receptor expression: Physiopathological implications. J. Neurosci. https://doi.org/10.1523/jneurosci.21-19-07463.2001

Hinton, D.J., Vázquez, M.S., Geske, J.R., Hitschfeld, M.J., Ho, A.M.C., Karpyak, V.M., Biernacka, J.M., Choi, D.S., 2017. Metabolomics biomarkers to predict acamprosate treatment response in alcohol-dependent subjects. Sci. Rep. https://doi.org/10.1038/s41598-017-02442-4

Holtze, M., Saetre, P., Engberg, G., Schwieler, L., Werge, T., Andreassen, O.A., Hall, H., Terenius, L., Agartz, I., Jönsson, E.G., Schalling, M., Erhardt, S., 2012. Kynurenine 3-monooxygenase polymorphisms: Relevance for kynurenic acid synthesis in patients with schizophrenia and healthy controls. J. Psychiatry Neurosci. https://doi.org/10.1503/jpn.100175

Holtze, M., Saetre, P., Erhardt, S., Schwieler, L., Werge, T., Hansen, T., Nielsen, J., Djurovic, S., Melle, I., Andreassen, O.A., Hall, H., Terenius, L., Agartz, I., Engberg, G., Jönsson, E.G., Schalling, M., 2011. Kynurenine 3-monooxygenase (KMO) polymorphisms in schizophrenia: An association study. Schizophr. Res. https://doi.org/10.1016/j.schres.2010.10.002

Idänpään-Heikkilä, J., Alhava, E., Olkinuora, M., Palva, I.P., 1977. Agranulocytosis during treatment with clozapine. Eur. J. Clin. Pharmacol. https://doi.org/10.1007/BF00606409

Imbeault, S., Goiny, M., Liu, X., Erhardt, S., 2019. Effects of IDO1 and TDO2 inhibition on cognitive deficits and anxiety following LPS-induced neuroinflammation. Acta Neuropsychiatr. 1–38. https://doi.org/10.1017/neu.2019.44

Jardemark, K.E., Ninan, I., Liang, X., Wang, R.Y., 2003. Protein kinase C is involved in clozapine's facilitation of N-methyl-D-aspartate- and electrically evoked responses in pyramidal cells of the medial prefrontal cortex. Neuroscience. https://doi.org/10.1016/S0306-4522(02)00976-4

Javitt, D.C., 2007. Glutamate and Schizophrenia: Phencyclidine, N-Methyl-d-Aspartate Receptors, and Dopamine-Glutamate Interactions. Int. Rev. Neurobiol. https://doi.org/10.1016/S0074-7742(06)78003-5

Javitt, D.C., Duncan, L., Balla, A., Sershen, H., 2005. Inhibition of System A-mediated glycine transport in cortical synaptosomes by therapeutic concentrations of clozapine: Implications for mechanisms of action. Mol. Psychiatry. https://doi.org/10.1038/sj.mp.4001552

Jentsch, J.D., Dazzi, L., Chhatwal, J.P., Verrico, C.D., Roth, R.H., 1998a. Reduced prefrontal cortical dopamine, but not acetylcholine, release in vivo after repeated, intermittent

phencyclidine administration to rats. Neurosci. Lett. https://doi.org/10.1016/S0304-3940(98)00879-9

Jentsch, J.D., Elsworth, J.D., Taylor, J.R., Eugene Redmond, D., Roth, R.H., 1997a. Dysregulation of Mesoprefrontal Dopamine Neurons Induced by Acute and Repeated Phencyclidine Administration in the Nonhuman Primate: Implications for Schizophrenia. Adv. Pharmacol. https://doi.org/10.1016/S1054-3589(08)60870-4

Jentsch, J.D., Roth, R.H., 1999. The neuropsychopharmacology of phencyclidine: From NMDA receptor hypofunction to the dopamine hypothesis of schizophrenia. Neuropsychopharmacology. https://doi.org/10.1016/S0893-133X(98)00060-8

Jentsch, J.D., Taylor, J.R., Roth, R.H., 1998b. Subchronic phencyclidine administration increases mesolimbic dopaminergic system responsivity and augments stress- and psychostimulant- induced hyperlocomotion. Neuropsychopharmacology. https://doi.org/10.1016/S0893-133X(98)00004-9

Jentsch, J.D., Tran, A., Le, D., Youngren, K.D., Roth, R.H., 1997b. Subchronic phencyclidine administration reduces mesoprefrontal dopaminev utilization and impairs prefrontal cortical-dependent cognition in the rat. Neuropsychopharmacology. https://doi.org/10.1016/S0893-133X(97)00034-1

Kaddurah-Daouk, R., Boyle, S.H., Matson, W., Sharma, S., Matson, S., Zhu, H., Bogdanov, M.B., Churchill, E., Krishnan, R.R., Rush, A.J., Pickering, E., Delnomdedieu, M., 2011. Pretreatment metabotype as a predictor of response to sertraline or placebo in depressed outpatients: A proof of concept. Transl. Psychiatry. https://doi.org/10.1038/tp.2011.22

Kaddurah-Daouk, R., McEvoy, J., Baillie, R.A., Lee, D., Yao, J.K., Doraiswamy, P.M., Krishnan, K.R.R., 2007. Metabolomic mapping of atypical antipsychotic effects in schizophrenia. Mol. Psychiatry. https://doi.org/10.1038/sj.mp.4002000

Kahn, R.S., Sommer, I.E., Murray, R.M., Meyer-Lindenberg, A., Weinberger, D.R., Cannon, T.D., O'Donovan, M., Correll, C.U., Kane, J.M., van Os, J., Insel, T.R., 2015. Schizophrenia. Nat. Rev. Dis. Prim. 1, 15067. https://doi.org/10.1038/nrdp.2015.67

Kalivas, P.W., Churchill, L., Klitenick, M.A., 1993. GABA and enkephalin projection from the nucleus accumbens and ventral pallidum to the ventral tegmental area. Neuroscience. https://doi.org/10.1016/0306-4522(93)90048-K

Kane, J., Honigfeld, G., Singer, J., Meltzer, H., 1988. Clozapine for the Treatment-Resistant Schizophrenic: A Double-blind Comparison With Chlorpromazine. Arch. Gen. Psychiatry. https://doi.org/10.1001/archpsyc.1988.01800330013001

Kapur, S., Seeman, P., 2001. Does fast dissociation from the dopamine D2 receptor explain the action of atypical antipsychotics?: A new hypothesis. Am. J. Psychiatry. https://doi.org/10.1176/appi.ajp.158.3.360

Karlsson, H., 2003. Viruses and schizophrenia, connection or coincidence? Neuroreport. https://doi.org/10.1097/00001756-200303240-00001

Kessler, M., Terramani, T., Lynch, G., Baudry, M., 1989. A Glycine Site Associated with N-Methyl-d-Aspartic Acid Receptors: Characterization and Identification of a New Class of Antagonists. J. Neurochem. https://doi.org/10.1111/j.1471-4159.1989.tb01881.x

Khoury, R., Nasrallah, H.A., 2018. Inflammatory biomarkers in individuals at clinical high risk for psychosis (CHR-P): State or trait? Schizophr. Res.

https://doi.org/10.1016/j.schres.2018.04.017

King, D.J., 1998. Drug treatment of the negative symptoms of schizophrenia. Eur. Neuropsychopharmacol. https://doi.org/10.1016/S0924-977X(97)00041-2

Kirkbride, J.B., Fearon, P., Morgan, C., Dazzan, P., Morgan, K., Murray, R.M., Jones, P.B., 2007. Neighbourhood variation in the incidence of psychotic disorders in Southeast London. Soc. Psychiatry Psychiatr. Epidemiol. https://doi.org/10.1007/s00127-007-0193-0

Kozak, R., Campbell, B.M., Strick, C.A., Horner, W., Hoffmann, W.E., Kiss, T., Chapin, D.S., McGinnis, D., Abbott, A.L., Roberts, B.M., Fonseca, K., Guanowsky, V., Young, D.A., Seymour, P.A., Dounay, A., Hajos, M., Williams, G. V., Castner, S.A., 2014. Reduction of brain kynurenic acid improves cognitive function. J. Neurosci. https://doi.org/10.1523/JNEUROSCI.1107-14.2014

Krupp, P., Barnes, P., 1992. Clozapine-associated agranulocytosis: Risk and aetiology. Br. J. Psychiatry. https://doi.org/10.1192/s0007125000296906

Krystal, J.H., Karper, L.P., Seibyl, J.P., Freeman, G.K., Delaney, R., Bremner, J.D., Heninger, G.R., Bowers, M.B., Charney, D.S., 1994. Subanesthetic Effects of the Noncompetitive NMDA Antagonist, Ketamine, in Humans: Psychotomimetic, Perceptual, Cognitive, and Neuroendocrine Responses. Arch. Gen. Psychiatry. https://doi.org/10.1001/archpsyc.1994.03950030035004

Krystal, J.H., Perry, E.B., Gueorguieva, R., Belger, A., Madonick, S.H., Abi-Dargham, A., Cooper, T.B., MacDougall, L., Abi-Saab, W., Cyril D'Souza, D., 2005. Comparative and interactive human psychopharmacologic effects of ketamine and amphetamine: Implications for glutamatergic and dopaminergic model psychoses and cognitive function. Arch. Gen. Psychiatry. https://doi.org/10.1001/archpsyc.62.9.985

Lahti, A.C., Koffel, B., Laporte, D., Tamminga, C.A., 1995. Subanesthetic doses of ketamine stimulate psychosis in schizophrenia. Neuropsychopharmacology. https://doi.org/10.1016/0893-133X(94)00131-I

Lahti, A.C., Weiler, M.A., Michaelidis, T., Parwani, A., Tamminga, C.A., 2001. Effects of ketamine in normal and schizophrenic volunteers. Neuropsychopharmacology. https://doi.org/10.1016/S0893-133X(01)00243-3

Larsson, M.K., Faka, A., Bhat, M., Imbeault, S., Goiny, M., Orhan, F., Oliveros, A., Ståhl, S., Liu, X.C., Choi, D.S., Sandberg, K., Engberg, G., Schwieler, L., Erhardt, S., 2016. Repeated LPS Injection Induces Distinct Changes in the Kynurenine Pathway in Mice. Neurochem. Res. https://doi.org/10.1007/s11064-016-1939-4

Laruelle, M., Abi-Dargham, A., 1999. Dopamine as the wind of the psychotic fire: New evidence from brain imaging studies, in: Journal of Psychopharmacology. https://doi.org/10.1177/026988119901300405

Laruelle, M., Abi-Dargham, A., Van Dyck, C.H., Gil, R., D'Souza, C.D., Erdos, J., Mccance, E., Rosenblatt, W., Fingado, C., Zoghbi, S.S., Baldwin, R.M., Seibyl, J.P., Krystal, J.H., Charney, D.S., Innis, R.B., 1996. Single photon emission computerized tomography imaging of amphetamine-induced dopamine release in drug-free schizophrenic subjects. Proc. Natl. Acad. Sci. U. S. A. https://doi.org/10.1073/pnas.93.17.9235

Laursen, T.M., Nordentoft, M., Mortensen, P.B., 2014. Excess Early Mortality in Schizophrenia. Annu. Rev. Clin. Psychol. https://doi.org/10.1146/annurev-clinpsy-

032813-153657

Lavebratt, C., Olsson, S., Backlund, L., Frisén, L., Sellgren, C., Priebe, L., Nikamo, P., Träskman-Bendz, L., Cichon, S., Vawter, M.P., Ösby, U., Engberg, G., Landén, M., Erhardt, S., Schalling, M., 2014. The KMO allele encoding Arg 452 is associated with psychotic features in bipolar disorder type 1, and with increased CSF KYNA level and reduced KMO expression. Mol. Psychiatry. https://doi.org/10.1038/mp.2013.11

Lee, S.Y., Choi, H.K., Lee, K.J., Jung, J.Y., Hur, G.Y., Jung, K.H., Kim, J.H., Shin, C., Shim, J.J., In, K.H., Kang, K.H., Yoo, S.H., 2009. The immune tolerance of cancer is mediated by IDO that is inhibited by COX-2 inhibitors through regulatory T cells. J. Immunother. https://doi.org/10.1097/CJI.0b013e31818ac2f7

Leklem, J.E., 1971. Quantitative aspects of tryptophan metabolism in humans and other species: a review. Am. J. Clin. Nutr. https://doi.org/10.1093/ajcn/24.6.659

Li, W., Yang, Y., Lin, J., Wang, S., Zhao, J., Yang, G., Wang, X., Ding, M., Zhang, H., Lv, L., 2013. Association of serotonin transporter gene (SLC6A4) polymorphisms with schizophrenia susceptibility and symptoms in a Chinese-Han population. Prog. Neuro-Psychopharmacology Biol. Psychiatry. https://doi.org/10.1016/j.pnpbp.2013.04.003

Linderholm, K.R., Alm, M.T., Larsson, M.K., Olsson, S.K., Goiny, M., Hajos, M., Erhardt, S., Engberg, G., 2016. Inhibition of kynurenine aminotransferase II reduces activity of midbrain dopamine neurons. Neuropharmacology. https://doi.org/10.1016/j.neuropharm.2015.10.028

Linderholm, K.R., Andersson, A., Olsson, S., Olsson, E., Snodgrass, R., Engberg, G., Erhardt, S., 2007. Activation of rat ventral tegmental area dopamine neurons by endogenous kynurenic acid: A pharmacological analysis. Neuropharmacology. https://doi.org/10.1016/j.neuropharm.2007.09.003

Linderholm, K.R., Skogh, E., Olsson, S.K., Dahl, M.L., Holtze, M., Engberg, G., Samuelsson, M., Erhardt, S., 2012. Increased levels of kynurenine and kynurenic acid in the CSF of patients with schizophrenia. Schizophr. Bull. https://doi.org/10.1093/schbul/sbq086

Liu, X.C., Holtze, M., Powell, S.B., Terrando, N., Larsson, M.K., Persson, A., Olsson, S.K., Orhan, F., Kegel, M., Asp, L., Goiny, M., Schwieler, L., Engberg, G., Karlsson, H., Erhardt, S., 2014. Behavioral disturbances in adult mice following neonatal virus infection or kynurenine treatment - Role of brain kynurenic acid. Brain. Behav. Immun. https://doi.org/10.1016/j.bbi.2013.10.010

MacDowell, K.S., Pinacho, R., Leza, J.C., Costa, J., Ramos, B., García-Bueno, B., 2017. Differential regulation of the TLR4 signalling pathway in post-mortem prefrontal cortex and cerebellum in chronic schizophrenia: Relationship with SP transcription factors. Prog. Neuro-Psychopharmacology Biol. Psychiatry. https://doi.org/10.1016/j.pnpbp.2017.08.005

Mangas, A., Yajeya, J., González, N., Ruiz, I., Duleu, S., Geffard, M., Coveñas, R., 2017. Overexpression of kynurenic acid in stroke: An endogenous neuroprotector? Ann. Anat. https://doi.org/10.1016/j.aanat.2017.01.002

Marsden, C.D., Jenner, P., 1980. The pathophysiology of extrapyramidal side-effects of neuroleptic drugs. Psychol. Med. https://doi.org/10.1017/S003329170003960X

McGrath, J., Saha, S., Chant, D., Welham, J., 2008. Schizophrenia: A concise overview of

incidence, prevalence, and mortality. Epidemiol. Rev. https://doi.org/10.1093/epirev/mxn001

Meltzer, H.Y., Huang, M., 2008. In vivo actions of atypical antipsychotic drug on serotonergic and dopaminergic systems. Prog. Brain Res. https://doi.org/10.1016/S0079-6123(08)00909-6

Millan, M.J., 2005. N-Methyl-d-aspartate receptors as a target for improved antipsychotic agents: Novel insights and clinical perspectives. Psychopharmacology (Berl). https://doi.org/10.1007/s00213-005-2199-1

Miller, C.L., Llenos, I.C., Dulay, J.R., Barillo, M.M., Yolken, R.H., Weis, S., 2004. Expression of the kynurenine pathway enzyme tryptophan 2,3-dioxygenase is increased in the frontal cortex of individuals with schizophrenia. Neurobiol. Dis. https://doi.org/10.1016/j.nbd.2003.12.015

Miller, C.L., Llenos, I.C., Dulay, J.R., Weis, S., 2006. Upregulation of the initiating step of the kynurenine pathway in postmortem anterior cingulate cortex from individuals with schizophrenia and bipolar disorder. Brain Res. https://doi.org/10.1016/j.brainres.2005.12.056

Molteni, R., Macchi, F., Zecchillo, C., Dell'Agli, M., Colombo, E., Calabrese, F., Guidotti, G., Racagni, G., Riva, M.A., 2013. Modulation of the inflammatory response in rats chronically treated with the antidepressant agomelatine. Eur. Neuropsychopharmacol. https://doi.org/10.1016/j.euroneuro.2013.03.008

Mortensen, P.B., Pedersen, C.B., Westergaard, T., Wohlfahrt, J., Ewald, H., Mors, O., Andersen, P.K., Melbye, M., 1999. Effects of family history and place and season of birth on the risk of schizophrenia. N. Engl. J. Med. https://doi.org/10.1056/NEJM199902253400803

Müller, N., 2018. Inflammation in schizophrenia: Pathogenetic aspects and therapeutic considerations. Schizophr. Bull. https://doi.org/10.1093/schbul/sby024

Müller, N., Weidinger, E., Leitner, B., Schwarz, M.J., 2015. The role of inflammation in schizophrenia. Front. Neurosci. https://doi.org/10.3389/fnins.2015.00372

Munn, D.H., Mellor, A.L., 2016. IDO in the Tumor Microenvironment: Inflammation, Counter-Regulation, and Tolerance. Trends Immunol. https://doi.org/10.1016/j.it.2016.01.002

Murase, S., Mathé, J.M., Grenhoff, J., Svensson, T.H., 1993. Effects of dizocilpine (MK-801) on rat midbrain dopamine cell activity: differential actions on firing pattern related to anatomical localization. J. Neural Transm. https://doi.org/10.1007/BF01244915

Murrough, J.W., Abdallah, C.G., Mathew, S.J., 2017. Targeting glutamate signalling in depression: Progress and prospects. Nat. Rev. Drug Discov. https://doi.org/10.1038/nrd.2017.16

Musso, T., Gusella, G.L., Brooks, A., Longo, D.L., Varesio, L., 1994. Interleukin-4 inhibits indoleamine 2,3-dioxygenase expression in human monocytes. Blood.

Nakamura, T., Niimi, S., Nawa, K., Noda, C., Ichihara, A., Takagi, Y., Anai, M., Sakaki, Y., 1987. Multihormonal regulation of transcription of the tryptophan 2,3-dioxygenase gene in primary cultures of adult rat hepatocytes with special reference to the presence of a transcriptional protein mediating the action of glucocorticoids. J. Biol. Chem.

Nilsson, L.K., Linderholm, K.R., Engberg, G., Paulson, L., Blennow, K., Lindström, L.H., Nordin, C., Karanti, A., Persson, P., Erhardt, S., 2005. Elevated levels of kynurenic acid in the cerebrospinal fluid of male patients with schizophrenia. Schizophr. Res. https://doi.org/10.1016/j.schres.2005.07.013

Nilsson, L.K., Linderholm, K.R., Erhardt, S., 2006. Subchronic treatment with kynurenine and probenecid: Effects on prepulse inhibition and firing of midbrain dopamine neurons. J. Neural Transm. https://doi.org/10.1007/s00702-005-0343-z

Nilsson, L.K., Nordin, C., Jönsson, E.G., Engberg, G., Linderholm, K.R., Erhardt, S., 2007. Cerebrospinal fluid kynurenic acid in male and female controls - Correlation with monoamine metabolites and influences of confounding factors. J. Psychiatr. Res. https://doi.org/10.1016/j.jpsychires.2005.12.001

Ninan, I., Jardemark, K.E., Wang, R.Y., 2003. Olanzapine and clozapine but not haloperidol reverse subchronic phencyclidine-induced functional hyperactivity of N-methyl-D-aspartate receptors in pyramidal cells of the rat medial prefrontal cortex. Neuropharmacology. https://doi.org/10.1016/S0028-3908(03)00033-9

Nucifora, F.C., Mihaljevic, M., Lee, B.J., Sawa, A., 2017. Clozapine as a Model for Antipsychotic Development. Neurotherapeutics. https://doi.org/10.1007/s13311-017-0552-9

O'Connor, J.C., Lawson, M.A., André, C., Moreau, M., Lestage, J., Castanon, N., Kelley, K.W., Dantzer, R., 2009. Lipopolysaccharide-induced depressive-like behavior is mediated by indoleamine 2,3-dioxygenase activation in mice. Mol. Psychiatry. https://doi.org/10.1038/sj.mp.4002148

Okuno, E., Nakamura, M., Schwarcz, R., 1991. Two kynurenine aminotransferases in human brain. Brain Res. https://doi.org/10.1016/0006-8993(91)91583-M

Oliveros, A., Starski, P., Lindberg, D., Choi, S., Heppelmann, C.J., Dasari, S., Choi, D.S., 2017a. Label-Free Neuroproteomics of the Hippocampal-Accumbal Circuit Reveals Deficits in Neurotransmitter and Neuropeptide Signaling in Mice Lacking Ethanol-Sensitive Adenosine Transporter. J. Proteome Res. https://doi.org/10.1021/acs.jproteome.6b00830

Oliveros, A., Wininger, K., Sens, J., Larsson, M.K., Liu, X.C., Choi, S., Faka, A., Schwieler, L., Engberg, G., Erhardt, S., Choi, D.S., 2017b. LPS-induced cortical kynurenic acid and neurogranin-NFAT signaling is associated with deficits in stimulus processing during Pavlovian conditioning. J. Neuroimmunol. 313, 1–9. https://doi.org/10.1016/j.jneuroim.2017.09.010

Olsson, S.K., Andersson, A.S., Linderholm, K.R., Holtze, M., Nilsson-Todd, L.K., Schwieler, L., Olsson, E., Larsson, K., Engberg, G., Erhardt, S., 2009. Elevated levels of kynurenic acid change the dopaminergic response to amphetamine: Implications for schizophrenia. Int. J. Neuropsychopharmacol. https://doi.org/10.1017/S1461145708009383

Olsson, S.K., Larsson, M.K., Erhardt, S., 2012a. Subchronic elevation of brain kynurenic acid augments amphetamine-induced locomotor response in mice. J. Neural Transm. https://doi.org/10.1007/s00702-011-0706-6

Olsson, S.K., Sellgren, C., Engberg, G., Landén, M., Erhardt, S., 2012b. Cerebrospinal fluid kynurenic acid is associated with manic and psychotic features in patients with bipolar I disorder. Bipolar Disord. https://doi.org/10.1111/bdi.12009

Orhan, F., Fatouros-Bergman, H., Goiny, M., Malmqvist, A., Piehl, F., Cervenka, S., Collste, K., Victorsson, P., Sellgren, C.M., Flyckt, L., Erhardt, S., Engberg, G., 2018. CSF GABA is reduced in first-episode psychosis and associates to symptom severity. Mol. Psychiatry. https://doi.org/10.1038/mp.2017.25

Parrott, J.M., Redus, L., Santana-Coelho, D., Morales, J., Gao, X., O'Connor, J.C., 2016. Neurotoxic kynurenine metabolism is increased in the dorsal hippocampus and drives distinct depressive behaviors during inflammation. Transl. Psychiatry. https://doi.org/10.1038/tp.2016.200

Parsons, C.G., Danysz, W., Quack, G., Hartmann, S., Lorenz, B., Wollenburg, C., Baran, L., Przegalinski, E., Kostowski, W., Krzascik, P., Chizh, B., Headley, P.M., 1997. Novel systemically active antagonists of the glycine site of the N- methyl-D-aspartate receptor: Electrophysiological, biochemical and behavioral characterization. J. Pharmacol. Exp. Ther.

Patton, M.H., Bizup, B.T., Grace, A.A., 2013. The infralimbic cortex bidirectionally modulates mesolimbic dopamine neuron activity via distinct neural pathways. J. Neurosci. https://doi.org/10.1523/JNEUROSCI.2449-13.2013

Paxinos, G., Watson, C., 2005. The Rat Brain in Stereotaxic Coordinates, fifth ed. Elsevier Acadmic Press.

Pedersen, C.B., Mortensen, P.B., 2001. Evidence of a dose-response relationship between urbanicity during upbringing and schizophrenia risk. Arch. Gen. Psychiatry. https://doi.org/10.1001/archpsyc.58.11.1039

Perkins, M.N., Stone, T.W., 1982. An iontophoretic investigation of the actions of convulsant kynurenines and their interaction with the endogenous excitant quinolinic acid. Brain Res. https://doi.org/10.1016/0006-8993(82)91048-4

Perry, W., Minassian, A., Paulus, M.P., Young, J.W., Kincaid, M.J., Ferguson, E.J., Henry, B.L., Zhuang, X., Masten, V.L., Sharp, R.F., Geyer, M.A., 2009. A reverse-translational study of dysfunctional exploration in psychiatric disorders: From mice to men. Arch. Gen. Psychiatry. https://doi.org/10.1001/archgenpsychiatry.2009.58

Petrulli, J.R., Kalish, B., Nabulsi, N.B., Huang, Y., Hannestad, J., Morris, E.D., 2017. Systemic inflammation enhances stimulant-induced striatal dopamine elevation. Transl. Psychiatry. https://doi.org/10.1038/tp.2017.18

Peyton, L., Oliveros, A., Tufvesson-Alm, M., Schwieler, L., Starski, P., Engberg, G., Erhardt, S., Choi, D.S., 2019. Lipopolysaccharide increases cortical kynurenic acid and deficits in reference memory in mice. Int. J. Tryptophan Res. In press.

Phillipson, O.T., 1979. Afferent projections to the ventral tegmental area of Tsai and interfascicular nucleus: A horseradish peroxidase study in the rat. J. Comp. Neurol. https://doi.org/10.1002/cne.901870108

Plitman, E., Iwata, Y., Caravaggio, F., Nakajima, S., Chung, J.K., Gerretsen, P., Kim, J., Takeuchi, H., Chakravarty, M.M., Remington, G., Graff-Guerrero, A., 2017. Kynurenic Acid in Schizophrenia: A Systematic Review and Meta-analysis. Schizophr. Bull. https://doi.org/10.1093/schbul/sbw221

Pucak, M.L., Grace, A.A., 1996. Effects of haloperidol on the activity and membrane physiology of substantia nigra dopamine neurons recorded in vitro. Brain Res. https://doi.org/10.1016/0006-8993(95)01460-8

Pucak, M.L., Grace, A.A., 1994. Evidence that systemically administered dopamine antagonists activate dopamine neuron firing primarily by blockade of somatodendritic autoreceptors. J. Pharmacol. Exp. Ther.

Pucci, L., Perozzi, S., Cimadamore, F., Orsomando, G., Raffaelli, N., 2007. Tissue expression and biochemical characterization of human 2-amino 3-carboxymuconate 6-semialdehyde decarboxylase, a key enzyme in tryptophan catabolism. FEBS J. https://doi.org/10.1111/j.1742-4658.2007.05635.x

Rao, J.S., Kim, H.W., Harry, G.J., Rapoport, S.I., Reese, E.A., 2013. Increased neuroinflammatory and arachidonic acid cascade markers, and reduced synaptic proteins, in the postmortem frontal cortex from schizophrenia patients. Schizophr. Res. https://doi.org/10.1016/j.schres.2013.02.017

Rassoulpour, A., Wu, H.Q., Ferre, S., Schwarcz, R., 2005. Nanomolar concentrations of kynurenic acid reduce extracellular dopamine levels in the striatum. J. Neurochem. https://doi.org/10.1111/j.1471-4159.2005.03134.x

Rassoulpour, A., Wu, H.Q., Poeggeler, B., Schwarcz, R., 1998. Systemic d-amphetamine administration causes a reduction of kynurenic acid levels in rat brain. Brain Res. https://doi.org/10.1016/S0006-8993(98)00577-0

Remus, J.L., Dantzer, R., 2016. Inflammation models of depression in rodents: Relevance to psychotropic drug discovery. Int. J. Neuropsychopharmacol. https://doi.org/10.1093/ijnp/pyw028

Rodrigues-Amorim, D., Rivera-Baltanás, T., Spuch, C., Caruncho, H.J., González-Fernandez, Á., Olivares, J.M., Agís-Balboa, R.C., 2018. Cytokines dysregulation in schizophrenia: A systematic review of psychoneuroimmune relationship. Schizophr. Res. https://doi.org/10.1016/j.schres.2017.11.023

Rossi, F., Schwarcz, R., Rizzi, M., 2008. Curiosity to kill the KAT (kynurenine aminotransferase): structural insights into brain kynurenic acid synthesis. Curr. Opin. Struct. Biol. https://doi.org/10.1016/j.sbi.2008.09.009

Saha, S., Chant, D., McGrath, J., 2007. A systematic review of mortality in schizophrenia: Is the differential mortality gap worsening over time? Arch. Gen. Psychiatry. https://doi.org/10.1001/archpsyc.64.10.1123

Salazar, A., Gonzalez-Rivera, B.L., Redus, L., Parrott, J.M., O'Connor, J.C., 2012. Indoleamine 2,3-dioxygenase mediates anhedonia and anxiety-like behaviors caused by peripheral lipopolysaccharide immune challenge. Horm. Behav. https://doi.org/10.1016/j.yhbeh.2012.03.010

Sasayama, D., Hattori, K., Wakabayashi, C., Teraishi, T., Hori, H., Ota, M., Yoshida, S., Arima, K., Higuchi, T., Amano, N., Kunugi, H., 2013. Increased cerebrospinal fluid interleukin-6 levels in patients with schizophrenia and those with major depressive disorder. J. Psychiatr. Res. https://doi.org/10.1016/j.jpsychires.2012.12.001

Sathyasaikumar, K. V., Stachowski, E.K., Wonodi, I., Roberts, R.C., Rassoulpour, A., McMahon, R.P., Schwarcz, R., 2011. Impaired kynurenine pathway metabolism in the prefrontal cortex of individuals with schizophrenia. Schizophr. Bull. https://doi.org/10.1093/schbul/sbq112

Schmidt, W., Guidetti, P., Okuno, E., Schwarcz, R., 1993. Characterization of human brain kynurenine aminotransferases using [3H]kynurenine as a substrate. Neuroscience.

https://doi.org/10.1016/0306-4522(93)90464-Q

Schwarcz, R., 2016. Kynurenines and Glutamate. Multiple Links and Therapeutic Implications., in: Advances in Pharmacology. https://doi.org/10.1016/bs.apha.2016.01.005

Schwarcz, R., Bruno, J.P., Muchowski, P.J., Wu, H.Q., 2012. Kynurenines in the mammalian brain: When physiology meets pathology. Nat. Rev. Neurosci. https://doi.org/10.1038/nrn3257

Schwarcz, R., Pellicciari, R., 2002. Manipulation of brain kynurenines: Glial targets, neuronal effects, and clinical opportunities. J. Pharmacol. Exp. Ther. https://doi.org/10.1124/jpet.102.034439

Schwarcz, R., Rassoulpour, A., Wu, H.Q., Medoff, D., Tamminga, C.A., Roberts, R.C., 2001. Increased cortical kynurenate content in schizophrenia. Biol. Psychiatry. https://doi.org/10.1016/S0006-3223(01)01078-2

Schwarcz, R., Stone, T.W., 2017. The kynurenine pathway and the brain: Challenges, controversies and promises. Neuropharmacology. https://doi.org/10.1016/j.neuropharm.2016.08.003

Schwieler, L., Engberg, G., Erhardt, S., 2004. Clozapine Modulates Midbrain Dopamine Neuron Firing Via Interaction with the NMDA Receptor Complex. Synapse. https://doi.org/10.1002/syn.20008

Schwieler, L., Erhardt, S., 2003. Inhibitory action of clozapine on rat ventral tegmental area dopamine neurons following increased levels of endogenous kynurenic acid. Neuropsychopharmacology. https://doi.org/10.1038/sj.npp.1300255

Schwieler, L., Erhardt, S., Erhardt, C., Engberg, G., 2005. Prostaglandin-mediated control of rat brain kynurenic acid synthesis - Opposite actions by COX-1 and COX-2 isoforms. J. Neural Transm. https://doi.org/10.1007/s00702-004-0231-y

Schwieler, L., Erhardt, S., Nilsson, L., Linderholm, K., Engberg, G., 2006. Effects of COX-1 and COX-2 inhibitors on the firing of rat midbrain dopaminergic neurons - Possible involvement of endogenous kynurenic acid. Synapse. https://doi.org/10.1002/syn.20241

Schwieler, L., Larsson, M.K., Skogh, E., Kegel, M.E., Orhan, F., Abdelmoaty, S., Finn, A., Bhat, M., Samuelsson, M., Lundberg, K., Dahl, M.L., Sellgren, C., Schuppe-Koistinen, I., Svensson, C.I., Erhardt, S., Engberg, G., 2015. Increased levels of IL-6 in the cerebrospinal fluid of patients with chronic schizophrenia - Significance for activation of the kynurenine pathway. J. Psychiatry Neurosci. https://doi.org/10.1503/jpn.140126

Schwieler, L., Linderholm, K.R., Nilsson-Todd, L.K., Erhardt, S., Engberg, G., 2008. Clozapine interacts with the glycine site of the NMDA receptor: Electrophysiological studies of dopamine neurons in the rat ventral tegmental area. Life Sci. https://doi.org/10.1016/j.lfs.2008.05.014

Seeman, P., Lee, T., 1975. Antipsychotic drugs: direct correlation between clinical potency and presynaptic action on dopamine neurons. Science (80-.). https://doi.org/10.1126/science.1145194

Sellgren, C.M., Gracias, J., Watmuff, B., Biag, J.D., Thanos, J.M., Whittredge, P.B., Fu, T., Worringer, K., Brown, H.E., Wang, J., Kaykas, A., Karmacharya, R., Goold, C.P., Sheridan, S.D., Perlis, R.H., 2019. Increased synapse elimination by microglia in

schizophrenia patient-derived models of synaptic pruning. Nat. Neurosci. https://doi.org/10.1038/s41593-018-0334-7

Sellgren, C.M., Kegel, M.E., Bergen, S.E., Ekman, C.J., Olsson, S., Larsson, M., Vawter, M.P., Backlund, L., Sullivan, P.F., Sklar, P., Smoller, J.W., Magnusson, P.K.E., Hultman, C.M., Walther-Jallow, L., Svensson, C.I., Lichtenstein, P., Schalling, M., Engberg, G., Erhardt, S., Landén, M., 2016. A genome-wide association study of kynurenic acid in cerebrospinal fluid: Implications for psychosis and cognitive impairment in bipolar disorder. Mol. Psychiatry. https://doi.org/10.1038/mp.2015.186

Sesack, S.R., Deutch, A.Y., Roth, R.H., Bunney, B.S., 1989. Topographical organization of the efferent projections of the medial prefrontal cortex in the rat: An anterograde tract-tracing study with Phaseolus vulgaris leucoagglutinin. J. Comp. Neurol. https://doi.org/10.1002/cne.902900205

Shaltiel, G., Shamir, A., Levi, I., Bersudsky, Y., Agam, G., 2006. Lymphocyte G-protein receptor kinase (GRK)3 mRNA levels in bipolar disorder. Int. J. Neuropsychopharmacol. https://doi.org/10.1017/S146114570500636X

Shave, S., McGuire, K., Pham, N.T., Mole, D.J., Webster, S.P., Auer, M., 2018. Diclofenac Identified as a Kynurenine 3-Monooxygenase Binder and Inhibitor by Molecular Similarity Techniques. ACS Omega. https://doi.org/10.1021/acsomega.7b02091

Shi, J., Levinson, D.F., Duan, J., Sanders, A.R., Zheng, Y., Péer, I., Dudbridge, F., Holmans, P.A., Whittemore, A.S., Mowry, B.J., Olincy, A., Amin, F., Cloninger, C.R., Silverman, J.M., Buccola, N.G., Byerley, W.F., Black, D.W., Crowe, R.R., Oksenberg, J.R., Mirel, D.B., Kendler, K.S., Freedman, R., Gejman, P. V., 2009. Common variants on chromosome 6p22.1 are associated with schizophrenia. Nature. https://doi.org/10.1038/nature08192

Slifstein, M., Van De Giessen, E., Van Snellenberg, J., Thompson, J.L., Narendran, R., Gil, R., Hackett, E., Girgis, R., Ojeil, N., Moore, H., D'Souza, D., Malison, R.T., Huang, Y., Lim, K., Nabulsi, N., Carson, R.E., Lieberman, J.A., Abi-Dargham, A., 2015. Deficits in prefrontal cortical and extrastriatal dopamine release in schizophrenia a positron emission tomographic functional magnetic resonance imaging study. JAMA Psychiatry. https://doi.org/10.1001/jamapsychiatry.2014.2414

Snyder, S., Greenberg, D., Yamamura, H.I., 1974. Antischizophrenic Drugs and Brain Cholinergic Receptors: Affinity for Muscarinic Sites Predicts Extrapyramidal Effects. Arch. Gen. Psychiatry. https://doi.org/10.1001/archpsyc.1974.01760130040006

Snyder, S.H., 1973. Amphetamine psychosis: a "model" schizophrenia mediated by catecholamines. Am. J. Psychiatry. https://doi.org/10.1176/ajp.130.1.61

Söderlund, J., Schröder, J., Nordin, C., Samuelsson, M., Walther-Jallow, L., Karlsson, H., Erhardt, S., Engberg, G., 2009. Activation of brain interleukin-1B in schizophrenia. Mol. Psychiatry. https://doi.org/10.1038/mp.2009.52

Solle, M., Labasi, J., Perregaux, D.G., Stam, E., Petrushova, N., Koller, B.H., Griffiths, R.J., Gabel, C.A., 2001. Altered cytokine production in mice lacking P2X7 receptors. J. Biol. Chem. https://doi.org/10.1074/jbc.M006781200

Song, C., Clark, S.M., Vaughn, C.N., Nicholson, J.D., Murphy, K.J., Mou, T.C.M., Schwarcz, R., Hoffman, G.E., Tonelli, L.H., 2018. Quantitative Analysis of Kynurenine Aminotransferase II in the Adult Rat Brain Reveals High Expression in Proliferative

Zones and Corpus Callosum. Neuroscience. https://doi.org/10.1016/j.neuroscience.2017.11.001

Squires, R.F., Saederup, E., 1997. Clozapine and some other antipsychotic drugs may preferentially block the same subset of GABA(A) receptors. Neurochem. Res. https://doi.org/10.1023/A:1027359422433

Stilo, S.A., Murray, R.M., 2010. The epidemiology of schizophrenia: replacing dogma with knowledge. Dialogues Clin. Neurosci.

Stone, T.W., 1993. Neuropharmacology of quinolinic and kynurenic acids. Pharmacol. Rev.

Stone, T.W., Forrest, C.M., Darlington, L.G., 2012. Kynurenine pathway inhibition as a therapeutic strategy for neuroprotection. FEBS J. https://doi.org/10.1111/j.1742-4658.2012.08487.x

Stone, T.W., Perkins, M.N., 1981. Quinolinic acid: A potent endogenous excitant at amino acid receptors in CNS. Eur. J. Pharmacol. https://doi.org/10.1016/0014-2999(81)90587-2

Sullivan, P.F., Kendler, K.S., Neale, M.C., 2003. Schizophrenia as a Complex Trait: Evidence from a Meta-analysis of Twin Studies. Arch. Gen. Psychiatry. https://doi.org/10.1001/archpsyc.60.12.1187

Susser, E., Bresnahan, M., 2002. Epidemiologic approaches to neurodevelopmental disorders. Mol. Psychiatry. https://doi.org/10.1038/sj.mp.4001161

Susser, E.S., Lin, S.P., 1992. Schizophrenia After Prenatal Exposure to the Dutch Hunger Winter of 1944-1945. Arch. Gen. Psychiatry. https://doi.org/10.1001/archpsyc.1992.01820120071010

Tan, K.R., Yvon, C., Turiault, M., Mirzabekov, J.J., Doehner, J., Labouèbe, G., Deisseroth, K., Tye, K.M., Lüscher, C., 2012. GABA Neurons of the VTA Drive Conditioned Place Aversion. Neuron. https://doi.org/10.1016/j.neuron.2012.02.015

Tavares, R.G., Tasca, C.I., Santos, C.E.S., Alves, L.B., Porciúncula, L.O., Emanuelli, T., Souza, D.O., 2002. Quinolinic acid stimulates synaptosomal glutamate release and inhibits glutamate uptake into astrocytes. Neurochem. Int. https://doi.org/10.1016/S0197-0186(01)00133-4

Tonohiro, T., Tanabe, M., Kaneko, T., Iwata, N., 1990. Is picolinic acid a glycine agonist at strychnine-sensitive receptors? Brain Res. https://doi.org/10.1016/0006-8993(90)90937-7

Trecartin, K. V., Bucci, D.J., 2011. Administration of kynurenine during adolescence, but not during adulthood, impairs social behavior in rats. Schizophr. Res. https://doi.org/10.1016/j.schres.2011.08.014

Tsuang, M., 2000. Schizophrenia: Genes and environment. Biol. Psychiatry. https://doi.org/10.1016/S0006-3223(99)00289-9

Tufvesson-Alm, M., Schwieler, L., Schwarcz, R., Goiny, M., Erhardt, S., Engberg, G., 2018. Importance of kynurenine 3-monooxygenase for spontaneous firing and pharmacological responses of midbrain dopamine neurons: Relevance for schizophrenia. Neuropharmacology. https://doi.org/10.1016/j.neuropharm.2018.06.003

Upthegrove, R., Manzanares-Teson, N., Barnes, N.M., 2014. Cytokine function in medication-naive first episode psychosis: A systematic review and meta-analysis. Schizophr. Res. https://doi.org/10.1016/j.schres.2014.03.005

Uwai, Y., Honjo, H., Iwamoto, K., 2012. Interaction and transport of kynurenic acid via human organic anion transporters hOAT1 and hOAT3. Pharmacol. Res. https://doi.org/10.1016/j.phrs.2011.11.003

Van Heesch, F., Prins, J., Konsman, J.P., Korte-Bouws, G.A.H., Westphal, K.G.C., Rybka, J., Olivier, B., Kraneveld, A.D., Korte, S.M., 2014. Lipopolysaccharide increases degradation of central monoamines: An in vivo microdialysis study in the nucleus accumbens and medial prefrontal cortex of mice. Eur. J. Pharmacol. https://doi.org/10.1016/j.ejphar.2014.01.014

Van Os, J., Selten, J.P., 1998. Prenatal exposure to maternal stress and subsequent schizophrenia. The May 1940 invasion of The Netherlands. Br. J. Psychiatry. https://doi.org/10.1016/s0920-9964(97)88329-6

Van Zessen, R., Phillips, J.L., Budygin, E.A., Stuber, G.D., 2012. Activation of VTA GABA Neurons Disrupts Reward Consumption. Neuron. https://doi.org/10.1016/j.neuron.2012.02.016

Vrooman, L., Jhamandas, K., Boegman, R.J., Beninger, R.J., 1993. Picolinic acid modulates kainic acid-evoked glutamate release from the striatum in vitro. Brain Res. https://doi.org/10.1016/0006-8993(93)90320-M

Walker, A.K., Budac, D.P., Bisulco, S., Lee, A.W., Smith, R.A., Beenders, B., Kelley, K.W., Dantzer, R., 2013. NMDA receptor blockade by ketamine abrogates lipopolysaccharide-induced depressive-like behavior in C57BL/6J mice. Neuropsychopharmacology. https://doi.org/10.1038/npp.2013.71

Weickert, C.S., Fung, S.J., Catts, V.S., Schofield, P.R., Allen, K.M., Moore, L.T., Newell, K.A., Pellen, D., Huang, X.F., Catts, S. V., Weickert, T.W., 2013. Molecular evidence of N-methyl-D-aspartate receptor hypofunction in schizophrenia. Mol. Psychiatry. https://doi.org/10.1038/mp.2012.137

Wonodi, I., Stine, O.C., Sathyasaikumar, K. V., Roberts, R.C., Mitchell, B.D., Hong, L.E., Kajii, Y., Thaker, G.K., Schwarcz, R., 2011. Downregulated kynurenine 3-monooxygenase gene expression and enzyme activity in schizophrenia and genetic association with schizophrenia endophenotypes. Arch. Gen. Psychiatry. https://doi.org/10.1001/archgenpsychiatry.2011.71

Wu, H. -Q, Baran, H., Ungerstedt, U., Schwarcz, R., 1992. Kynurenic Acid in the Quinolinate-lesioned Rat Hippocampus: Studies In Vitro and In Vivo. Eur. J. Neurosci. https://doi.org/10.1111/j.1460-9568.1992.tb00152.x

Xi, Z.X., Stein, E.A., 1999. Baclofen inhibits heroin self-administration behavior and mesolimbic dopamine release. J. Pharmacol. Exp. Ther.

Xuan, J., Pan, G., Qiu, Y., Yang, L., Su, M., Liu, Y., Chen, J., Feng, G., Fang, Y., Jia, W., Xing, Q., He, L., 2011. Metabolomic profiling to identify potential serum biomarkers for schizophrenia and risperidone action. J. Proteome Res. https://doi.org/10.1021/pr2006796

Yolken, R.H., Torrey, E.F., 2008. Are some cases of psychosis caused by microbial agents? A review of the evidence. Mol. Psychiatry. https://doi.org/10.1038/mp.2008.5

Young, J.W., Minassian, A., Geyer, M.A., 2016. Locomotor profiling from rodents to the clinic and back again, in: Current Topics in Behavioral Neurosciences. https://doi.org/10.1007/7854_2015_5015

Zakrocka, I., Targowska-Duda, K.M., Wnorowski, A., Kocki, T., Jóźwiak, K., Turski, W.A., 2019. Influence of Cyclooxygenase-2 Inhibitors on Kynurenic Acid Production in Rat Brain in Vitro. Neurotox. Res. https://doi.org/10.1007/s12640-018-9952-9

Zavitsanou, K., Lim, C.K., Purves-Tyson, T., Karl, T., Kassiou, M., Banister, S.D., Guillemin, G.J., Weickert, C.S., 2014. Effect of maternal immune activation on the kynurenine pathway in preadolescent rat offspring and on MK801-induced hyperlocomotion in adulthood: Amelioration by COX-2 inhibition. Brain. Behav. Immun. https://doi.org/10.1016/j.bbi.2014.05.011

Zheng, W., Cai, D. Bin, Yang, X.H., Ungvari, G.S., Ng, C.H., Müller, N., Ning, Y.P., Xiang, Y.T., 2017. Adjunctive celecoxib for schizophrenia: A meta-analysis of randomized, double-blind, placebo-controlled trials. J. Psychiatr. Res. https://doi.org/10.1016/j.jpsychires.2017.04.004

Zuckerman, L., Weiner, I., 2005. Maternal immune activation leads to behavioral and pharmacological changes in the adult offspring. J. Psychiatr. Res. https://doi.org/10.1016/j.jpsychires.2004.08.008

Zunszain, P.A., Anacker, C., Cattaneo, A., Choudhury, S., Musaelyan, K., Myint, A.M., Thuret, S., Price, J., Pariante, C.M., 2012. Interleukin-1β: A new regulator of the kynurenine pathway affecting human hippocampal neurogenesis. Neuropsychopharmacology. https://doi.org/10.1038/npp.2011.277